

SDPMflut User's guide, version 0.6

G. Dimitriadis

January 2025

1 Introduction

SDPMflut is a Python package to perform subsonic compressible aerodynamic and aeroelastic analysis on wings and bodies using the compressible unsteady Source and Doublet Panel Method (SDPM). It is largely based on Unsteady Aerodynamics: Potential and Vortex Methods by G. Dimitriadis [1] and its core components are similar to those included in the companion site of the textbook, albeit written in Python instead of Matlab. The present unsteady aerodynamic formulation of the SDPM is also described in [2, 3], while the aeroelastic formulation of the SDPM is presented in [4, 5, 6].

2 Theoretical background

Under inviscid, irrotational and isentropic flow assumptions and for small perturbations the continuity equation simplifies to the linearized small disturbance equation

$$(1 - M_\infty^2)\phi_{xx} + \phi_{yy} + \phi_{zz} - \frac{2M_\infty}{a_\infty}\phi_{xt} - \frac{1}{a_\infty^2}\phi_{tt} = 0 \quad (1)$$

where $M_\infty = Q_\infty/a_\infty$ is the free stream Mach number, Q_∞ is the free stream airspeed along the x direction, a_∞ is the free stream speed of sound and ϕ is the velocity perturbation potential, defined from

$$u = \frac{\partial\phi}{\partial x}, \quad v = \frac{\partial\phi}{\partial y}, \quad w = \frac{\partial\phi}{\partial z}$$

and u, v, w are the perturbation velocities in the x, y, z directions. Under the same assumptions, the momentum equations can be integrated and expanded up to second order, such that

$$c_p = 1 - \frac{Q^2}{Q_\infty^2} + \frac{M_\infty^2}{Q_\infty^2}\phi_x^2 - \frac{2}{Q_\infty^2}\phi_t + \frac{M_\infty^2}{Q_\infty^4}\phi_t^2 + \frac{2M_\infty^2}{Q_\infty^3}\phi_x\phi_t \quad (2)$$

where c_p is the pressure coefficient

$$c_p = \frac{p - p_\infty}{\frac{1}{2}\rho_\infty Q_\infty^2}$$

where p is the pressure at any point in the flow and p_∞ is the free stream pressure, $Q^2 = u^2 + v^2 + w^2$ and ρ_∞ the free stream density.

The present source and doublet panel method solves equation 1 for the velocity potential $\phi(t)$ on the surface of a wing or other body and then calculates the pressure coefficient on the surface from equation 2. Both solutions are evaluated after applying the Fourier and Prandtl-Glauert transformations. The latter consists in expressing the geometry in coordinates ξ, η, ζ , such that

$$\xi = x/\beta, \quad \eta = y, \quad \zeta = z \quad (3)$$

where $\beta^2 = 1 - M_\infty^2$. Furthermore, the quasi-fixed geometry assumption is enforced, such that:

- all deformations of all bodies are small so that their geometry can be approximated as constant in time.
- the deformations are represented mathematically by means of the relative velocity between the fluid and the surface.

All the assumptions mentioned above mean that the SDPM is a fast and accurate aerodynamic modelling method as long as structural deformations are small, there is no significant flow separation and there are no shock waves in contact with the surface. Furthermore, as the present formulation of the SDPM is purely subsonic, the free stream Mach number must be less than one. Extensions to supersonic and transonic flow conditions are under development.

2.1 Calculating the potential on the surface

The fundamental equation of the unsteady compressible Source and Doublet Panel Method (SDPM) is Green's theorem in the frequency domain [7, 8]

$$\left(\hat{\mathbf{B}}_\phi(k) - \frac{1}{2}\mathbf{I} \right) \boldsymbol{\mu}(k) + \hat{\mathbf{C}}_\phi(k) \boldsymbol{\mu}_w(k) = -\hat{\mathbf{A}}_\phi(k) \boldsymbol{\sigma}(k) \quad (4)$$

Equation 4 is written out for the N panels on the surface of a wing and the N_w panels on the flat wake, such that $k = \omega c_0 / 2Q_\infty$ is the reduced frequency, ω is the frequency in rad/s, c_0 is a reference chord length, $\hat{\mathbf{A}}_\phi(k)$, $\hat{\mathbf{B}}_\phi(k)$ are $N \times N$ unsteady source and doublet influence coefficient matrices, $\hat{\mathbf{C}}_\phi(k)$ is the $N \times N_w$ unsteady doublet influence coefficient matrix of the wake on the wing, $\boldsymbol{\sigma}(k)$, $\boldsymbol{\mu}(k)$ are $N \times 1$ vectors of the source and doublet strengths on the wing panels and $\boldsymbol{\mu}_w(k)$ is the $N_w \times 1$ vector of the doublet strengths on the wake panels. The doublet strength on the surface is equal to the unknown potential on the surface, the source strength on the surface is determined from the impermeability boundary condition and the doublet strength in the wake is determined from the Kutta condition

$$\boldsymbol{\mu}_w(k) = \mathbf{P}_e(k) \mathbf{P}_c \boldsymbol{\mu}(k) \quad (5)$$

where

$$\mathbf{P}_c = (\mathbf{0}_{n \times (2m-1)n} \ \mathbf{I}_n) - (\mathbf{I}_n \ \mathbf{0}_{n \times (2m-1)n}) \quad (6)$$

$$\mathbf{P}_e(k) = \begin{pmatrix} \mathbf{I}_n e^{-i2k/m} \\ \mathbf{I}_n e^{-i4k/m} \\ \vdots \\ \mathbf{I}_n e^{-i2m_w k/m} \end{pmatrix} \quad (7)$$

Applying these two conditions leads to the solution for the doublet strength on the surface

$$\boldsymbol{\mu}(k) = \boldsymbol{\phi}(k) = -\mathbf{K}(k)\boldsymbol{\mu}_n(k) \quad (8)$$

where

$$\begin{aligned} \mathbf{K}(k) &= \left(\frac{2ikM_\infty^2}{c_0\beta} \hat{\mathbf{A}}_\phi(k) \circ \mathbf{n}_\xi + \hat{\mathbf{B}}_\phi(k) - \frac{1}{2}\mathbf{I} + \hat{\mathbf{C}}_\phi(k)\mathbf{P}_e(k)\mathbf{P}_c \right)^{-1} \hat{\mathbf{A}}_\phi(k) \\ \boldsymbol{\mu}_n(k) &= - \left(\frac{1}{\beta} \mathbf{u}_m(k) \circ \mathbf{n}_\xi + \mathbf{v}_m(k) \circ \mathbf{n}_\eta + \mathbf{w}_m(k) \circ \mathbf{n}_\zeta \right) \end{aligned} \quad (9)$$

\mathbf{n}_ξ , \mathbf{n}_η , \mathbf{n}_ζ are the three components of the unit vectors normal to the panels and pointing outwards written in Prandtl-Glauert coordinates, and the Hadamard operator \circ is used to denote the element-by-element multiplication of vectors or of each of the columns of a matrix by the same column vector. It should be noted that $\mathbf{K}(k)$ has dimensions of meters while $\boldsymbol{\mu}_n(k)$ has dimensions of m/s, such that $\boldsymbol{\mu}(k)$ has dimensions of m²/s.

Once the doublet strengths on the surface, $\boldsymbol{\mu}(k)$, have been evaluated, the next step is to calculate the perturbation velocities on the surface by numerically differentiating $\boldsymbol{\mu}(k)$. The result is

$$\phi_x(k) = \mathbf{K}_x(k)\boldsymbol{\mu}_n(k), \quad \phi_y(k) = \mathbf{K}_y(k)\boldsymbol{\mu}_n(k), \quad \phi_z(k) = \mathbf{K}_z(k)\boldsymbol{\mu}_n(k) \quad (10)$$

where $\mathbf{K}_x(k)$, $\mathbf{K}_y(k)$, $\mathbf{K}_z(k)$ are non-dimensional functions of the geometry and finite difference matrices and are detailed in [3, 4]. The total flow velocities on the surface are given by

$$\mathbf{u}(k) = \mathbf{u}_m(k) + \phi_x(k), \quad \mathbf{v}(k) = \mathbf{v}_m(k) + \phi_y(k), \quad \mathbf{w}(k) = \mathbf{w}_m(k) + \phi_z(k) \quad (11)$$

where $\mathbf{u}_m(k)$, $\mathbf{v}_m(k)$, $\mathbf{w}_m(k)$ are the relative velocities between the flow and the surface due to the motion.

The steady solution is obtained for $k = 0$, such that equation 8 becomes

$$\boldsymbol{\mu}(0) = \boldsymbol{\phi}(0) = -\mathbf{K}(0)\boldsymbol{\mu}_n(0) \quad (12)$$

where

$$\mathbf{K}(0) = \left(\mathbf{B}_\phi - \frac{1}{2}\mathbf{I} + \mathbf{C}_\phi\mathbf{P}_e(0)\mathbf{P}_c \right)^{-1} \mathbf{A}_\phi \quad (13)$$

$$\boldsymbol{\mu}_n(0) = - \left(\frac{1}{\beta} U_\infty \mathbf{n}_\xi + V_\infty \mathbf{n}_\eta + W_\infty \mathbf{n}_\zeta \right) \quad (14)$$

$$\mathbf{P}_e(0) = \begin{pmatrix} \mathbf{I}_n \\ \mathbf{I}_n \\ \vdots \\ \mathbf{I}_n \end{pmatrix} \quad (15)$$

$$\boldsymbol{\phi}_x(0) = \mathbf{K}_x(0)\boldsymbol{\mu}_n(0), \quad \boldsymbol{\phi}_y(0) = \mathbf{K}_y(0)\boldsymbol{\mu}_n(0), \quad \boldsymbol{\phi}_z(0) = \mathbf{K}_z(0)\boldsymbol{\mu}_n(0) \quad (16)$$

$$\mathbf{u}(0) = U_\infty + \boldsymbol{\phi}_x(0), \quad \mathbf{v}(0) = V_\infty + \boldsymbol{\phi}_y(0), \quad \mathbf{w}(0) = W_\infty + \boldsymbol{\phi}_z(0) \quad (17)$$

with $Q_\infty^2 = U_\infty^2 + V_\infty^2 + W_\infty^2$, \mathbf{A}_ϕ , \mathbf{B}_ϕ , \mathbf{C}_ϕ being the steady influence coefficient matrices. Note that the form of equation 1 implies that $V_\infty \ll U_\infty$ and $W_\infty \ll U_\infty$, such that only U_∞ is comparable to a_∞ . In other words, the direction of compressibility is the x axis.

2.2 Calculating the pressure on the surface

Appendix A shows that, after substituting equations 8 to 17 is the Fourier transform of equation 2, the pressure coefficient on the panel control points is given by

$$\begin{aligned} \mathbf{c}_p(k) = & -\frac{1}{\beta}\bar{\mathbf{C}}_0(k)(\mathbf{n}_\xi \circ \bar{\mathbf{u}}_m(k)) - 2\bar{\mathbf{u}}(0) \circ \bar{\mathbf{u}}_m(k) - \bar{\mathbf{C}}_0(k)(\mathbf{n}_\eta \circ \bar{\mathbf{v}}_m(k)) - 2\bar{\mathbf{v}}(0) \circ \bar{\mathbf{v}}_m(k) \\ & -\bar{\mathbf{C}}_0(k)(\mathbf{n}_\zeta \circ \bar{\mathbf{w}}_m(k)) - 2\bar{\mathbf{w}}(0) \circ \bar{\mathbf{w}}_m(k) - \frac{2ik}{c_0\beta}\bar{\mathbf{C}}_1(k)(\mathbf{n}_\xi \circ \bar{\mathbf{u}}_m(k)) \\ & -\frac{2ik}{c_0}\bar{\mathbf{C}}_1(k)(\mathbf{n}_\eta \circ \bar{\mathbf{v}}_m(k)) - \frac{2ik}{c_0}\bar{\mathbf{C}}_1(k)(\mathbf{n}_\zeta \circ \bar{\mathbf{w}}_m(k)) \end{aligned} \quad (18)$$

where

$$\begin{aligned} \bar{\mathbf{C}}_0(k) &= -2\mathbf{K}_x(k) \circ \bar{\mathbf{u}}(0) - 2\mathbf{K}_y(k) \circ \bar{\mathbf{v}}(0) - 2\mathbf{K}_z(k) \circ \bar{\mathbf{w}}(0) + 2M_\infty^2\mathbf{K}_x(k) \circ \bar{\boldsymbol{\phi}}_x(0) \\ \bar{\mathbf{C}}_1(k) &= 2\mathbf{K}(k) - 2M_\infty^2\mathbf{K}(k) \circ \bar{\boldsymbol{\phi}}_x(0) \end{aligned} \quad (19)$$

and the overbars denote the normalized potential and velocities $\bar{\boldsymbol{\phi}}(k) = \boldsymbol{\phi}(k)/Q_\infty$, $\bar{\mathbf{u}}(k) = \mathbf{u}(k)/Q_\infty$, $\bar{\mathbf{v}}(k) = \mathbf{v}(k)/Q_\infty$, $\bar{\mathbf{w}}(k) = \mathbf{w}(k)/Q_\infty$, $\bar{\mathbf{u}}_m(k) = \mathbf{u}_m(k)/Q_\infty$, $\bar{\mathbf{v}}_m(k) = \mathbf{v}_m(k)/Q_\infty$, $\bar{\mathbf{w}}_m(k) = \mathbf{w}_m(k)/Q_\infty$, $\bar{\boldsymbol{\phi}}_x(k) = \boldsymbol{\phi}_x(k)/Q_\infty$, $\bar{\boldsymbol{\phi}}_y(k) = \boldsymbol{\phi}_y(k)/Q_\infty$, $\bar{\boldsymbol{\phi}}_z(k) = \boldsymbol{\phi}_z(k)/Q_\infty$, $\bar{U}_\infty = U_\infty/Q_\infty$, $\bar{V}_\infty = V_\infty/Q_\infty$, $\bar{W}_\infty = W_\infty/Q_\infty$. It should be noted that both $\bar{\boldsymbol{\phi}}(k)$ and $\bar{\mathbf{C}}_1(k)$ have dimensions of meters, such that $\mathbf{c}_p(k)$ is non-dimensional. Substituting the same normalized quantities into equation 42, such that the steady pressure coefficient becomes

$$\mathbf{c}_{p_0} = 1 - (\bar{\mathbf{u}}(0) \circ \bar{\mathbf{u}}(0) + \bar{\mathbf{v}}(0) \circ \bar{\mathbf{v}}(0) + \bar{\mathbf{w}}(0) \circ \bar{\mathbf{w}}(0)) + M_\infty^2 (\bar{\boldsymbol{\phi}}_x(0) \circ \bar{\boldsymbol{\phi}}_x(0)) \quad (20)$$

Equations 20 and 18 are the required steady and unsteady pressure distributions around the surface. In order to calculate them, the free stream and relative motion between the flow and the surface must be specified. The free stream is straightforward; it depends on the prescribed flight condition, which are usually described by the angle of attack α_0 and the angle of sideslip β_0 , such that

$$\bar{U}_\infty = \cos \alpha_0 \cos \beta_0, \quad \bar{V}_\infty = -\sin \beta_0, \quad \bar{W}_\infty = \sin \alpha_0 \cos \beta_0 \quad (21)$$

The relative velocity due to the unsteady motion at frequency k can be rigid and/or flexible. For rigid motion around the body's centre of gravity, having set the latter as the origin of the coordinate system, the linearized motion-induced velocities are given by

$$\begin{aligned}\bar{\mathbf{u}}_m(k) &= \bar{V}_\infty\psi(k) - \bar{W}_\infty\theta(k) - \bar{q}(k)\mathbf{z}_c + \bar{r}(k)\mathbf{y}_c - \bar{u}(k) \\ \bar{\mathbf{v}}_m(k) &= -\bar{U}_\infty\psi(k) + \bar{W}_\infty\phi(k) + \bar{p}(k)\mathbf{z}_c - \bar{r}(k)\mathbf{x}_c - \bar{v}(k)(k) \\ \bar{\mathbf{w}}_m(k) &= \bar{U}_\infty\theta(k) - \bar{V}_\infty\phi(k) + \bar{q}(k)\mathbf{x}_c - \bar{p}(k)\mathbf{y}_c - \bar{w}(k)\end{aligned}\quad (22)$$

where \mathbf{x}_c , \mathbf{y}_c , \mathbf{z}_c are the coordinates of the panel control points, $u(k)$, $v(k)$, $w(k)$ are the rigid-body translation velocities, $p(k)$, $q(k)$, $r(k)$ are the rigid-body roll, pitch and yaw velocities, $\phi(k)$, $\theta(k)$, $\psi(k)$ are the roll, pitch and yaw angles and $\bar{u}(k) = u(k)/Q_\infty$, $\bar{v}(k) = v(k)/Q_\infty$, $\bar{w}(k) = w(k)/Q_\infty$, $\bar{p}(k) = p(k)/Q_\infty$, $\bar{q}(k) = q(k)/Q_\infty$, $\bar{r}(k) = r(k)/Q_\infty$. Note that $\bar{p}(k)$, $\bar{q}(k)$, $\bar{r}(k)$ have dimensions of 1/m so that $\bar{\mathbf{u}}_m(k)$, $\bar{\mathbf{v}}_m(k)$, $\bar{\mathbf{w}}_m(k)$, are non-dimensional.

Flexible deformations are modelled in `SDPMflut` using a modal description. The body's deformation is written as

$$\mathbf{x}_{FE}(t) = \mathbf{\Phi}\mathbf{q}(t)$$

where $\mathbf{x}_{FE}(t)$ is the $6N_{FE} \times 1$ vector of degrees of freedom of a finite element model, N_{FE} is the number of nodes in the model, $\mathbf{\Phi}$ is a $6N_{FE} \times K$ matrix of mode shapes, K is the number of retained modes and $\mathbf{q}(t)$ is a $K \times 1$ vector of generalized coordinates. The mode shape matrix $\mathbf{\Phi}$ contains translations in the x , y , z directions and rotations around the x , y , z axes. Then, it can be decomposed as

$$\mathbf{\Phi} = \begin{pmatrix} \mathbf{\Phi}_x \\ \mathbf{\Phi}_y \\ \mathbf{\Phi}_z \\ \mathbf{\Phi}_\phi \\ \mathbf{\Phi}_\theta \\ \mathbf{\Phi}_\psi \end{pmatrix}$$

where $\mathbf{\Phi}_x$, $\mathbf{\Phi}_y$, $\mathbf{\Phi}_z$ are $N_{FE} \times K$ translation mode shapes and $\mathbf{\Phi}_\phi$, $\mathbf{\Phi}_\theta$, $\mathbf{\Phi}_\psi$ are $N_{FE} \times K$ rotation mode shapes in the roll, pitch and yaw directions respectively. The mode shapes of the finite element model must be interpolated onto the control points of the SDPM grid, such that they become $N \times K$ matrices $\tilde{\mathbf{\Phi}}_x$, $\tilde{\mathbf{\Phi}}_y$, $\tilde{\mathbf{\Phi}}_z$, $\tilde{\mathbf{\Phi}}_\phi$, $\tilde{\mathbf{\Phi}}_\theta$, $\tilde{\mathbf{\Phi}}_\psi$, the tilde denoting interpolated quantities and N being the number of SDPM panels. Consequently, the motion-induced velocities are given by

$$\begin{aligned}\bar{\mathbf{u}}_m(k) &= \bar{V}_\infty\tilde{\mathbf{\Phi}}_\psi\mathbf{q}(k) - \bar{W}_\infty\tilde{\mathbf{\Phi}}_\theta\mathbf{q}(k) - \frac{2ik}{c_0}\tilde{\mathbf{\Phi}}_x\mathbf{q}(k) \\ \bar{\mathbf{v}}_m(k) &= -\bar{U}_\infty\tilde{\mathbf{\Phi}}_\psi\mathbf{q}(k) + \bar{W}_\infty\tilde{\mathbf{\Phi}}_\phi\mathbf{q}(k) - \frac{2ik}{c_0}\tilde{\mathbf{\Phi}}_y\mathbf{q}(k) \\ \bar{\mathbf{w}}_m(k) &= \bar{U}_\infty\tilde{\mathbf{\Phi}}_\theta\mathbf{q}(k) - \bar{V}_\infty\tilde{\mathbf{\Phi}}_\phi\mathbf{q}(k) - \frac{2ik}{c_0}\tilde{\mathbf{\Phi}}_z\mathbf{q}(k)\end{aligned}\quad (23)$$

Substituting equations 22 and/or 23 into expression 18 results in the numerical values of the oscillatory pressure distribution at frequency k . Note that $\mathbf{c}_p(k)$ is a complex

quantity. Note that $u(k)$, $v(k)$, $w(k)$, $p(k)$, $q(k)$, $r(k)$ and $\mathbf{q}(k)$ are known if the motion is prescribed. If the motion is free, the pressure distribution can be written in the form of pressure derivatives. Then, the pressure distribution due to the rigid motion is written as

$$\begin{aligned}
\mathbf{c}_p(k) = & \mathbf{c}_{p_u}(k)u(k) + \mathbf{c}_{p_v}(k)v(k) + \mathbf{c}_{p_w}(k)w(k) + \mathbf{c}_{p_\theta}(k)\theta(k) \\
& + \mathbf{c}_{p_\psi}(k)\psi(k) + \mathbf{c}_{p_p}(k)p(k) + \mathbf{c}_{p_q}(k)q(k) + \mathbf{c}_{p_r}(k)r(k) \\
& + \mathbf{c}_{p_{\dot{u}}}(k)u(k) + ik\mathbf{c}_{p_{\dot{v}}}(k)v(k) + ik\mathbf{c}_{p_{\dot{w}}}(k)w(k) + ik\mathbf{c}_{p_{\dot{p}}}(k)p(k) \\
& + ik\mathbf{c}_{p_{\dot{q}}}(k)q(k) + ik\mathbf{c}_{p_{\dot{r}}}(k)r(k)
\end{aligned} \tag{24}$$

and SDPMflut calculates the $N \times 1$ pressure derivative vectors $\mathbf{c}_{p_u}(k)$, $\mathbf{c}_{p_v}(k)$, etc, expressions for which are given in appendix B. For flexible motion, the pressure distribution is written as

$$\begin{aligned}
\mathbf{c}_p(k) = & (\mathbf{c}_{p_\phi}(k) + \mathbf{c}_{p_\theta}(k) + \mathbf{c}_{p_\psi}(k)) \mathbf{q}(k) \\
& + ik \left(\mathbf{c}_{p_{\dot{x}}}(k) + \mathbf{c}_{p_{\dot{y}}}(k) + \mathbf{c}_{p_{\dot{z}}}(k) + \mathbf{c}_{p_{\dot{\phi}}}(k) + \mathbf{c}_{p_{\dot{\theta}}}(k) + \mathbf{c}_{p_{\dot{\psi}}}(k) \right) \mathbf{q}(k) \\
& + (ik)^2 (\mathbf{c}_{p_{\ddot{x}}}(k) + \mathbf{c}_{p_{\ddot{y}}}(k) + \mathbf{c}_{p_{\ddot{z}}}(k)) \mathbf{q}(k)
\end{aligned} \tag{25}$$

and SDPMflut calculates the $N \times K$ pressure derivative matrices $\mathbf{c}_{p_\phi}(k)$, $\mathbf{c}_{p_\theta}(k)$, $\mathbf{c}_{p_\psi}(k)$ etc, expressions for which are given in appendix D.

2.3 Calculating the aerodynamic loads

The steady aerodynamic loads acting on each panel are given by

$$\begin{aligned}
\mathbf{F}_x(0) &= -\mathbf{c}_{p_0} \circ \mathbf{s} \circ \mathbf{n}_x \\
\mathbf{F}_y(0) &= -\mathbf{c}_{p_0} \circ \mathbf{s} \circ \mathbf{n}_y \\
\mathbf{F}_z(0) &= -\mathbf{c}_{p_0} \circ \mathbf{s} \circ \mathbf{n}_z \\
\mathbf{M}_x(0) &= (\mathbf{y}_c - y_{f_0})\mathbf{F}_z(0) - (\mathbf{z}_c - z_{f_0})\mathbf{F}_y(0) \\
\mathbf{M}_y(0) &= -(\mathbf{x}_c - x_{f_0})\mathbf{F}_z(0) + (\mathbf{z}_c - z_{f_0})\mathbf{F}_x(0) \\
\mathbf{M}_z(0) &= (\mathbf{x}_c - x_{f_0})\mathbf{F}_y(0) - (\mathbf{y}_c - y_{f_0})\mathbf{F}_x(0)
\end{aligned} \tag{26}$$

where $\mathbf{F}_x(0)$, $\mathbf{F}_y(0)$, $\mathbf{F}_z(0)$ are $N \times 1$ vectors of aerodynamic force per Pascal, $\mathbf{M}_x(0)$, $\mathbf{M}_y(0)$, $\mathbf{M}_z(0)$ are $N \times 1$ vectors of aerodynamic moment per Pascal around point $(x_{f_0}, y_{f_0}, z_{f_0})$, \mathbf{n}_x , \mathbf{n}_y , \mathbf{n}_z , are the $N \times 1$ components of the unit vectors normal to the panels in cartesian coordinates, \mathbf{s} is the $N \times 1$ vector of the areas of the panels, \mathbf{c}_{p_0} is calculated from equation 20. The negative signs in these equations are due to the fact that the unit vectors normal to the surfaces are pointing outwards. Similarly, the unsteady aerodynamic loads at k are calculated from

$$\begin{aligned}
\mathbf{F}_x(k) &= -\mathbf{c}_p(k) \circ \mathbf{s} \circ \mathbf{n}_x \\
\mathbf{F}_y(k) &= -\mathbf{c}_p(k) \circ \mathbf{s} \circ \mathbf{n}_y \\
\mathbf{F}_z(k) &= -\mathbf{c}_p(k) \circ \mathbf{s} \circ \mathbf{n}_z
\end{aligned} \tag{27}$$

$$\begin{aligned}
\mathbf{M}_x(k) &= (\mathbf{y}_c - y_{f_0})\mathbf{F}_z(k) - (\mathbf{z}_c - z_{f_0})\mathbf{F}_y(k) \\
\mathbf{M}_x(k) &= -(\mathbf{x}_c - x_{f_0})\mathbf{F}_z(k) + (\mathbf{z}_c - z_{f_0})\mathbf{F}_x(k) \\
\mathbf{M}_x(k) &= (\mathbf{x}_c - x_{f_0})\mathbf{F}_y(k) - (\mathbf{y}_c - y_{f_0})\mathbf{F}_x(k)
\end{aligned}$$

where $\mathbf{c}_p(k)$ is calculated from equation 24 or 25.

2.4 Calculating the flutter solution

The aeroelastic equation for flexible motion is given by

$$\mathbf{A}\ddot{\mathbf{q}} + \mathbf{C}\dot{\mathbf{q}} + \mathbf{E}\mathbf{q} = \frac{1}{2}\rho_\infty Q_\infty^2 (\mathbf{Q}_0(k) + ik\mathbf{Q}_1(k) + (ik)^2\mathbf{Q}_2(k)) \mathbf{q} \quad (28)$$

where \mathbf{A} , \mathbf{C} , \mathbf{E} are $K \times K$ structural modal mass, damping and stiffness matrices and $\mathbf{Q}_0(k)$, $\mathbf{Q}_1(k)$, $\mathbf{Q}_2(k)$ are generalized aerodynamic stiffness, damping and mass matrices, given by

$$\begin{aligned}
\mathbf{Q}_0(k) &= \left(\tilde{\Phi}_x^T \mathbf{F}_{x_0}(k) + \tilde{\Phi}_y^T \mathbf{F}_{y_0}(k) + \tilde{\Phi}_z^T \mathbf{F}_{z_0}(k) \right) \\
\mathbf{Q}_1(k) &= \left(\tilde{\Phi}_x^T \mathbf{F}_{x_1}(k) + \tilde{\Phi}_y^T \mathbf{F}_{y_1}(k) + \tilde{\Phi}_z^T \mathbf{F}_{z_1}(k) \right) \\
\mathbf{Q}_2(k) &= \left(\tilde{\Phi}_x^T \mathbf{F}_{x_2}(k) + \tilde{\Phi}_y^T \mathbf{F}_{y_2}(k) + \tilde{\Phi}_z^T \mathbf{F}_{z_2}(k) \right)
\end{aligned} \quad (29)$$

where

$$\begin{aligned}
\mathbf{F}_{x_0}(k) &= -(\mathbf{c}_{p_\phi}(k) + \mathbf{c}_{p_\theta}(k) + \mathbf{c}_{p_\psi}(k)) \circ \mathbf{s} \circ \mathbf{n}_x \\
\mathbf{F}_{x_1}(k) &= -(\mathbf{c}_{p_{\dot{x}}}(k) + \mathbf{c}_{p_{\dot{y}}}(k) + \mathbf{c}_{p_z}(k) + \mathbf{c}_{p_{\dot{\phi}}}(k) + \mathbf{c}_{p_{\dot{\theta}}}(k) + \mathbf{c}_{p_{\dot{\psi}}}(k)) \circ \mathbf{s} \circ \mathbf{n}_x \\
\mathbf{F}_{x_2}(k) &= -(\mathbf{c}_{p_{\ddot{x}}}(k) + \mathbf{c}_{p_{\ddot{y}}}(k) + \mathbf{c}_{p_{\ddot{z}}}(k)) \circ \mathbf{s} \circ \mathbf{n}_x \\
\mathbf{F}_{y_0}(k) &= -(\mathbf{c}_{p_\phi}(k) + \mathbf{c}_{p_\theta}(k) + \mathbf{c}_{p_\psi}(k)) \circ \mathbf{s} \circ \mathbf{n}_y \\
\mathbf{F}_{y_1}(k) &= -(\mathbf{c}_{p_{\dot{x}}}(k) + \mathbf{c}_{p_{\dot{y}}}(k) + \mathbf{c}_{p_z}(k) + \mathbf{c}_{p_{\dot{\phi}}}(k) + \mathbf{c}_{p_{\dot{\theta}}}(k) + \mathbf{c}_{p_{\dot{\psi}}}(k)) \circ \mathbf{s} \circ \mathbf{n}_y \\
\mathbf{F}_{y_2}(k) &= -(\mathbf{c}_{p_{\ddot{x}}}(k) + \mathbf{c}_{p_{\ddot{y}}}(k) + \mathbf{c}_{p_{\ddot{z}}}(k)) \circ \mathbf{s} \circ \mathbf{n}_y \\
\mathbf{F}_{z_0}(k) &= -(\mathbf{c}_{p_\phi}(k) + \mathbf{c}_{p_\theta}(k) + \mathbf{c}_{p_\psi}(k)) \circ \mathbf{s} \circ \mathbf{n}_z \\
\mathbf{F}_{z_1}(k) &= -(\mathbf{c}_{p_{\dot{x}}}(k) + \mathbf{c}_{p_{\dot{y}}}(k) + \mathbf{c}_{p_z}(k) + \mathbf{c}_{p_{\dot{\phi}}}(k) + \mathbf{c}_{p_{\dot{\theta}}}(k) + \mathbf{c}_{p_{\dot{\psi}}}(k)) \circ \mathbf{s} \circ \mathbf{n}_z \\
\mathbf{F}_{z_2}(k) &= -(\mathbf{c}_{p_{\ddot{x}}}(k) + \mathbf{c}_{p_{\ddot{y}}}(k) + \mathbf{c}_{p_{\ddot{z}}}(k)) \circ \mathbf{s} \circ \mathbf{n}_z
\end{aligned} \quad (30)$$

Equation 28 is solved using determinant iteration for the system eigenvalues at each selected value of the free stream airspeed. The objective is to solve

$$\begin{aligned}
\left| \left(\frac{2Q_\infty^2}{c_0^2} \mathbf{A} - \frac{1}{2}\rho_\infty Q_\infty^2 \mathbf{Q}_2(k) \right) p^2 + \left(\frac{2Q_\infty}{c_0} \mathbf{A} - \frac{1}{2}\rho_\infty Q_\infty^2 \mathbf{Q}_1(k) \right) p \right. \\
\left. + \left(\mathbf{E} - \frac{1}{2}\rho_\infty Q_\infty^2 \mathbf{Q}_0(k) \right) \right| = 0 \quad (31)
\end{aligned}$$

for the reduced eigenvalue $p = g + ik$, where g is the reduced damping and k the reduced frequency. Both the real and imaginary parts of the determinant must be equal to zero,

so that there are two equations with two unknowns, g and k . The problem is nonlinear so it must be solved iteratively, starting from an initial guess $g = 0$ and $k = \omega_{n_i} c_0 / 2Q_\infty$, where ω_{n_i} is the i th wind-off natural frequency of the system. Once p_i has been evaluated for one airspeed, it is used as the initial guess for the next airspeed and so on, until p_i is available at all Q_∞ values of interest. Then, the entire process is repeated for all the other wind-off natural frequencies. Finally, the i th system eigenvalue at Q_∞ is calculated from

$$\lambda_i(Q_\infty) = \frac{2Q_\infty}{c_0} p_i(Q_\infty)$$

for $i = 1, \dots, K$. The fact that k varies during the determinant iteration procedure means that $\mathbf{Q}_0(k)$, $\mathbf{Q}_1(k)$ and $\mathbf{Q}_2(k)$ must be calculated at each current value of k . In order to reduce the cost of the flutter solution, $\mathbf{Q}_0(k)$, $\mathbf{Q}_1(k)$ and $\mathbf{Q}_2(k)$ are calculated at a number of pre-selected k values and then interpolated as needed.

The system is stable as long as all $\lambda_i(Q_\infty)$ have negative real parts. This condition is expressed in `SDPMflut` in terms of the damping ratio

$$\zeta_i(Q_\infty) = -\frac{\Re(\lambda_i(Q_\infty))}{|\lambda_i(Q_\infty)|}$$

so that $\zeta_i(Q_\infty) > 0$ for stability. If any $\zeta_i(Q_\infty)$ becomes negative inside the airspeed range of interest, `SDPMflut` repeats the determinant iteration procedure in the neighbourhood of the sign change in order to pinpoint accurately the flutter airspeed Q_F at which $\zeta_i(Q_F) = 0$. Note that, since $g = 0$ at the flutter speed, then the flutter eigenvalue becomes $p = ik_F$, k_F being the flutter reduced frequency; consequently, this second round of determinant iterations solves the problem

$$\left| \left(\frac{2Q_F^2}{c_0^2} \mathbf{A} - \frac{1}{2} \rho_\infty Q_F^2 \mathbf{Q}_2(k_F) \right) (ik_F)^2 + \left(\frac{2Q_F}{c_0} \mathbf{A} - \frac{1}{2} \rho_\infty Q_F^2 \mathbf{Q}_1(k_F) \right) ik_F + \left(\mathbf{E} - \frac{1}{2} \rho_\infty Q_F^2 \mathbf{Q}_0(k_F) \right) \right| = 0 \quad (32)$$

for the two unknowns Q_F and k_F . Then, the dimensional flutter frequency is obtained from

$$\omega_F = \frac{2Q_F}{c_0} k_F$$

3 Installing and running SDPMflut

`SDPMflut` is written in Python and C. To run it you need to have a recent Python distribution and a C compiler installed on your system. The installation steps are the following:

1. Unzip the `SDPMflut_v0.6.zip` file, place anywhere in your file space, then edit the line starting with `install_dir=` in
 - `AGARD445_6/flutter_SDPM_AGARD.py`

- NACARML5/unsteady_SDPM_delta.py
- NACARML5/unsteady_SDPM_straight.py
- NACARML5/unsteady_SDPM_swept.py
- NASATMX72799/flutter_SDPM_NASATMX72799.py
- NASATND344/unsteady_SDPM_NASATND344.py
- NASATM84367/steady_SDPM_NASATM84367.py
- PAPA/flutter_SDPM_NACA0012.py
- PAPA/flutter_SDPM_BSCW.py
- PAPA/flutter_SDPM_NACA64A010.py
- T_tail/flutter_SDPM_Ttail.py.
- Theodorsen/flutter_SDPM_Theodorsen.py.

You need to give the absolute path to the Common directory, as installed on your system. Mac OS/Linux example:

```
install_dir=r"/Users/Username/Documents/Python/SDPMflut_v0.6/Common/"
```

Windows example:

```
install_dir=r"C:\Users\Username\Documents\Python\SDPMflut\Common"
```

2. Compile the C codes `sdpminfso.c` and `sdpminf_unsteady_subsonicso.c` found in directory `Common`. At your C compiler's terminal type:

- `gcc -fPIC -shared -o sdpminfso.so sdpminfso.c`
- `gcc -fPIC -shared -o sdpminf_unsteadyso.so sdpminf_unsteadyso.c`

assuming that you have GNU C installed. The same commands with `cc` instead of `gcc` may work.

If you do not have a Python distribution or IDE on your system you can install Anaconda and Spyder:

1. Download Anaconda from <https://docs.anaconda.com/anaconda/install/>.
2. Run the installer, selecting the default installation options.
3. On Windows, Anaconda installs its own version of the DOS command window, called Anaconda Prompt. Launch Anaconda Prompt.
4. On Mac OS/Linux launch the terminal.
5. Type `conda --version` (no space between the dashes).
6. Instal Spyder from <https://www.spyder-ide.org>.
7. Launch Spyder and go to Preferences->Python interpreter

8. Click on `Use the following Python interpreter` and select `/opt/anaconda3/bin/python` or whatever version has been installed by Anaconda.
9. Click `Apply`, `OK` and then from the `Consoles` menu select `Restart kernel`
10. It is likely that Spyder will complain that the interpreter you selected does not have the right version of the Spyder Kernels.
11. Launch the Anaconda Prompt or terminal as Administrator. Type:


```
conda install spyder-kernels=3.0
```

 or whatever version Spyder has asked for.
12. Quit and restart Spyder.

If you do not have a C compiler on your system, you can install one depending on your system architecture:

- On Mac OS install Xcode and the command line tools. You can also optionally instal GCC (GNU Compiler Collection).
- On Linux install GCC (GNU Compiler Collection).
- On Windows there are many options. For example, you can download MinGW from <https://www.mingw-w64.org/downloads/>. Extract the zip file to `C:\Prog` or wherever else you wish. Launch the Command Prompt and set the path:
 - Temporary option: type `set path=C:\Prog\mingw64\bin;%PATH%`
 - Permanent option: type `setx PATH ^%PATH^%;"C:\Prog\mingw64\bin"`

To run `SDPMflut`, Launch Spyder and open one of the test cases. For example, you can open `PAPA/flutter_SDPM_NACA0012.py`. Click on `Rune file` or type `F5`.

4 Structure of `SDPMflut`

`SDPMflut` does not have a user interface. For each test case there is a subdirectory inside the installation directory that contains one or more `.py` files and may also contain one or more `.mat` files. The file names of the files to run end with `.py` and start with

- `steady_SDPM_`: These files calculate only steady aerodynamic pressures and loads.
- `unsteady_SDPM_`: These files calculate both steady and unsteady aerodynamic pressures and loads.
- `flutter_SDPM_`: These files calculate steady and unsteady aerodynamic pressures and loads, as well as flutter solutions.

The current distribution contains the following test cases:

- **AGARD445_6**: Flutter solution for the weakened AGARD 445.6 wing described in [9].
- **NACARML5**: Calculation of aerodynamic stability derivatives for a straight tapered wing, a swept tapered wing and a delta wing, described in [10, 11, 12, 13].
- **NASATMX72799**: Flutter solution for the flat plate swept wing with and without winglets described in [14].
- **NASATND344**: Steady and unsteady pressure calculation for the rectangular wing forced to oscillate in [15].
- **NASATM84367**: Steady pressure calculation for the swept wing described in [16].
- **PAPA**: Flutter solution for the rectangular NACA 0012, NACA 64A010 and BSCW wings tested by NASA on the Pitch and Plunge Apparatus (PAPA) described in [17, 18, 19].
- **T-tail**: Flutter solution for the rectangular Van Zyl T-tail described in [20, 21, 22].
- **Theodorsen**: Flutter solution for a 2D infinitely thin flat plate airfoil with pitch and plunge degrees of freedom at incompressible conditions and comparison to Theodorsen theory results [23].

The filename of each of the run files ends with the name of the test case. When the file is run, it calls functions in the `Common` directory; it may also call functions in the test case directory and load data from `.mat` files in the test case directory.

The structure of each run file is the following:

1. Load libraries, C functions and data types.
2. Define flight conditions.
3. Input geometries for all bodies in the flow.
4. Optional: Input structural models for all bodies.
5. For each of the selected flight conditions:
 - Calculate the steady aerodynamic pressures and loads at prescribed values of the Mach number, angle of attack and angle of sideslip.
 - Optional: For each of the selected reduced frequencies calculate the unsteady aerodynamic pressures derivatives with respect to rigid-body or flexible motion coordinates.
 - Optional: Carry out flutter analysis to calculate the flutter speed and frequency.
6. Plot results.

4.1 Geometry definition

Only wing geometry definitions are included in the current distribution; fuselage definitions will be included in a future release. Wings are defined using trapezoidal sections, defined in the `tp_trap` data type. Each element of `tp_trap` is a trapezoidal section with the following parameters:

- **rootchord**: The chord length of the root of the current trapezoidal section.
- **xledist**: The chordwise distance of the root of the current trapezoidal section to the tip of the previous trapezoidal section.
- **span**: The span of the current trapezoidal section.
- **taper**: The taper ratio of the current trapezoidal section, i.e. the ratio of the tip chord to the root chord of the trapezoidal section.
- **sweepLE**: The sweep angle at the leading edge of the current trapezoidal section.
- **roottwist**: The twist angle at the root of the current trapezoidal section.
- **tiptwist**: The twist angle at the tip of the current trapezoidal section.
- **twistcent**: The non-dimensional chordwise position of the axis around which the wing is twisted, taking values between 0 and 1.
- **dihedral**: The dihedral angle of the current trapezoidal section.
- **rootairfoil**: The name of the root airfoil of the current trapezoidal section. This name must be a function defined in `Common/airfoils.py`. If your airfoil is not already defined (most likely), you need to write a function for it in `Common/airfoils.py`.
- **rootairfoilparams**: The parameters of the root airfoil. These depend on the airfoil type and its definition; they may be thickness, camber, NACA number etc. For NACA four- and five-digit airfoils the parameter `teclosed` determines the thickness of the trailing edge. If `teclosed=0`, the original thickness equation is used and the trailing edge thickness is finite. If `teclosed=1`, a modified thickness equation is used and the trailing edge thickness is zero.
- **tipairfoil**: The name of the tip airfoil of the current trapezoidal section. The root and tip airfoils are interpolated linearly to obtain the airfoil shape in between.
- **tipairfoilparams**: The parameters of the tip airfoil.

There can be any number of trapezoidal sections; new sections are needed when any of the parameters defined in `tp_trap` change. The root and tip airfoil and their parameters can be identical. The SDPM grid for the complete wing is created using the parameters for all trapezoidal sections by calling function `SDPMgeometry_trap_fun` in package `SDPMgeometry.py` with the following inputs:

- **body**: Structured array of type `tp_body` (see later) holding the SDPM grid information for all bodies present in the flow.
- **ibody**: The index of `body` for which the SDPM grid is to be calculated.
- **m**: Number of chordwise panels on the upper surface of the wing. There will be another `m` panels on the lower side for a total of `2*m` panels. The value of `m` is constant for all trapezoidal sections.
- **mw**: Number of chordwise panels in the wake. This is calculated as `mw=m*nchords`, where `nchords` is the length of the wake in root chord lengths. Recommended value: `nchords=10`.
- **nhalf**: Number of spanwise panels on the half-wing (semispan wing). If a full-span wing is requested (`mirroredwing=2`, see later), there will be another `nhalf` on the other half for a total of `2*nhalf` panels.
- **mirroredwing**: How to arrange the wing. Each wing is initially created as a right half-wing (semispan wing). If `mirroredwing=-1` it is changed to a left half-wing. If `mirroredwing=1` it remains a right half-wing. If `mirroredwing=2` a full-span wing is created by mirroring the right half-wing to the left.
- **linchord**: The distribution of chordwise panels. if `linchord=0` the distribution will be such that panel density is highest around the leading edge and lowest around the trailing edge. If `linchord=1` the chordwise distribution will have constant density.
- **linspan**: The distribution of spanwise panels. if `linspan=0` the distribution will be such that panel density is highest near the wingtip and root. If `linspan=1` the spanwise distribution will have constant density.
- **trap**: Structured array of type `tp_trap` containing the geometrical information for all trapezoidal sections for the current wing.
- **name**: The name of the wing. This is not important for the calculation, it only helps identify the wing when more than one wings are defined.
- **dir_tau**: Direction in which the unit tangent vector for this wing has a zero component. `dir_tau=1` denotes the x direction and is suitable for fuselages. `dir_tau=2` denotes the y direction and is suitable for horizontal wings. `dir_tau=3` denotes the z direction and is suitable for vertical wings and fins.
- **rollpitchyaw**: A three-element vector containing angles by which to roll, pitch and yaw the complete wing. To define a fin, set:
`rollpitchyaw=np.array([0, 0, 90])*np.pi/180`
Do not use `rollpitchyaw` to impose a dihedral angle, use the `dihedral` parameter of the `tp_trap` data type instead.
- **rollpitchyaw_cent**: The point around which the rotations defined in `rollpitchyaw` are performed.

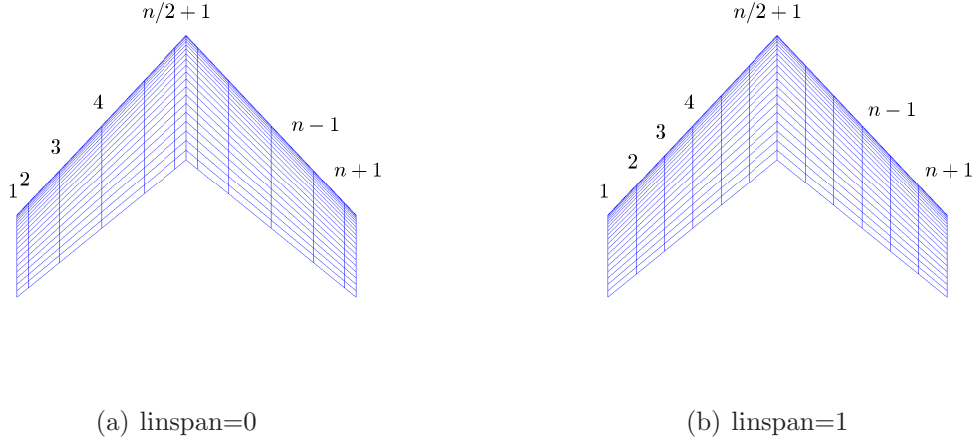


Figure 2: Spanwise panel numbering and distributions

axis system is different to the usual body-fixed axes used in flight dynamics, whereby the x axis points upstream and the z axis downwards. Finally, the figure also plots a section of the wake model; the wake panels are attached to the lower trailing edge segments of their corresponding wing panels and extend downstream in the x direction. The chordwise spacing of the panels is set to c_0/m , where c_0 is the wing's root chord.

The geometries of all the bodies of a particular test case are stored in an array of type `tp_body`. Each element of this array type contains the following data:

- **m**: Number of chordwise panels on the upper surface of the wing.
- **n**: Number of spanwise panels on the upper surface of the wing. This number is set by function `SDPMgeometry_trap_fun`, depending on the values of `nhalf`, `nmin` and `mirroredwing`.
- **mw**: Number of chordwise panels in the wake.
- **Xp0, Yp0, Zp0**: $(2m + 1) \times (n + 1)$ matrices containing the x, y, z coordinates of the wing panel vertices in cartesian coordinates.
- **Xc0, Yc0, Zc0**: $2m \times n$ matrices containing the x, y, z coordinates of the wing panel control points (centroids) in cartesian coordinates.
- **Xc0all, Yc0all, Zc0all**: $2mn \times 1$ vectors containing the x, y, z coordinates of the wing panel control points (centroids) in cartesian coordinates.
- **Xw0, Yw0, Zw0**: $(m_w + 1) \times (n + 1)$ matrices containing the x, y, z coordinates of the wake panel vertices in cartesian coordinates.
- **nx0, ny0, nz0**: $2m \times n$ matrices containing the x, y, z components of unit vectors normal to the wing panels and pointing outwards in cartesian coordinates.

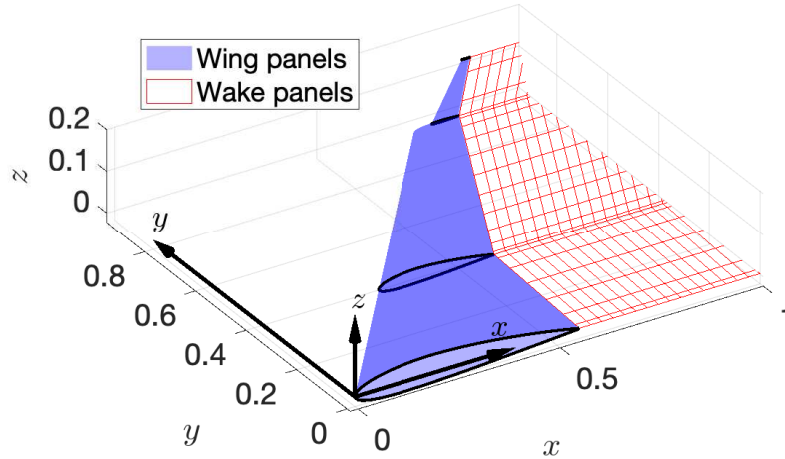


Figure 3: Coordinate system used by SDPMflut

- $\mathbf{nx0all}$, $\mathbf{ny0all}$, $\mathbf{nz0all}$: $2mn \times 1$ vectors containing the x , y , z components of unit vectors normal to the wing panels and pointing outwards in cartesian coordinates.
- $\mathbf{s0}$: $2m \times n$ matrix containing the surface areas of the wing panels in cartesian coordinates.
- $\mathbf{s0all}$: $2mn \times 1$ vector containing the surface areas of the wing panels in cartesian coordinates.
- $\mathbf{c0}$: A reference chord length, currently it is the root chord.
- \mathbf{b} : The total span, calculated from the trapezoidal section information stored in array `trap`.
- \mathbf{S} : The planform area, calculated from the trapezoidal section information stored in array `trap`.
- \mathbf{AR} : Aspect ratio of the full-span wing.
- \mathbf{Xp} , \mathbf{Yp} , \mathbf{Zp} : $(2m + 1) \times (n + 1)$ matrices containing the ξ , η , ζ coordinates of the wing panel vertices in Prandtl-Glauert coordinates.
- \mathbf{Xc} , \mathbf{Yc} , \mathbf{Zc} : $2m \times n$ matrices containing the ξ , η , ζ coordinates of the wing panel control points (centroids) in Prandtl-Glauert coordinates.
- \mathbf{Xcall} , \mathbf{Ycall} , \mathbf{Zcall} : $2mn \times 1$ vectors containing the ξ , η , ζ coordinates of the wing panel control points (centroids) in Prandtl-Glauert coordinates.

- X_w, Y_w, Z_w : $(m_w + 1) \times (n + 1)$ matrices containing the ξ, η, ζ coordinates of the wake panel vertices in Prandtl-Glauert coordinates.
- nx, ny, nz : $2m \times n$ matrices containing the ξ, η, ζ components of unit vectors normal to the wing panels and pointing outwards in Prandtl-Glauert coordinates.
- $nx_{all}, ny_{all}, nz_{all}$: $2mn \times 1$ vectors containing the ξ, η, ζ components of unit vectors normal to the wing panels and pointing outwards in Prandtl-Glauert coordinates.
- s : $2m \times n$ matrix containing the surface areas of the wing panels in Prandtl-Glauert coordinates.
- s_{all} : $2mn \times 1$ vector containing the surface areas of the wing panels in Prandtl-Glauert coordinates.
- $tauxx, tauxy, tauxz$: $2m \times n$ matrices containing the ξ, η, ζ components of unit vectors tangent to the wing panels in Prandtl-Glauert coordinates. These vectors are aligned according to the value of `dir_tau`.
- $tauyx, tauyy, tauyz$: $2m \times n$ matrices containing the ξ, η, ζ components of another set of unit vectors tangent to the wing panels in Prandtl-Glauert coordinates. These vectors are orthogonal to vectors nx, ny, nz and $tauxx, tauxy, tauxz$.
- tmx, tmy, tmz : $2m \times n$ matrices containing the ξ, η, ζ components of unit vectors tangent to the wing panels and pointing in the chordwise direction in Prandtl-Glauert coordinates.
- tnx, tny, tnz : $2m \times n$ matrices containing the ξ, η, ζ components of unit vectors tangent to the wing panels and pointing in the spanwise direction in Prandtl-Glauert coordinates.
- sm, sn : $2m \times n$ matrices containing the mean chordwise and spanwise lengths, respectively, of the wing panels in Prandtl-Glauert coordinates.
- X_{cw}, Y_{cw}, Z_{cw} : $m_w \times n$ matrices containing the ξ, η, ζ coordinates of the wake panel control points (centroids) in Prandtl-Glauert coordinates.
- nx_w, ny_w, nz_w : $m_w \times n$ matrices containing the ξ, η, ζ components of unit vectors normal to the wake panels and pointing upwards in Prandtl-Glauert coordinates.
- $tauxx_w, tauxy_w, tauxz_w$: $m_w \times n$ matrices containing the ξ, η, ζ components of unit vectors tangent to the wake panels in Prandtl-Glauert coordinates. These vectors are aligned according to the value of `dir_tau`.
- $tauyx_w, tauyy_w, tauyz_w$: $m_w \times n$ matrices containing the ξ, η, ζ components of another set of unit vectors tangent to the wake panels in Prandtl-Glauert coordinates. These vectors are orthogonal to vectors nx_w, ny_w, nz_w and $tauxx_w, tauxy_w, tauxz_w$.

- **cp0**: $2m \times n$ matrix containing the steady pressure coefficients on the wing panels.
- **Fx0, Fy0, Fz0**: $2m \times n$ matrices containing the x, y, z components of the aerodynamic forces acting on the wing panels in Newtons per Pascal. In order to obtain the aerodynamic forces in Newtons they must be multiplied by the free stream dynamic pressure. In order to obtain the forces in force coefficient form they must be divided by the reference area.
- **Mx0, My0, Mz0**: $2m \times n$ matrices containing the aerodynamic moments acting on the wing panels around the x, y, z axes in Newton meters per Pascal. In order to obtain the aerodynamic moments in Newtons they must be multiplied by the free stream dynamic pressure and a reference length. In order to obtain the moments in moment coefficient form they must be divided by the reference area.
- **mu0**: $2m \times n$ matrix containing the steady doublet strengths on the wing panels.
- **muw0**: $2m \times n$ matrix containing the steady doublet strengths on the wake panels.
- **Phi_xall, Phi_yall, Phi_zall**: $2mn \times K$ vectors containing the modal translations in the x, y, z directions at the wing panel control points.
- **Phi_phiall, Phi_thetaall, Phi_psi**: $2mn \times K$ vectors containing the modal rotations around the x, y, z axes at the wing panel control points.

Function `SDPMgeometry_trap_fun` calculates all quantities in cartesian coordinates. All quantities in Prandtl-Glauert coordinates are calculated by function `PGtransform` in package `SDPMcalcs.py`. The steady aerodynamic calculations are carried out in the run file. The modal translations and rotations are calculated by function `SDPMmodeinterp` in package `FEmodes.py`.

5 Structural model input

The structural model is composed of the $K \times K$ structural modal matrices \mathbf{A} , \mathbf{C} , \mathbf{E} and the $N_{FE} \times K$ mode shape matrices $\Phi_x, \Phi_y, \Phi_z, \Phi_\phi, \Phi_\theta, \Phi_\psi$ calculate on a finite element grid defined by the $N_{FE} \times 1$ vectors $\mathbf{x}_{FE}, \mathbf{y}_{FE}$ and, optionally, \mathbf{z}_{FE} . Currently, two types of mode shapes are used in `SDPMflut`:

- **Beam mode shapes**: Translation and rotation mode shapes of beams with coordinates $\mathbf{x}_{FE}, \mathbf{y}_{FE}, \mathbf{z}_{FE}$. This type of mode shape is used in test case `T_tail/flutter_SDPMTtail.py`.
- **Plate mode shapes**: Translation and rotation mode shapes of flat plates with coordinates $\mathbf{x}_{FE}, \mathbf{y}_{FE}, \mathbf{z}_{FE}$, with $\mathbf{z}_{FE} = 0.0$. This type of mode shape is used in all other flexible flutter test cases.

The mode shapes in all the test cases are normalized such that the mass matrix \mathbf{A} is the unit matrix. The damping and stiffness matrices are calculated by functions `FE_matrices` or `FE_matrices_beam` in package `FEmodes.py`, which takes the following inputs:

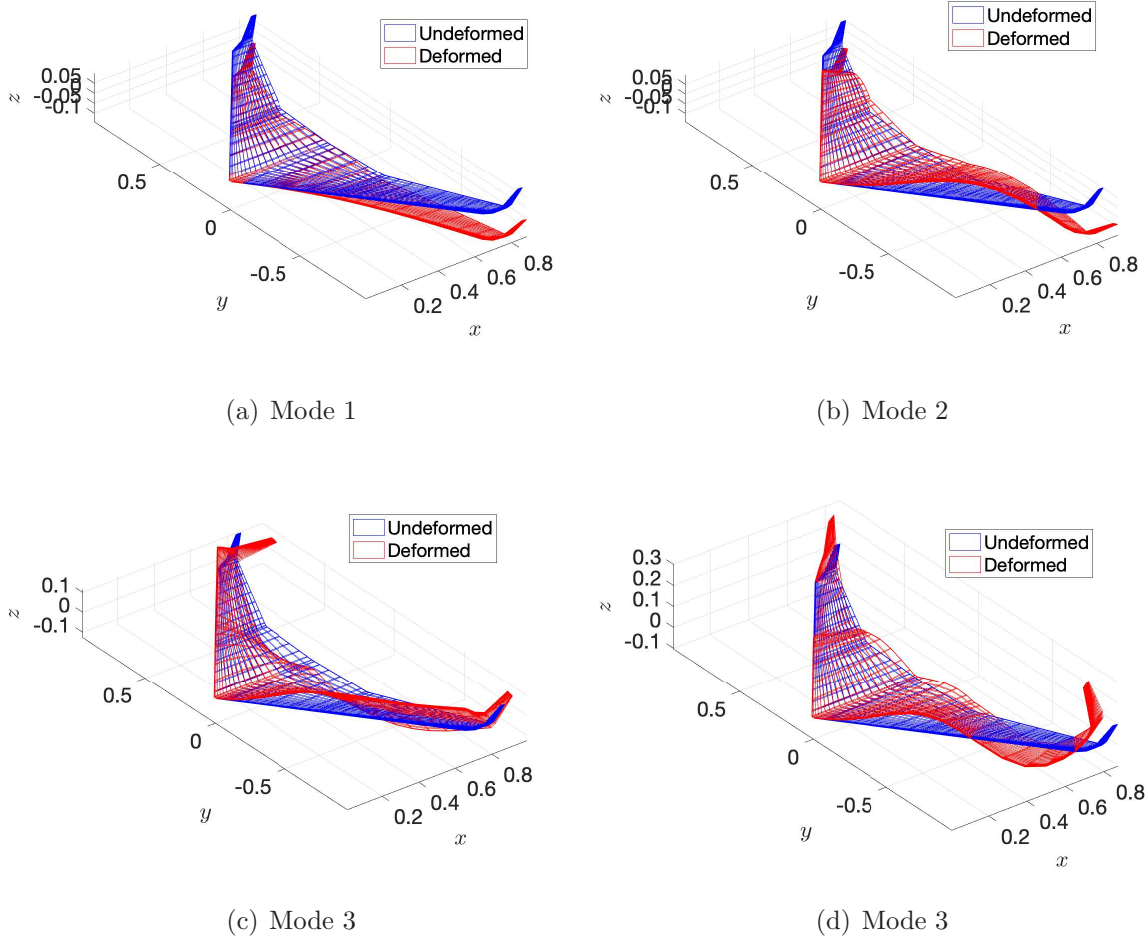


Figure 4: First four mode shapes of the NASA TMX 72799 wing with heavy winglet.

- **fname**: The name of a `.mat` file in the current working directory that contains the structural mass and stiffness matrices, \mathbf{A} and \mathbf{E} , as well as Φ_x , Φ_y , Φ_z , Φ_ϕ , Φ_θ , Φ_ψ , \mathbf{x}_{FE} , \mathbf{y}_{FE} and \mathbf{z}_{FE} . Currently, the only means for inputting structural information to `SDPMflut` is by means of Matlab `.mat` files. Future versions will introduce other input methods.
- **nmodes**: The number of modes, K , selected by the user for the flutter analysis. The maximum number of modes is the number of modes contained in **fname**. Fewer modes can be specified.
- **zeta0**: A 1D array with **nmodes** elements containing the values of the structural damping ratios corresponding to each mode.

Once the modal matrices and mode shapes have been acquired, the latter are interpolated onto the SDPM grids of all the bodies in the flow using function `SDPMmodeinterp` in package `FEmodes.py`, except for test case `T_tail/flutter_SDPM_Ttail.py` for which

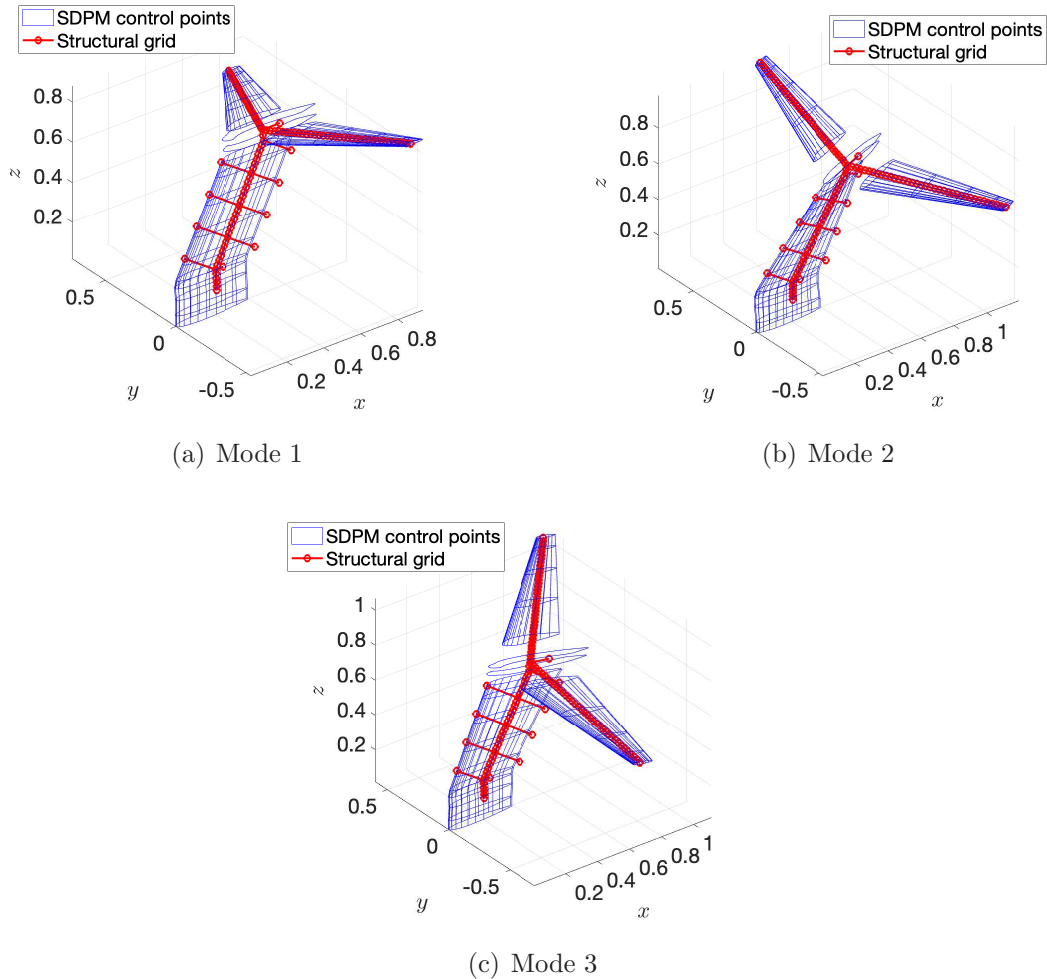


Figure 5: T-tail deformed parallel to the first three mode shapes[3].

function `ttailmodesinterp` in package `VanZylTtail.py` is used instead. Currently, function `SDPMmodeinterp` works only for single wings with flat plate mode shapes. The wings are cantilevered at the root so that the mode shapes are defined on the right half-wing, on a x - y grid with N_{FE} nodes. These mode shapes are interpolated onto the mean surface (camber surface) of the right-hand side of the SDPM grid using 2D scattered data cubic interpolation, with respect to the x and y coordinates of the mean surface. The interpolated mode shapes are mirrored to the left half-wing and applied to both the upper and lower surfaces. Figure 4 plots the first four mode shapes of the NASA TMX 72799 wing with heavy winglet, corresponding to test case `flutter_SDPM_NASATMX72799.py` with option `winglet=3`. It can be seen that the interpolated mode shapes are symmetric across the $y = 0$ plane. Mode 1 is mostly first wing bending, mode 2 second wing bending with a bit of first wing torsion, mode 3 second wing torsion with a bit of winglet bending and mode four third wing bending with a bit of torsion.

Function `ttailmodesinterp` works for all the components of the Van Zyl T-tail (fin, left and right horizontal tailplanes and fin fairing) and beam mode shapes. The T-

tail structural model is cantilevered at the root of the fin beam. The mode shapes are interpolated separately onto the fin, tailplanes and fin fairing using radial basis functions. The interpolation is carried out directly onto the two surfaces of each body, using x and z control point coordinates for the fin and fin fairing and x and y control point coordinates for the two tailplanes. Only the nodes of the structural model that are relevant to each body are used in the interpolations. Figure 5 plots the T-tail deformed parallel to the first three modes, comparing the deformed structural grid to the deformed SDPM grid.

6 Input file

Every SDPMflut input file starts with setting the value of `install_dir` to tell Python where to look for the files in `./Common`. Next, the necessary libraries and data types are imported:

```
# Input installation directory
install_dir=r"/Users/Username/Documents/Python/SDPMflut_v0.5/Common/"
# Import libraries and packages
import numpy as np
import matplotlib.pyplot as plt
import sys
sys.path.append(install_dir)
from SDPMgeometry import SDPMgeometry_trap_fun
import flutsol
import FEmodes
import SDPMcalcs
# Acquire SDPMflut trap and body data types
tp_trap, tp_body, _=SDPMcalcs.SDPMdtypes()
```

Additional libraries can be imported, depending on the needs of each project.

The next step is to define the flight conditions for the SDPMflut analysis. The minimum set of variables that need to be defined are:

- **Machdata**: The free stream Mach number.
- **rhodata**: The free stream density.
- **alpha0**: The steady (or mean) angle of attack
- **beta0**: The steady (or mean) angle of sideslip

Each of these variables can be a scalar or an array with `nruns` elements, where `nruns` is the desired number of runs of the SDPMflut analysis at different flight conditions. Note that different runs can be defined not only in terms of flight conditions, but also in terms of some geometric or structural parameter(s), such as the tailplane incidence in example `T_tail`. The units used in SDPMflut can SI or imperial, as long as they are consistent. All angles must given in rad and all frequencies in rad/s.

Next, the geometries of all the bodies present in the flow are defined. The first step is to set the number of bodies and to initialize the `body` structured array:

```

# Set number of bodies
nbody=1
# Initialize body struct array
body=np.zeros(nbody,dtype=tp_body)

```

Then, the geometry of each body must be inputted, starting with:

```

# Input first body
ibody=0          # Index of body
name='wing'     # Name of body
# Choose numbers of panels for this wing and its wake
nhalf=10        # Number of spanwise panels per half-wing.
m=20            # Number of chordwise panels
nchords=10      # Set length of wake in chord lengths
# Calculate number of chordwise wake rings
mw=m*nchords
# Set number of trapezoidal sections for this wing
ntrap=1
# Initialize trapezoidal section struct array
trap=np.zeros(ntrap,dtype=tp_trap)

```

These lines tell the software which body is being defined, what is its desired grid size and how many trapezoidal sections are necessary for its definition. The array `trap` is initialized and values for all of its fields must be given, as defined in section 4.1. Then, the geometric data of each trapezoidal section, are inputted into the `trap` array.

```

# Arrange all data into trapezoidal sections
trap[0]=np.array([(c0,xledist,bhalf,lamda,LamdaLE,roottwist,tiptwist,
    twistcent,dihedral,rootairfoil,rootairfoil_params,tipairfoil,
    tipairfoil_params)],dtype=tp_trap)

```

The panel aspect ratio, `panelAR`, can be defined for a complete body or for a trapezoidal section. For a complete wing, it is recommended that the panel aspect ratio should not take values less than 0.1; 2D test cases do not have to conform to this recommendation. The input files in the test cases check for this using:

```

# Calculate panel aspect ratio
panelAR=(c0/m)/(bhalf/nhalf)
if panelAR < 0.1:
    sys.exit('Panel aspect ratio too low. Increase n or decrease m.')
```

The user can remove these lines, they only serve as a warning.

Finally, the SDPM grid for body `ibody` is generated:

```

# Calculate vertices of wing panels
body=SDPMgeometry_trap_fun(body,ibody,m,mw,nhalf,mirroredwing,linchord,
    linspan,trap,name,dir_tau,rollpitchyaw,rollpitchyaw_cent,lexyz,nmin)

```

where all of the inputs to function `SDPMgeometry_trap_fun` must be set beforehand, as detailed in section 4.1. Once the SDPM grids for all bodies have been generated, the software will calculate the numbers and indices of panels, spanwise panels and wake panels in all bodies stored in struct array `body` and create structured array `allbodies`:

```
# Assemble the indices of the body panels, spanwise body panels, wake
# panels etc. for all bodies.
allbodies=SDPMcalcs.allbodyindex(body)
```

Array `allbodies` is of type `tp_allbodies` and contains only outputs of the software. It is a placeholder for information taken from all the bodies present in the flow. Six of its fields contain flow information that is not available elsewhere:

- `barphix0, barphiy0, barphiz0`: Normalized steady perturbation velocities at the control points of all the panels of all the bodies.
- `baruc0, barvc0, barwc0`: Normalized steady total velocities (including the free stream) at the control points of all the panels of all the bodies.

The other fields in `allbodies` concerning flow quantities (e.g. `cp0`) can also be found in the elements of `body`.

The next step is to carry out the desired analysis: there are three analysis types:

1. Calculation of steady aerodynamic pressures, surface velocities and loads on the control points of the panels of all the bodies.
2. Calculation of unsteady aerodynamic pressures, surface velocities and loads on the control points of the panels of all the bodies. This analysis requires the steady aerodynamic calculation.
3. Calculation of the flutter speed and frequency. This analysis requires both steady and unsteady aerodynamic calculations.

Each of the analysis will be demonstrated separately by means of the relevant test cases that come with the software.

6.1 Steady aerodynamic analysis

Once the flight conditions and body geometries have been defined, steady aerodynamic analysis is carried out by typing:

```
# Calculate steady aerodynamic pressures and loads
body,allbodies,Aphi,Bphi,Cphi,barUinf,barVinf,barWinf=
    SDPMcalcs.steadysolve(body,allbodies,cp_order,Mach,beta,alpha0,
        beta0,xf0,yf0,zf0,install_dir)
```

where `xf0, yf0, zf0` are the Cartesian coordinates of a point around which rotations and/or moments are to be calculated. This point can be the centre of gravity or any rotation axis; `xf0, yf0, zf0` can all be set to 0.0 if no rotations or moments are to be calculated. Function `SDPMcalcs.steadysolve` calculates:

1. `barUinf,barVinf,barWinf`: the non-dimensional free stream components, $\bar{U}_\infty, \bar{V}_\infty, \bar{W}_\infty$, of equation 21
2. the Prandtl-Glauert transformation of equation 3 for all geometries
3. `Pe0,Pc`: the matrices $\mathbf{P}_e(0)$ in equation 15 and \mathbf{P}_c in equation 6
4. `Aphi,Bphi,Cphi`: the steady aerodynamic influence coefficient matrices, $\mathbf{A}_\phi, \mathbf{B}_\phi, \mathbf{C}_\phi$, in equation 13
5. `mu0`: the steady doublet strength on the body panels, $\bar{\boldsymbol{\mu}}(0) = \boldsymbol{\mu}(0)/Q_\infty$, from equations 12, 13 and 14
6. `muw0`: the steady doublet strength on the wake panels, $\bar{\boldsymbol{\mu}}_w(0) = \boldsymbol{\mu}_w(0)/Q_\infty$, from equation 5 for $k = 0$
7. `barphix0,barphiy0,barphiz0`: the steady perturbation velocities on the body panels, $\bar{\phi}_x(0) = \phi_x(0)/Q_\infty, \bar{\phi}_y(0) = \phi_y(0)/Q_\infty, \bar{\phi}_z(0) = \phi_z(0)/Q_\infty$, from equations 16
8. `baruc0,barvc0,barwc0`: the steady total velocities on the body panels, $\bar{\mathbf{u}}(0) = \mathbf{u}(0)/Q_\infty, \bar{\mathbf{v}}(0) = \mathbf{v}(0)/Q_\infty, \bar{\mathbf{w}}(0) = \mathbf{w}(0)/Q_\infty$, from equation 17
9. `cp0`: the steady pressure coefficient on the body panels, \mathbf{c}_{p0} , from equation 20
10. `Fx0,Fy0,Fz0`: the steady aerodynamic loads per dynamic pressure on the body panels, $\mathbf{F}_x(0), \mathbf{F}_y(0), \mathbf{F}_z(0)$, from equation 26

The function returns `barUinf,barVinf,barWinf` and `Aphi,Bphi,Cphi` directly to the input function's workspace so that they can be used in subsequent analyses. The variables `barphix0,barphiy0,barphiz0, baruc0,barvc0,barwc0, cp0, Fx0,Fy0,Fz0` and `Mx0,My0,Mz0` are stored in the respective fields of the `allbodies` structured array. For each of the bodies, the variables `mu0, muw0, cp0, Fx0,Fy0,Fz0` and `Mx0,My0,Mz0` are extracted, reshaped into $2m \times n$ matrices and stored in the respective fields of the respective element of the `body` structured array.

The NASATM84367 test case is an example of a purely steady aerodynamic analysis of a wing at different Mach numbers and angles of attack. The input file is

```
steady_SDPM_NASATM84367.py
```

and the different flight conditions are entered as numpy arrays:

```
# Free stream Mach number. The last two test cases are highly transonic
Machdata=np.array([0.501, 0.499, 0.601, 0.601, 0.695, 0.695, 0.794,
                   0.793])
# Mean angle of attack in degrees
alpha0data=np.array([0.0, 2.0, -2.0, 2.0, -2.0, 2.0, 2.0,
                    -2.0])*np.pi/180.0
# Total number of runs
nruns=Machdata.size
```

The experimental pressure measurements are loaded from the data file `dataNASATM84367`:

```
# Load experimental pressure data from .mat file
mat = scipy.io.loadmat("dataNASATM84367.mat")
```

The geometry input is carried out as described in section 6. Then, `SDPMcalcs.steadysolve` is called for each of the `nruns` runs:

```
print('Calculating flutter solutions for all experimental test cases')
for irun in range (0,nruns):
    print('Simulating run '+str(irun+1))

    # Set Mach number of current run
    Mach=Machdata[irun]
    # Set mean angle of attack
    alpha0=alpha0data[irun]
    # Calculate subsonic compressibility factor
    beta=np.sqrt(1-Mach**2)

    # Calculate steady aerodynamic pressures and loads
    body,allbodies,Aphi,Bphi,Cphi,barUinf,barVinf,barWinf=
        SDPMcalcs.steadysolve(body,allbodies,cp_order,Mach,beta,alpha0,
            beta0,0.0,0.0,0.0,install_dir)

    fig, axx = plt.subplots(subplot_kw={"projection": "3d"})
    # Plot SDPM pressure predictions
    axx.plot_surface(body['Xc0'][0][:,body['n'][0]//2:body['n'][0]],
        body['Yc0'][0][:,body['n'][0]//2:body['n'][0]],
        body['cp0'][0][:,body['n'][0]//2:body['n'][0]],
        edgecolor='royalblue',alpha=0.1)
    # Plot experimental pressure measurements
    axx.scatter(mat['x0data'],mat['y0data'],mat['cp0data'][:,irun],
        marker='o',color='r')
    axx.set_proj_type('ortho') # FOV = 0 deg
    axx.set_zlim(-1,0.6)
    axx.set_xlabel("$x/c_0$", labelpad=10)
    axx.set_ylabel("$y/b$", labelpad=10)
    axx.set_zlabel("$c_p(0)$", labelpad=-1)
    axx.view_init(26, -120)
    plt.show()
# End for
```

All the lines after the call to `SDPMcalcs.steadysolve` plot the pressure distribution around the half-wing, stored in `body['cp0'][0]` against the x and y coordinates of the panel control points, `body['Xc0'][0]`, `body['Yc0'][0]`. Note that `body['Xc0'][0]`, `body['Yc0'][0]` describe a full-span wing geometry; the right half-wing is contained in the columns of these arrays that have indices from $n/2$ to $n - 1$.

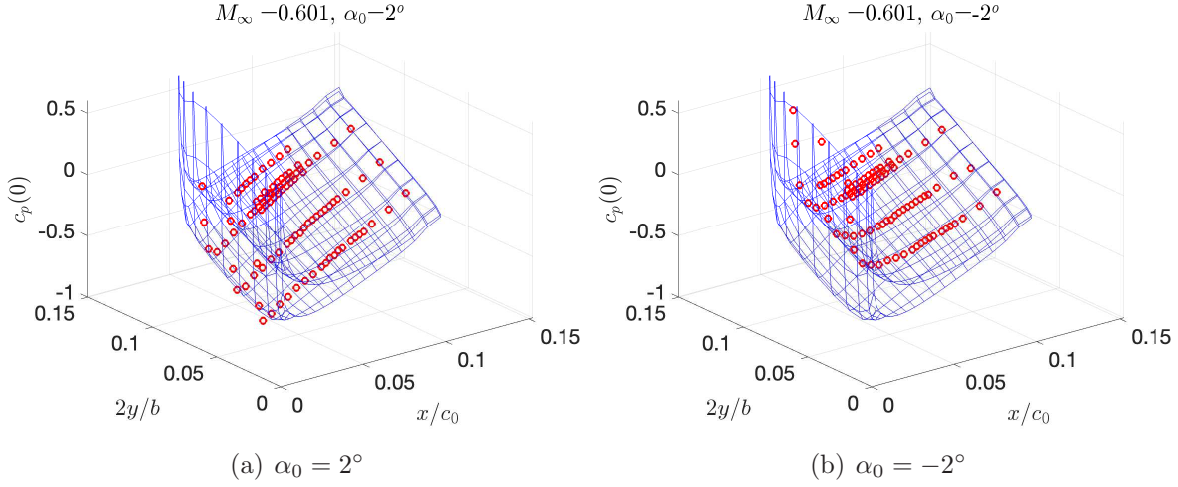


Figure 6: Steady pressure distributions for the NASATM8436 test case at $M_\infty = 0.6$

The pressure distributions calculated by the SDPM are compared to the experimental pressure measurements for each run. Pressure tappings were only installed on the upper surface of the wing, which is a suction surface for positive angles of attack and a pressure surface for negative angles of attack. Figure 6 plots the predicted and measured pressure distributions at $M_\infty = 0.6$ for $\alpha_0 = 2^\circ$ and $\alpha_0 = -2^\circ$ ¹. The experimental pressures are denoted by the red circles, which lie on the suction side on figure 6(a) and on the pressure side on figure 6(b). The SDPM predictions are quite accurate at this Mach number; at $M_\infty = 0.8$ there is a strong shock wave on the suction side that cannot be modelled by the SDPM.

The aerodynamic loads per dynamic pressure (dimensions of length squared) are stored in `body['Fx0'] [0]`, `body['Fy0'] [0]`, `body['Fz0'] [0]` as matrices with the same dimensions as `body['Xc0'] [0]`, `body['Yc0'] [0]`, `body['Zc0'] [0]`. To obtain the aerodynamic loads in force units type:

```
Fx0_dimensional=body['Fx0'] [0]*0.5*rhoinf*Qinf**2
Fy0_dimensional=body['Fy0'] [0]*0.5*rhoinf*Qinf**2
Fz0_dimensional=body['Fz0'] [0]*0.5*rhoinf*Qinf**2
```

where `rhoinf` is the free stream density, ρ_∞ , and `Qinf` the free stream airspeed, Q_∞ ; both must be defined before the calculation. To obtain aerodynamic load coefficients in the x , y and z directions type:

```
CX0=body['Fx0'] [0]/body['S'] [0]
CY0=body['Fy0'] [0]/body['S'] [0]
CZ0=body['Fz0'] [0]/body['S'] [0]
```

The total lift and drag coefficients acting on the wing are obtained from:

```
CL=np.sum(CZ0)*np.cos(alpha0)-np.sum(CX0)*np.sin(alpha0)
CD=np.sum(CZ0)*np.sin(alpha0)+np.sum(CX0)*np.cos(alpha0)
```

¹The figures in this document were plotted in Matlab and not Matplotlib.

6.2 Unsteady aerodynamic analysis

Unsteady aerodynamic analyses are carried out after the steady analysis. The only requirements are the definition of the motion kinematics of all the bodies and the input of a value for the reduced frequency, k , of the motion. The motion can be rigid translation and rotation around a given rotation centre or flexible and parallel to give mode shapes. Test case NASATND344 is an example of the latter; a rectangular wing was placed in the wind tunnel and forced to oscillate in bending around its first bending mode shape, with imposed amplitude and frequency. The test case input file, `unsteady_SDPM_NASATND344.py`, includes

```
# Bending tip amplitude (m)
bendtip_amp=0.2*0.0254
# Bending phase (rad)
Phi_bend=0.0
```

where `bendtip_amp` is the bending oscillation amplitude at the wingtip and `Phi_bend` is the phase angle of the oscillation, such that `Phi_bend=0.0` means that the motion is a pure cosine function of time. In the frequency domain, the displacement of the wingtip in the z direction at frequency k is given by

```
bendtip_amp/2.0*np.exp(1j*Phi_bend)
```

The bending mode shape, Φ_z , is created on a structural grid with `mFE` chordwise and `nFE` spanwise points,

```
# Choose number of modes to include in the flutter calculation
nmodes=1 # The wing was forced to oscillate in the first bending mode
# Set up structural modal grid
mFE=30 # Set desired number of chordwise points
nFE=30 # Set desired number of spanwise points
# Acquire mode shapes (only modeshapesz and its derivative modeshapesRx
# are non-zero)
xxplot,yyplot,modeshapesx,modeshapesy,modeshapesz,modeshapesRx,
    modeshapesRy,modeshapesRz=modes_NASATND344(mFE,nFE)
```

such that Φ_z is 0 at the root and 1 at the tip. It is assumed that there is no torsion, so that Φ_z is constant in the chordwise direction. As only bending was imposed, $\Phi_x = \Phi_y = \Phi_\psi = 0$. Consequently,

$$\Phi_\phi = -\frac{\partial\Phi_z}{\partial y}, \quad \Phi_\theta = -\frac{\partial\Phi_z}{\partial x}$$

Since Φ_z is constant in the chordwise direction, $\Phi_\theta = 0$, so that only Φ_ϕ and Φ_z are non-zero. Function `modes_NASATND344` returns in $m_{FE}n_{FE} \times 1$ arrays:

- `xxplot,yyplot`: The x and y coordinates of the structural grid.
- `modeshapesx,modeshapesy,modeshapesz`: The translation components of the mode shape, Φ_x , Φ_y , Φ_z .

- `modeshapesRx,modeshapesRy,modeshapesRz`: The rotation components of the mode shape, $\tilde{\Phi}_\phi, \tilde{\Phi}_\theta = 0, \tilde{\Phi}_\psi$.

Function `unsteady_SDPM_NASATND344.py` interpolates the components of the mode shape onto the SDPM grid, once have been acquired, using

```
# Interpolate mode shapes onto panel control points
body=FEmodes.SDPMmodeinterp(xxplot,yyplot,modeshapesx,modeshapesy,
    modeshapesz,modeshapesRx,modeshapesRy,modeshapesRz,body)
```

Function `FEmodes.SDPMmodeinterp` takes the x and y cartesian coordinates of the panel control points from `body['Xc0'][0]`, `body['Yc0'][0]`. The interpolation is carried out onto the mean surface (camber surface) of the right half-wing; it is then assigned to both the upper and lower surfaces and mirrored across the centreline of the wing. The interpolated mode shape components are $2mn \times 1$ arrays stored in struct array `body`:

- `body['Phi_xall'][0],body['Phi_yall'][0],body['Phi_zall'][0]`: The interpolated translation components of the mode shape, $\tilde{\Phi}_x, \tilde{\Phi}_y, \tilde{\Phi}_z$.
- `body['Phi_phiall'][0],body['Phi_thetaall'][0],body['Phi_psiall'][0]`: The interpolated rotation components of the mode shape, $\tilde{\Phi}_\phi, \tilde{\Phi}_\theta, \tilde{\Phi}_\psi$.

The next step in `unsteady_SDPM_NASATND344.py` is to concatenate the mode shape components for all the bodies:

```
# Assemble mode shapes for all bodies into global matrices
allbodies=SDPMcalcs.modeshape_assemble(body,allbodies,nmodes)
```

In the present case there is only one body so the only result of this operation is the copying of `body['Phi_xall'][0]`, `body['Phi_yall'][0]`, etc, into `allbodies['Phi_x'][0]`, `allbodies['Phi_y'][0]` etc.

For each of the experimental runs, the Mach number, reduced frequency, angle of attack, subsonic compressibility factor and effective angle of attack at the wingtip are set:

```
# Set Mach number of current run
Mach=Machdata[irun]
# Set reduced frequency
k=kdata[irun]
# Set mean angle of attack
alpha0=alpha0data[irun]
# Calculate subsonic compressibility factor
beta=np.sqrt(1-Mach**2);
# Calculate effective angle of attack at the wingtip
alpha_h=2.0/c0*k*bendtip_amp
```

where `irun` is the index of the current run. Next, the steady aerodynamic calculation is carried out

```

# Calculate steady aerodynamic pressures and loads
body,allbodies,Aphi,Bphi,Cphi,barUinf,barVinf,barWinf=
    SDPMcalcs.steadysolve(body,allbodies,cp_order,Mach,beta,alpha0,
        beta0,0.0,0.0,0.0,install_dir)

```

and the steady pressure distribution is plotted and compared to experimental data. Then, the unsteady aerodynamic analysis is carried out:

```

# Calculate the unsteady pressure coefficients
cp1,cp_0,cp_1,cp_2=SDPMcalcs.unsteadysolve_flex(body,allbodies,Aphi,
    Bphi,Cphi,barUinf,barVinf,barWinf,k,c0,Mach,beta,cp_order,
    install_dir)

```

Function `SDPMcalcs.unsteadysolve_flex` calculates the oscillatory pressure distribution for flexible motion using the mode shapes stored in array `body`. The function first calculates the non-dimensional frequency $\Omega = 2kM_\infty/c_0\beta$ and then the wake double strength decay matrix $\mathbf{P}_e(k)$ of equation 7, before computing the unsteady aerodynamic influence coefficient matrices using:

```

# Calculate unsteady influence coefficient matrices
Abarphi,Bbarphi,Cbarphi=unsteady_infcoef(body,allbodies,install_dir,
    Omega,Mach,Aphi,Bphi,Cphi)

```

where `Abarphi`, `Bbarphi`, `Cbarphi` are the matrices $\hat{\mathbf{A}}_\phi(k)$, $\hat{\mathbf{B}}_\phi(k)$, $\hat{\mathbf{C}}_\phi(k)$ appearing in equations 9. Then, it evaluates the matrices $\mathbf{K}(k)$, $\mathbf{K}_x(k)$, $\mathbf{K}_y(k)$, $\mathbf{K}_z(k)$ in equations 9 to 10, followed by the matrices $\mathbf{C}_0(k)$ and $\mathbf{C}_1(k)$ in equation 19. Finally, the function outputs the pressure derivative arrays `cp1`, `cp_0`, `cp_1`, `cp_2`, which have size `allbodies['allpanels'] × nmodes` and are given by

$$\begin{aligned}
 \mathbf{c}_{p_0}(k) &= \mathbf{c}_{p_\phi}(k) + \mathbf{c}_{p_\theta}(k) + \mathbf{c}_{p_\psi}(k) \\
 \mathbf{c}_{p_1}(k) &= \mathbf{c}_{p_{\dot{x}}}(k) + \mathbf{c}_{p_{\dot{y}}}(k) + \mathbf{c}_{p_z}(k) + \mathbf{c}_{p_{\dot{\phi}}}(k) + \mathbf{c}_{p_{\dot{\theta}}}(k) + \mathbf{c}_{p_{\dot{\psi}}}(k) \\
 \mathbf{c}_{p_2}(k) &= \mathbf{c}_{p_{\ddot{x}}}(k) + \mathbf{c}_{p_{\ddot{y}}}(k) + \mathbf{c}_{p_{\ddot{z}}}(k)
 \end{aligned}$$

where $\mathbf{c}_{p_\phi}(k)$, $\mathbf{c}_{p_\theta}(k)$ etc. appear in equation 25. The function also outputs the total pressure derivative array `cp1`, which has the same dimensions and is $\mathbf{c}_p(k)$ and is given by

$$\mathbf{c}_{p_0}(k) + ik\mathbf{c}_{p_1}(k) + (ik)^2\mathbf{c}_{p_2}(k) \quad (33)$$

Finally, `unsteady_SDPM_NASATND344.py` calculates $\mathbf{c}_p(k)$ in equation 25 by multiplying `cp1` by the tip bending amplitude:

```

# Multitply cp1 by tip bending amplitude and reshape to a matrix
cp1mat=bendtip_amp/2.0*np.exp(1j*Phi_bend)*np.reshape(cp1,
    (2*body['m'] [0],body['n'] [0]),order='C')

```

The array `cp1mat` has dimensions $2m \times n$ and is complex. It is the required oscillatory pressure distribution acting on the panel control points due to the imposed bending motion. The test case input file also calculates the pressure jump across the surface, $\Delta\mathbf{c}_p(k)$.

```
# Calculate pressure jump across the surface
Dcp1=np.flipud(cp1mat[0:m,:])-cp1mat[m:2*m,:]
```

The final step is to plot the real and imaginary parts of the unsteady pressure distribution and to compare them to experimental data. The original reference gives this data only for the $M_\infty = 0.24$ cases. Figure 7 plots the real and imaginary parts of the pressure distribution for $M_\infty = 24$, $\alpha_0 = 5^\circ$ and compares them to the experimental measurements. For all the Mach numbers, only the pressure jump distribution is given so this is what is plotted by `unsteady_SDPM_NASATND344.py`. Note that there are strong shock waves in the steady pressure distributions at $M_\infty = 0.9$ and $M_\infty = 0.7$ ($\alpha_0 = 5^\circ$ case), which also have an effect on the unsteady pressure jump distributions.

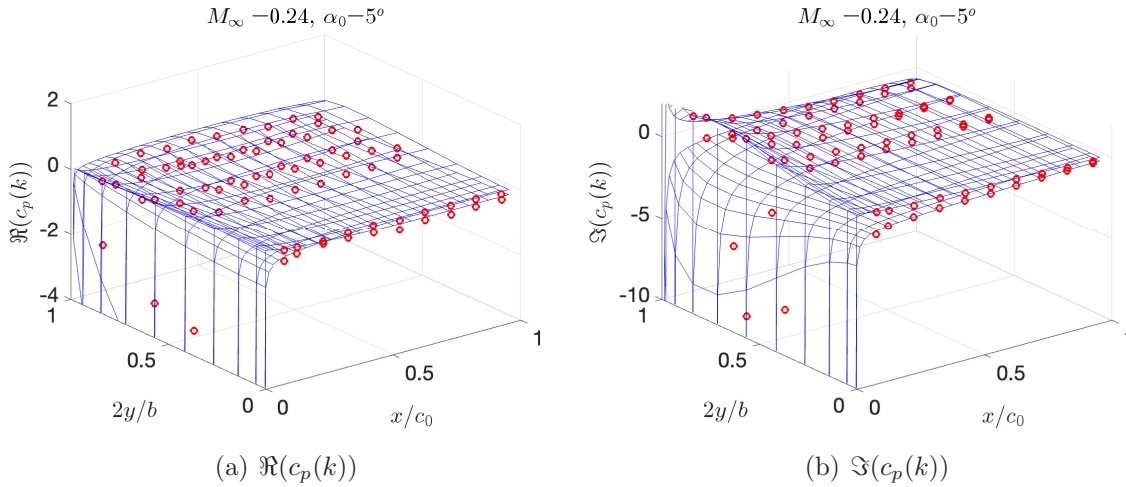


Figure 7: Real and imaginary parts of the pressure distribution for the NASATND344 test case at $M_\infty = 24$, $\alpha_0 = 5^\circ$

6.3 Calculation of aerodynamic stability derivatives

Test case NACARML5 calculates the lateral aerodynamic stability derivatives of a Delta, a straight, and a swept wing and compares them to experimentally determined values given in [10, 11, 12, 13]. Each of the wings has its own input file, `unsteady_SDPM_delta.py`, `unsteady_SDPM_straight.py` and `unsteady_SDPM_swept.py`. The analysis starts as usual, with the input of the flight conditions, the description of the wing geometry and the generation of the SDPM grid. Since the lateral stability derivatives are of interest, the straight and swept wings feature wingtips that block the lateral flow through the wing. The SDPM grid is created as follows:

```
# Calculate vertices of wing panels
body=SDPMgeometry_trap_fun(body,ibody,m,mw,nhalf,mirroredwing,linchord,
    linspan,trap,name,dir_tau,rollpitchyaw,rollpitchyaw_cent,lexyz,nmin)
# Calculate vertices of wingtip panels
body=makewingtips(body,ibody,mirroredwing)
```

Function `makewingtips` adds one or two new elements in structured array `body`, containing the SDPM grid coordinates of left and right wingtips attached to `body[ibody]`. The number of wingtips depends on the value of `mirroredwing`; if `mirroredwing=-1` a left wingtip is added, if `mirroredwing=1` a right wingtip is added and if `mirroredwing=2` both left and right wingtips are added. Figure 8 plots an example of a left wingtip added to the straight wing. Wingtip objects are identical in structure to all other `body` objects but they do not shed a wake, such that `mw=0`. The wingtip vertex matrices `Xp0`, `Yp0`, `Zp0` have $2m + 1$ lines, where m is the number of chordwise panels in the parent wing, and 3 columns:

- : Left wingtip: lower surface, mid surface and upper surface
- Right wingtip: upper surface, mid surface and lower surface

Consequently, wingtips have $2m$ chordwise and 2 heightwise panels. Aside from not shedding wakes, they are treated like all other elements of the `body` struct array.

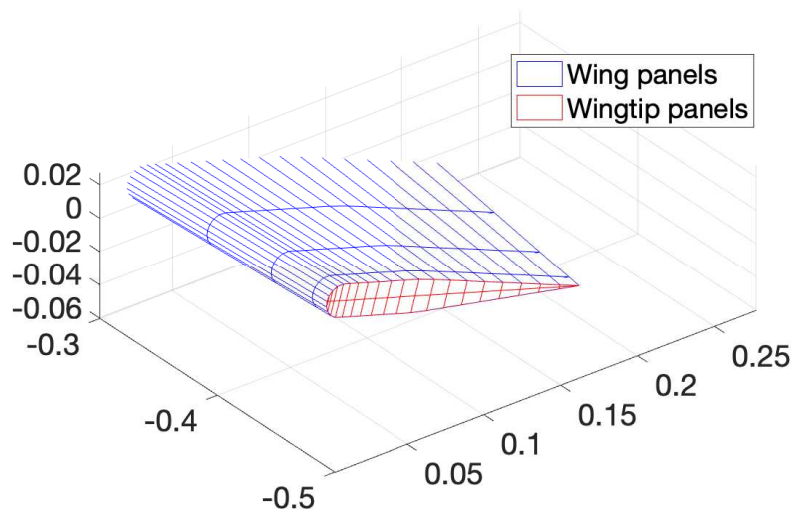


Figure 8: Wing and wingtip panels

The NACARML5 test cases calculate all the aerodynamic stability derivatives at a single reduced frequency, $k_b = \omega b / 2Q_\infty = 0.23$, where $b/2$ is the half-span, and a range of steady pitch angles. In order to simulate as closely as possible the experiments, the free stream angles of attack and sideslip are set to zero but the wing itself is rotated to the desired pitch angle, around the quarter of the mean aerodynamic chord. The rotation is carried by calling `SDPMgeometry_trap_fun` after setting

```
# Recreate the body at the current pitch angle value
# Define roll, pitch and yaw angles
```

```

rollpitchyaw=np.array([0, pitchdata[irun], 0])
# Define roll, pitch and yaw centre (x,y,z position of rotation centre)
rollpitchyaw_cent=np.array([xf0, yf0, zf0])

```

thus regenerating the SDPM grid at the current pitch angle, `pitchdata[irun]`. Then, the wingtips are recalculated to fit the new wing grid and `SDPMcalcs.steadysolve` is called to solve the steady flow at the current pitch angle. Recall that `SDPMflut` calculates forces and moments in Newtons per Pascal and Newton meters per Pascal respectively. These are converted to steady load coefficients by

```

# Calculate steady aerodynamic load coefficients on the panels
CD[irun]=np.sum(body['Fx0'][0])/Sref
CY[irun]=np.sum(body['Fy0'][0])/Sref
CL[irun]=np.sum(body['Fz0'][0])/Sref
Cl[irun]=np.sum(body['Mx0'][0])/Sref/bref
Cm[irun]=np.sum(body['My0'][0])/Sref/cref
Cn[irun]=np.sum(body['Mz0'][0])/Sref/bref

```

where `Sref` is the reference area, `bref` the reference span, `cref` the reference chord, `CD` is the drag coefficient, `CY` the sideforce coefficient, `CL` the lift coefficient, `Cl` the rolling moment coefficient, `Cm` the pitching moment coefficient and `Cn` the yawing moment coefficient.

For compatibility with the rest of the code, k_b is converted to the reduced frequency based on the half-chord

```

# Convert reduced frequency based on half-span
# to reduced frequency based on half-chord
k=kvec[ik]/bhalf*c0/2.0

```

The derivatives of the pressure with respect to the degrees of freedom are evaluated using equations 64 to 78. Both the pressure derivatives and the aerodynamic stability derivatives are calculated by function `SDPMcalcs.aerostabderiv`:

```

# Calculate aerodynamic stability derivatives
stabder=SDPMcalcs.aerostabderiv(body,allbodies,Aphi,Bphi,Cphi,barUinf,
    barVinf,barWinf,k,c0,Mach,beta,cp_order,xf0,yf0,zf0,Sref,bref,
    cref,install_dir)

```

The aerodynamic stability derivatives are stored in structure array `stabder`, of type `tp_stabder`. This array contains 21 longitudinal derivatives, from `CXu` to `Cmqdot`, and 24 lateral derivatives, from `CYv` to `Cnrndot`. Given the definitions of $\bar{v}(k)$ and $\bar{\dot{v}}(k)$ in appendix B, it can be shown that

$$C_{Y_\beta} = -C_{Y_v}, \quad C_{Y_{\dot{\beta}}} = -C_{Y_{\dot{v}}}, \quad C_{l_\beta} = -C_{l_v}, \quad C_{l_{\dot{\beta}}} = -C_{l_{\dot{v}}}, \quad C_{n_\beta} = -C_{n_v}, \quad C_{n_{\dot{\beta}}} = -C_{n_{\dot{v}}}$$

As an example, figure 9 plots the variation of the roll and yaw aerodynamic stability derivatives with respect to \bar{r} and β with steady pitch angle for the straight wing. The agreement between the SDPM predictions and experimental data is very good up to pitch

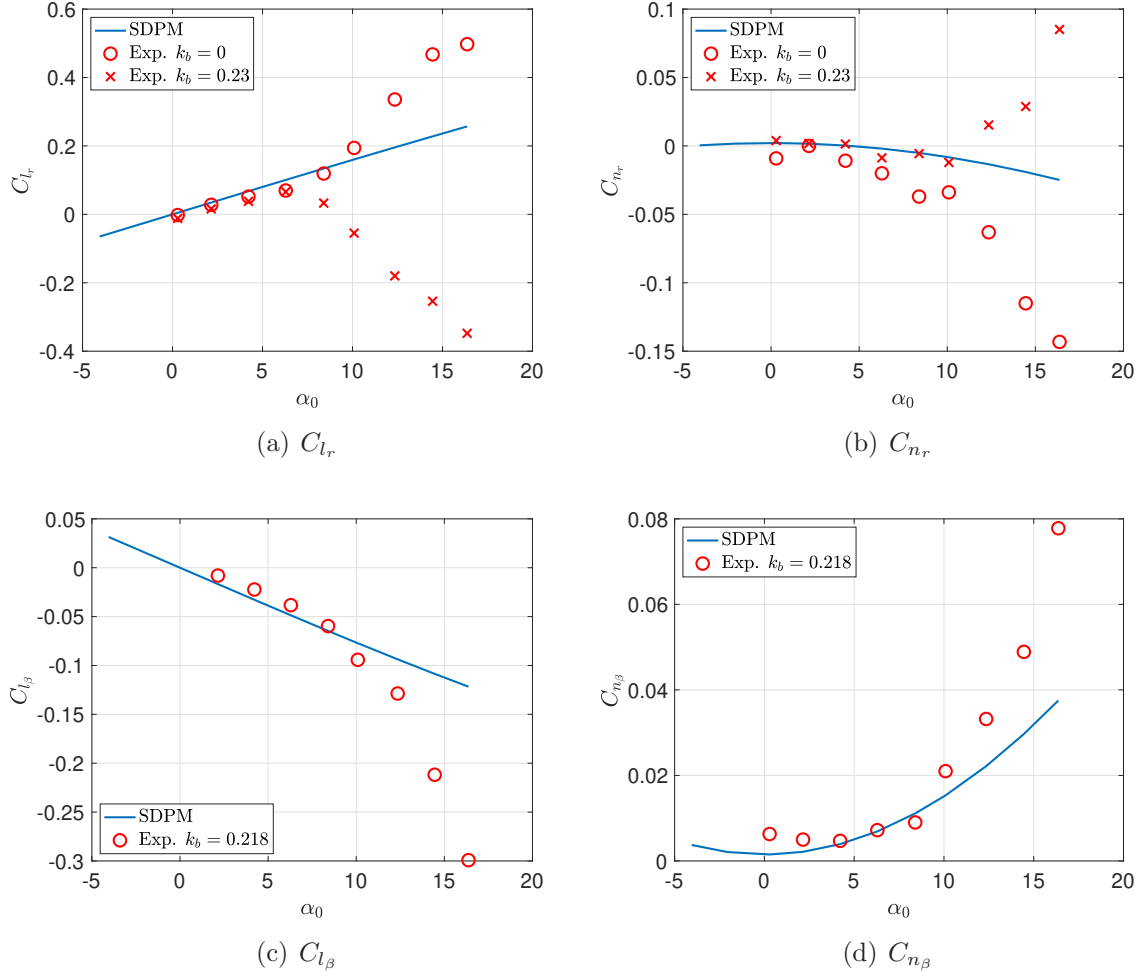


Figure 9: Variation of aerodynamic stability derivatives with steady pitch angle for the straight wing

angle values of around 8° . At higher angles, viscous phenomena become very important and the inviscid SDPM cannot predict them. For compatibility with the experimental data, only the real parts of the aerodynamic derivatives are plotted; the imaginary parts are very small compared to the real parts at this value of the reduced frequency.

The measured aerodynamic stability derivatives with respect to accelerations \dot{r} and $\dot{\beta}$ are quite flat at low pitch angles; it is only at the higher pitch angles that significant values are observed. The SDPM predicts very small values for these derivatives at all pitch angles. Finally, it should be noted that the sideslip derivatives predicted by the SDPM are less accurate than the roll and yaw derivatives.

6.4 Flutter analysis for flexible wings

The contents of an input file for flutter analysis are fairly similar to those of an input file for unsteady analysis. There are three flutter cases of flexible structures in the current

SDPM distribution:

- flutter_SDPM_AGARD.py
- flutter_SDPM_NASATMX72799.py
- flutter_SDPM_Ttail.py

The input files starts as usual but the `flutsol` package must also be imported. The definition of flight conditions and the input of the geometry are carried out as usual. The structural model is loaded from a `.mat` file, whose name is stored in `fname`, e.g.

```
# File name of Matlab mat file that contains the structural model
fname='modes_AGARD_Q4EPM.mat'
# Choose number of modes to include in the flutter calculation
nmodes=5 # Cannot exceed number of modes in FE model
zeta0=0.02*np.ones(nmodes) # Structural damping ratios
# Parameter to determine if the structural model concerns a half wing or a
# full wing.
halfwing=1 # halfwing=1: half-wing. halfwing=0: full wing
```

File `modes_AGARD_Q4EPM.mat` contains the `nmodes`×`nmodes` arrays `Mmodal` and `Kmodal`, the `mFE`×`nFE`× coordinate arrays `xxplot`, `yyplot`, and the `mFE`×`nFE`×`nmodes` mode shape arrays `modeshapesx`, `modeshapesy`, `modeshapesz`, `modeshapesRx`, `modeshapesRy`, `modeshapesRz`. The file is read using:

```
# Acquire structural matrices and mode shapes
A, C, E, wn, xxplot, yyplot, zzplot, modeshapesx, modeshapesy, modeshapesz,
    modeshapesRx, modeshapesRy, modeshapesRz=
    FEmodes.FE_matrices(fname,zeta0,nmodes)
```

Function `FEmodes.FE_matrices` also truncates the modal matrices and mode shapes to the first `nmodes` modes, sets the off-diagonal terms of the modal matrices to exactly zero², calculates the damping matrix given the wind-off structural damping ratios `zeta0`, and calculates the first `nmodes` natural frequencies, outputting them to array `wn`.

The user must also define the reduced frequencies and airspeeds at which to carry out the flutter analysis, e.g.:

```
# Select reduced frequency values
kvec=np.array([0.001, 0.01, 0.1, 0.2, 0.3, 0.4, 0.5, 0.7, 1.0, 2.0])

# Select airspeed range in m/s
Uv=np.linspace(100,400,num=101)
```

The values in `kvec` and `Uv` must be informed by the physics of the problem. The minimum value in $k = 0.001$ is probably adequate for most applications but the maximum value depends on the highest wind-off natural frequency, lowest airspeed and characteristic chord length. In other words:

²The modal matrices obtained from finite element packages are not always exactly diagonal, the off-diagonal terms may be non-zero but very small.

```
kmax=np.max(wn)*c0/2.0/np.min(Uv)
```

This calculation is not carried out by `SDPMflut` because the user may wish to select an even higher maximum value for k . The reduced frequency values must be denser towards the lowest range; flutter in aircraft occurs generally at $k < 1$ and often at $k < 0.4$. The airspeed range in `Uv` must be selected by trial and error, unless the flutter airspeed is known or suspected. For a complete aircraft, the entire speed range in the flight envelope can be assigned to `Uv`.

The only other difference between a flutter analysis input file and an unsteady analysis input file is the calling of the flutter solution function, e.g.:

```
Uflut,freqflut,kflut,dynpressflut,omega,zeta=
flutsol.flutsolve_flex(body,allbodies,kvec,Uv,
nmodes,Aphi,Bphi,Cphi,barUinf,barVinf,barWinf,c0,
Mach,beta,cp_order,A,C,E,rho,wn,halfwing,install_dir)
```

Function `flutsol.flutsolve_flex` starts with calculating the steady generalized aerodynamic load vector, $\mathbf{Q}_0(0)$, given by

$$\mathbf{Q}_0(0) = - \left(\tilde{\Phi}_x^T \mathbf{F}_x(0) + \tilde{\Phi}_y^T \mathbf{F}_y(0) + \tilde{\Phi}_z^T \mathbf{F}_z(0) \right)$$

where $\mathbf{F}_x(0)$, $\mathbf{F}_y(0)$, $\mathbf{F}_z(0)$ are defined in equation 26. If the structural model is a half-wing, it will divide $\mathbf{Q}_0(0)$ by two so that only the aerodynamic loads from one half-wing will be included in the aeroelastic equation. Currently, $\mathbf{Q}_0(0)$ is not used in any of the test cases included with `SDPMflut` but it could be used to carry out steady aeroelastic analysis by solving the steady version of equation 28

$$\left(\mathbf{E} - \frac{1}{2} \rho_\infty Q_F^2 \mathbf{Q}_0(0) \right) \mathbf{q}(0) = \frac{1}{2} \rho_\infty Q_F^2 \mathbf{Q}_s(0)$$

for the modal displacements $\mathbf{q}(0)$ induced by the steady aerodynamic loads. The procedure can also be iterative, deforming the SDPM geometry by $\tilde{\Phi}_x \mathbf{q}(0)$, $\tilde{\Phi}_y \mathbf{q}(0)$, $\tilde{\Phi}_z \mathbf{q}(0)$ and then re-calculating all the steady and unsteady aerodynamic influence coefficients and the generalized aerodynamic load vector and matrices.

The next step in `flutsol.flutsolve_flex` is to call

```
# Calculate the unsteady pressure coefficients
cp1,cp_0,cp_1,cp_2=SDPMcalcs.unsteadysolve_flex(body,allbodies,
Aphi,Bphi,Cphi,barUinf,barVinf,barWinf,k,c0,Mach,beta,
cp_order,install_dir)
```

to obtain the unsteady pressures and to calculate $\mathbf{Q}_0(k)$, $\mathbf{Q}_1(k)$, $\mathbf{Q}_2(k)$ using equations 29 and 30, for all specified values of the reduced frequency k . Once the loop for k has finished executing, if `halfwing=1`, all generalized aerodynamic load matrices are divided by 2. Then, the determinant iteration procedure of equation 31 is applied to evaluate the wind-on natural frequencies and damping ratios at all selected airspeeds:

```

# Calculate eigenvalues using determinant iteration
eigvals=detiterfun(A,C,E,Q_0,Q_1,Q_2,kvec,Uv,c0/2,rho,wn)
# Calculate natural frequencies and damping ratios
omega=np.absolute(eigvals)
zeta=-eigvals.real/np.absolute(eigvals)

```

where ω is a $n_{\text{modes}} \times \text{len}(Uv)$ array storing the natural frequencies, $\omega_n = |\lambda|$, and ζ is an array of the same size storing the damping ratios,

$$\zeta_n = \frac{-\Re(\lambda)}{|\lambda|}$$

If any of the damping ratios become negative within the airspeed range, a function will be called to pinpoint exactly the flutter condition by solving the determinant problem of equation 32:

```

# Calculate exact flutter velocity and frequency
Uflut,freqflut=flutfind(A,C,E,Q_0,Q_1,Q_2,kvec,Uini,c0/2.0,rho,wini)
# Calculate flutter reduced frequency
kflut=freqflut*c0/2.0/Uflut
# Calculate flutter dynamic pressure
dynpressflut=1/2.0*rho*Uflut**2.0

```

where U_{ini} and w_{ini} are initial guesses for the flutter velocity and frequency obtained from the crossing of ζ to negative values. The converged values for the flutter speed and frequency are stored in U_{flut} , $freq_{flut}$ respectively. The function also calculates the reduced flutter frequency, k_{flut} , and the flutter dynamic pressure, $dynpress_{flut}$ before returning.

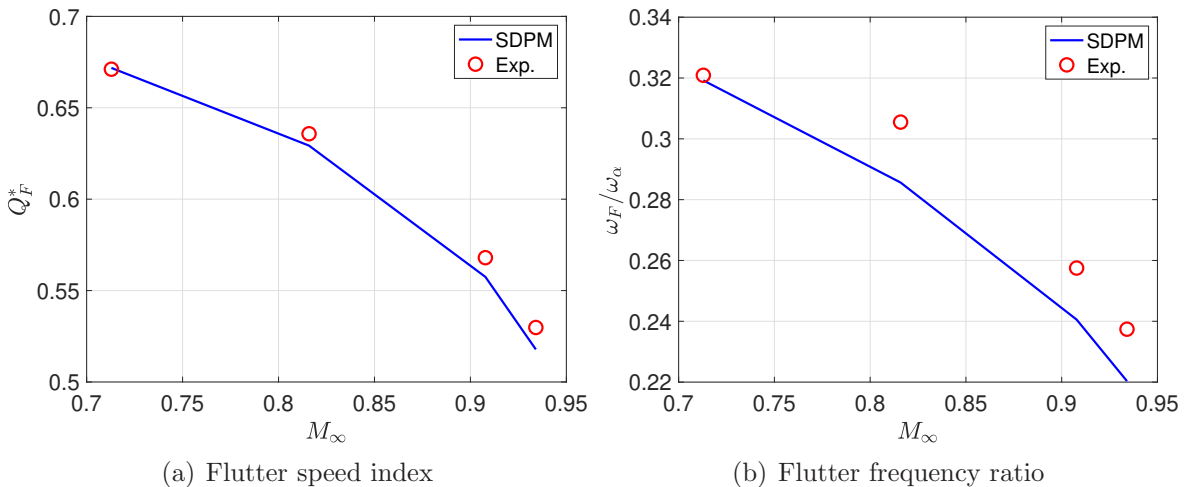


Figure 10: Variation of flutter speed index and flutter frequency ratio with Mach number for the NASATMX72799 test case with heavy winglets

Finally, the input file calculates the flutter speed index,

$$Q_F^* = \frac{Q_F}{(c_0/2)\omega_\alpha\sqrt{\mu}}$$

where ω_α is usually the first wind-off torsional natural frequency and μ is the mass ratio, i.e. the ratio of a mass of air enclosing a body to the mass of the body. Then, it plots the flutter results for all the runs. For example, figure 10 plots the variation of flutter speed index and flutter frequency ratio with Mach number for the NASATMX72799 test case with heavy winglets.



(a) T-tail fin fairing and horizontal tailplanes

(b) Exploded view

Figure 11: SDPM grids for the fin fairing and horizontal tailplanes

The `T_tail` case is particular in that there are many bodies in the flow and, more importantly, the horizontal tailplane is in contact with the fin fairing. When using panel methods, bodies that are in contact but do not share exactly the same contact vertices can cause significant numerical instabilities. The solution adopted in this test case is to create the fin fairing SDPM grid after creating that of the two tailplanes, such that the former shares the root vertices of the latter. As the angle of incidence of the horizontal tailplane varies between runs, the geometry is finalized inside the loop for `irun`; only the SDPM grid of the vertical fin is created before this loop. Figure 11 plots the SDPM grids for the horizontal tailplanes and fin fairing only, as well as an exploded view of these elements. It can be seen that the fin fairing is split into two bodies, the upper and lower fairings, so that its grid can be accommodated into 2D arrays. Each half of the fairing has $2m$ chordwise panels on the right side and another $2m$ on the left, while the horizontal tailplanes have m chordwise panels on the upper surface and m on the lower. The right half of the upper fairing shares m vertices with the upper surface of the right tailplane and the left half of the upper fairing shares m vertices with the upper surface of the left tailplane. Similarly, lower fairing shares vertices with the lower halves of the two tailplanes.

The other specificity of the `T_tail` test case is that it uses a dedicated mode interpolation function, instead of the one found in `Common`, that is:

```
# Interpolate mode shapes
body=VanZylTtail.ttai modesinterp(body,z_root_tip,nmodes,xxplot,yyplot,
    zzplot,modeshapesx,modeshapesy,modeshapesz,modeshapesRx,
    modeshapesRy,modeshapesRz)
```

There are two reasons for this specificity:

- The mode shapes are beam modes; when interpolating them onto surfaces there is quite a lot of extrapolation. This means that radial basis function interpolation is necessary to avoid NaNs when using SciPy.
- Different parts of the mode shapes are used when interpolating on different bodies; the nodes of the mode shape lying on $y = 0$ are used for the fin and fin fairing while the nodes lying on $y \neq 0$ are used for the tailplanes.

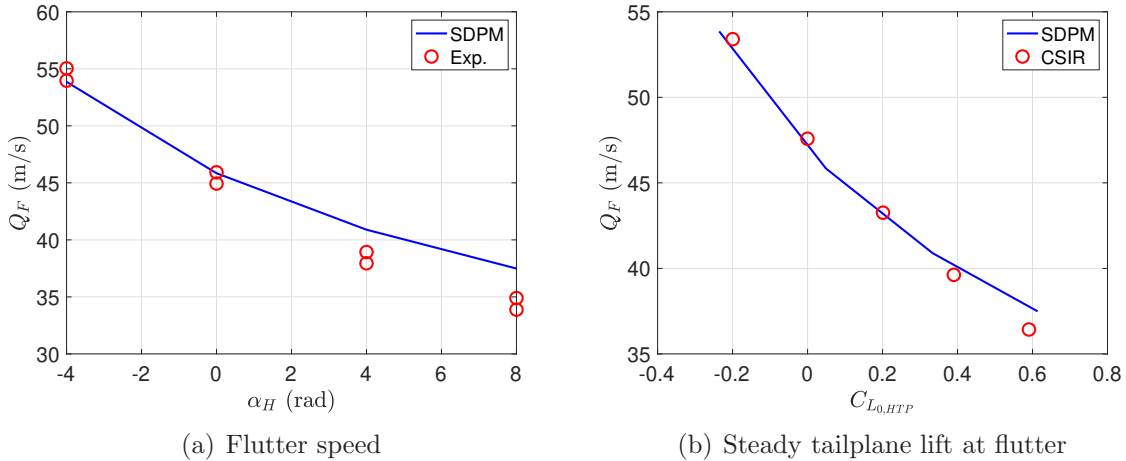


Figure 12: Variation of flutter speed with tailplane incidence and steady tailplane lift at flutter for the Van Zyl T-tail test case

The rest of the `flutter_SDPM_Ttail.py` input file is similar to the AGARD and NASA TMX72799 input files, except that the experimental flutter frequencies are not given in the original references. Figure 12 plots the variation of the dimensional flutter speed with tailplane incidence, as well as its variation with steady tailplane lift coefficient. Note that the CSIR data plotted in figure 12(b) are not experimental; they were obtained using a modelling method by [20].

6.5 Flutter analysis for pitching and plunging wings

The three test cases in the PAPA folder are rigid rectangular wings of exactly the same dimensions but with different airfoil sections, suspended from the same Pitching and Plunging Apparatus. The input files are identical except for the wind tunnel test conditions, airfoil sections and mass/stiffness characteristics. The difference with the flexible

flutter test cases discussed in section 6.4 is that dedicated functions are used for calculating the unsteady aerodynamic pressures and flutter solutions. The normalized upwash due to the motion is given by a simplified version of equations 22,

$$\begin{aligned}\bar{\mathbf{u}}_m(k) &= -\frac{q(k)}{Q_\infty}(\mathbf{z}_c - z_f) \\ \bar{\mathbf{v}}_m(k) &= 0 \\ \bar{\mathbf{w}}_m(k) &= \theta(k) + \frac{q(k)}{Q_\infty}(\mathbf{x}_c - x_f) - \frac{w(k)}{Q_\infty}\end{aligned}\tag{34}$$

where all the terms due to longitudinal, lateral, roll and yaw motion have been removed and x_f, y_f, z_f is the position of the pitch axis. Consequently, the unsteady pressure is given by a shorter version of equations 24, namely

$$\begin{aligned}\mathbf{c}_p(k) &= \mathbf{c}_{p_w}(k)w(k) + \mathbf{c}_{p_\theta}(k)\theta(k) + \mathbf{c}_{p_q}(k)q(k) + ik\mathbf{c}_{p_{\dot{w}}}(k)w(k) \\ &\quad + ik\mathbf{c}_{p_{\dot{q}}}(k)q(k)\end{aligned}$$

The pitch and plunge aeroelastic equations [23] are written in terms of the pitch displacement, $\alpha(k) = \theta(k)$, and plunge displacement $h(k)$, such that $q(k) = ik\alpha(k)$ and $w(k) = ikh(k)$. Substituting into the equation for the oscillatory pressure yields

$$\begin{aligned}\mathbf{c}_p(k) &= ik\mathbf{c}_{p_{\dot{h}}}(k)h(k) + \mathbf{c}_{p_\alpha}(k)\alpha(k) + ik\mathbf{c}_{p_{\dot{\alpha}}}(k)\alpha(k) + (ik)^2\mathbf{c}_{p_{\ddot{h}}}(k)h(k) \\ &\quad + (ik)^2\mathbf{c}_{p_{\ddot{\alpha}}}(k)\alpha(k)\end{aligned}\tag{35}$$

where expressions for the pressure derivatives $\mathbf{c}_{p_{\dot{h}}}(k), \mathbf{c}_{p_\alpha}(k)$, etc. are given in [4]. The aerodynamic load and moment derivatives around the pitch axis are given by

$$\begin{aligned}\mathbf{F}_{z_\alpha}(k) &= -\mathbf{c}_{p_\alpha}(k) \circ \mathbf{s} \circ \mathbf{n}_z \\ \mathbf{M}_{y_\alpha}(k) &= -\mathbf{F}_{z_\alpha}(k) \circ (\mathbf{x}_c - x_f)\end{aligned}$$

and similarly for the derivatives with respect to $\dot{h}, \dot{\alpha}, \ddot{h}, \ddot{\alpha}$. Consequently, the generalized aerodynamic stiffness, damping and mass matrices are given by

$$\begin{aligned}\mathbf{Q}_0(k_0) &= \begin{pmatrix} 0 & -\sum_{i=1}^N \mathbf{F}_{z_\alpha}(k_0) \\ 0 & \sum_{i=1}^N \mathbf{M}_{y_\alpha}(k_0) \end{pmatrix}, \quad \mathbf{Q}_1(k_0) = \begin{pmatrix} -\sum_{i=1}^N \mathbf{F}_{z_{\dot{h}}}(k_0) & -\sum_{i=1}^N \mathbf{F}_{z_{\dot{\alpha}}}(k_0) \\ \sum_{i=1}^N \mathbf{M}_{y_{\dot{h}}}(k_0) & \sum_{i=1}^N \mathbf{M}_{y_{\dot{\alpha}}}(k_0) \end{pmatrix} \\ \mathbf{Q}_2(k_0) &= \begin{pmatrix} -\sum_{i=1}^N \mathbf{F}_{z_{\ddot{h}}}(k_0) & -\sum_{i=1}^N \mathbf{F}_{z_{\ddot{\alpha}}}(k_0) \\ \sum_{i=1}^N \mathbf{M}_{y_{\ddot{h}}}(k_0) & \sum_{i=1}^N \mathbf{M}_{y_{\ddot{\alpha}}}(k_0) \end{pmatrix}\end{aligned}\tag{36}$$

noting that the lift is defined as positive downwards in Theodorsen theory. Similarly, the steady generalized aerodynamic load vector becomes

$$\mathbf{Q}_s(k_0) = \begin{pmatrix} -\sum_{i=1}^N \mathbf{F}_z(0) \\ \sum_{i=1}^N \mathbf{M}_y(0) \end{pmatrix}\tag{37}$$

where

$$\begin{aligned}\mathbf{F}_z(0) &= -\mathbf{c}_p(0) \circ \mathbf{s} \circ \mathbf{n}_z \\ \mathbf{M}_y(0) &= -\mathbf{F}_z(0) \circ (\mathbf{x}_c - x_f)\end{aligned}$$

The PAPA input files

- flutter_SDPM_BSCW.py
- flutter_SDPM_NACA0012.py
- flutter_SDPM_NACA64A010.py

do not import or interpolate any mode shapes since the motion is described by the pitch and plunge degrees of freedom. The structural mass and stiffness matrices are calculated from

$$\mathbf{A} = \begin{pmatrix} m_h & S_{h\alpha} \\ S_{h\alpha} & I_\alpha \end{pmatrix}, \quad \mathbf{E} = \begin{pmatrix} K_h & 0 \\ 0 & K_\alpha \end{pmatrix}$$

where m_h is the mass of the wing, $S_{h\alpha}$ its static imbalance around the pitch axis, I_α its moment of inertia around the pitch axis, K_h the stiffness of the plunge spring and K_α that of the pitch spring. The values of all these parameters are given in the original references, noting that $S_{h\alpha} = 0$. The rest of the PAPA input files are identical to those of the flexible test cases, except for

```
# Calculate flutter solution for pitch-plunge motion
Uflut,freqflut,kflut,dynpressflut,omega,zeta=
  flutsol.flutsolve_pitchplunge(body,allbodies,kvec,Uv,nmodes,
  Aphi,Bphi,Cphi,barUinf,barVinf,barWinf,c0,Mach,beta,cp_order,
  A,C,E,rho,wn,halfwing,xf0,yf0,zf0,install_dir)
```

Function `flutsol.flutsolve_pitchplunge` calculates the generalized aerodynamic load vector and matrices using equations 35 to 37. As an example, figure 13 plots the flutter speed index and flutter frequency ratio variation with Mach number for the NACA0012 test case.

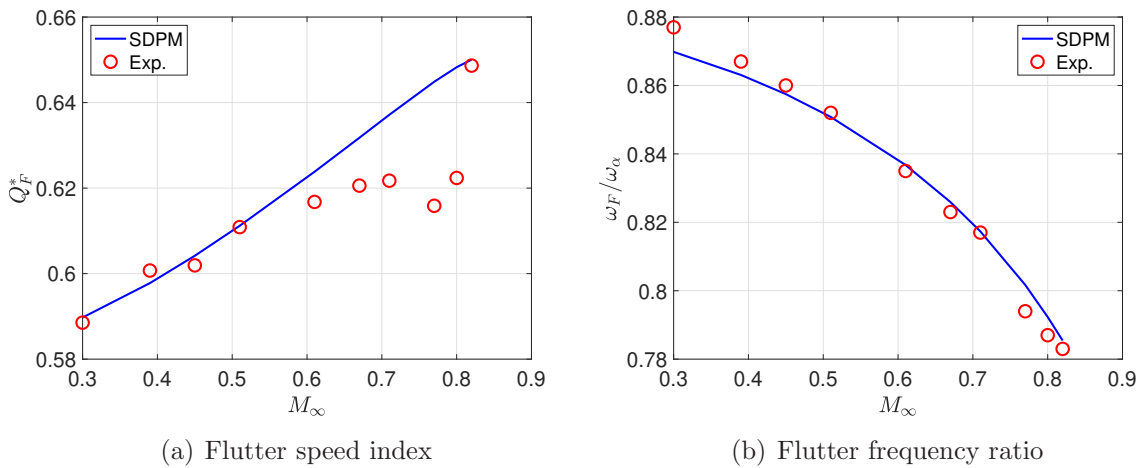


Figure 13: Variation of flutter speed index and flutter frequency ratio with Mach number for the NACA0012 test case

7 Summary

The `SDPMflut` package is a collection of functions for calculating the steady and unsteady aerodynamic loads acting on exact wing geometries and for calculating flutter solutions, if a structural model is given. It does not create any structural models, with the exception of the pitch and plunge test cases; modal models must be imported from a `.mat` file that has been created elsewhere. The package includes functions for creating SDPM grids for wing geometries but not for fuselages, as yet. Future versions will also include fuselage grid generation functions. The user can of course choose to use their own SDPM grids `Xp0`, `Yp0`, `Zp0`, if they have created them elsewhere. The only constraint is that the grid coordinates must be arranged in 2D arrays, such that there are m chordwise panels on the lower and upper surfaces for a total of $2m$ chordwise panels, the first and last rows are the lower and upper trailing edges, respectively, while the first and last columns are the wingtips. Then, the user can employ the functions in `SDPMflut` to calculate the coordinates of the control points, the components of the normal and tangential vectors, the panel areas etc., and place everything in the `body` array.

When using `SDPMflut`, the assumptions behind the source and doublet panel method must always be kept in mind:

- The flow is inviscid, irrotational and isentropic
- All deformations and displacements are small
- The flow remains attached to the surface and separated smoothly at the trailing edge
- There are no shock waves on the surface

Some of the test cases included in the package feature transonic flow with shocks on the surface; the pressure distribution around the surface for such cases cannot be modelled accurately by the SDPM. Consequently, any flutter solutions will ignore the effect of the shock waves and will fail to predict the transonic flutter dip. Future versions will include functions to correct the unsteady pressure distributions using higher fidelity steady results [6].

All drag estimates obtained from `SDPMflut` ignore viscous drag contributions. The flat plate analogy can be used to obtain an empirical estimate of steady skin friction drag, see for example [3]. The required wetted area of all the bodies in the flow can be calculated conveniently from the sums of the panel area fields, `s0`, of each element of the `body` structured array.

References

- [1] Dimitriadis, G., *Unsteady Aerodynamics - Potential and Vortex Methods*, Wiley, 2023, <https://doi.org/10.1002/9781119762560>.

- [2] Sánchez Martínez, M. and Dimitriadis, G., “Subsonic source and doublet panel methods,” *Journal of Fluids and Structures*, Vol. 113, 2022, pp. 103624, <https://doi.org/10.1016/j.jfluidstructs.2022.103624>.
- [3] Dimitriadis, G., Panagiotou, P., Dimopoulos, T., and Yakinthos, K., “Aerodynamic stability derivative calculations using the compressible source and doublet panel method,” *Journal of Aircraft*, Vol. 61, No. 4, 2024, pp. 1034–1046, <https://doi.org/10.2514/1.C037747>.
- [4] Dimitriadis, G., Kilimtzidis, S., Kostopoulos, V., Laraspata, V., and Soria, L., “Flutter calculations using the unsteady source and doublet panel method,” *Journal of Aircraft*, Vol. 62, No. 1, 2024, pp. 117–131, <https://arc.aiaa.org/doi/10.2514/1.C037891>.
- [5] Dimitriadis, G., Kilimtzidis, S., Kostopoulos, V., Laraspata, V., and Soria, L., “Application of the unsteady compressible source and doublet panel method to flutter calculations,” *Proceedings of the International Forum on Aeroelasticity and Structural Dynamics*, No. IFASD2024-199, The Hague, Netherlands, June 2024.
- [6] Dimitriadis, G., Crovato, A., Sánchez Martínez, M., Laraspata, V., Soria, L., Kilimtzidis, S., and Kostopoulos, V., “Transonic corrections for the unsteady compressible Source and Doublet Panel Method,” *Journal of Aircraft*, Vol. In print, 2024.
- [7] Morino, L., “A general theory of unsteady compressible potential aerodynamics,” Contractor Report CR-2464, NASA, 1974.
- [8] Morino, L., Chen, L., and Suciú, E. O., “Steady and Oscillatory Subsonic and Supersonic Aerodynamics around Complex Configurations,” *AIAA Journal*, Vol. 13, No. 3, 1975, pp. 368–374, <https://doi.org/10.2514/3.49706>.
- [9] Carson Yates, Jr, E., “AGARD standard aeroelastic configurations for dynamic response I – Wing 445.6,” Report AGARD-R-765, AGARD, 1988.
- [10] Riley, D. R., Bird, J. D., and Fisher, L. R., “Experimental determination of the aerodynamic derivatives arising from acceleration in sideslip for a triangular, a swept, and an unswept wing,” Research Memorandum RM L55A07, NACA, 1955.
- [11] Queijo, M. J., Fletcher, H. S., Marple, C. G., and Hughes, F. M., “Preliminary measurements of the aerodynamic yawing derivatives of a triangular, a swept, and an unswept wing performing pure yawing oscillations, with a description of the instrumentation employed,” Research Memorandum RM L55L14, NACA, 1956.
- [12] Fisher, L. R., “Experimental determination of effects of frequency and amplitude on the lateral stability derivatives for a Delta, a swept, and an unswept wing oscillating in yaw,” Report 1357, NACA, 1958.
- [13] Lichtenstein, J. H. and Williams, J. L., “Low speed investigation of the effects of frequency and amplitude of oscillation in sideslip on the lateral stability derivatives of 60° Delta wing, a 45° sweptback wing, and an unswept wing,” Research Memorandum RM L58B26, NACA, 1958.

- [14] Doggett, Jr, R. V. and Farmer, M. G., “A preliminary study of the effects of vortex diffusers (winglets) on wing flutter,” Technical Memorandum NASA TMX 72799, NASA, 1975.
- [15] Lessing, H. C., Troutman, J. L., and Menees, G. P., “Experimental determination of the pressure distribution on a rectangular wing oscillating in the first bending mode for Mach numbers from 0.24 to 1.30,” Technical Note TN-D-344, NASA, 1960.
- [16] Lockman, W. K. and Lee Seegmiller, H., “An Experimental Investigation of the Subcritical and Supercritical Flow About a Swept Semispan Wing,” Technical Memorandum TM-84367, NASA, 1983.
- [17] Dansberry, B. E., Durham, M. H., Turnock, D. L., Silva, W. A., and Rivera, Jr., J. A., “Physical Properties of the Benchmark Models Program Supercritical Wing,” Technical Memorandum TM 4457, NASA, 1993.
- [18] Bennett, R. M., “Test Cases for a Rectangular Supercritical Wing Undergoing Pitching Oscillations,” *Verification and Validation Data for Computational Unsteady Aerodynamics*, edited by L. P. Ruiz-Calavera, No. RTO-TR-26, Research and Technology Organization North Atlantic Treaty Organization, Neuilly-sur-Seine, France, 2000.
- [19] Rivera, Jr, J. A., Dansberry, B. E., Durham, M. H., Bennett, R. M., and Silva, W. A., “Pressure measurements on a rectangular wing with a NACA0012 airfoil during conventional flutter,” Technical Memorandum TM-104211, NASA, 1992.
- [20] Murua, J., Martínez, P., Climent, H., van Zyl, L., and Palacios, R., “Applications of the unsteady vortex-lattice method in aircraft aeroelasticity and flight dynamics,” *Progress in Aerospace Sciences*, Vol. 55, 2012, pp. 46–72.
- [21] van Zyl, L. and Mathews, E. H., “Aeroelastic Analysis of T-Tails Using an Enhanced Doublet Lattice Method,” *Journal of Aircraft*, Vol. 48, No. 3, 2011, pp. 823–831, <https://doi.org/10.2514/1.C001000>.
- [22] van Zyl, L., *Advanced linear methods for T-tail aeroelasticity*, Ph.D. thesis, North-West University, 2011.
- [23] Theodorsen, T., “General theory of aerodynamic instability and the mechanism of flutter,” Technical Report TR-496, NACA, 1935.

A Fourier transform of nonlinear pressure equation

In applying the Fourier transform to equation 2, all the multiplications in the time domain become convolutions in the frequency domain. The Fourier transform can be written as

$$c_p(\omega) = \delta(\omega) - \frac{u(\omega) * u(\omega) + v(\omega) * v(\omega) + w(\omega) * w(\omega)}{Q_\infty^2} + \frac{M_\infty^2}{Q_\infty^2} \phi_x(\omega) * \phi_x(\omega) - \frac{2}{Q_\infty^2} i\omega\phi(\omega) + \frac{M_\infty^2}{Q_\infty^4} (i\omega\phi(\omega)) * (i\omega\phi(\omega)) + \frac{2M_\infty^2}{Q_\infty^3} \phi_x(\omega) * (i\omega\phi(\omega)) \quad (38)$$

where $\delta(\omega)$ is the Kronecker Delta function and the operator $*$ denotes convolution. For sinusoidal motion at frequency ω_0 , the various terms in equation 38 can be written as vectors with three elements, their frequency components at $-\omega_0$, 0 and ω_0 , such that

$$\begin{aligned} \phi(\omega) &= (\phi^*(\omega_0), \phi(0), \phi(\omega_0)) \\ i\omega\phi(\omega) &= (-i\omega_0\phi^*(\omega_0), 0, i\omega_0\phi(\omega_0)) \\ \phi_x(\omega) &= (\phi_x^*(\omega_0), \phi_x(0), \phi_x(\omega_0)) \\ \phi_y(\omega) &= (\phi_y^*(\omega_0), \phi_y(0), \phi_y(\omega_0)) \\ \phi_z(\omega) &= (\phi_z^*(\omega_0), \phi_z(0), \phi_z(\omega_0)) \\ u(\omega) &= (u_m^*(\omega_0) + \phi_x^*(\omega_0), U_\infty + \phi_x(0), u_m(\omega_0) + \phi_x(\omega_0)) \\ v(\omega) &= (v_m^*(\omega_0) + \phi_y^*(\omega_0), V_\infty + \phi_y(0), v_m(\omega_0) + \phi_y(\omega_0)) \\ w(\omega) &= (w_m^*(\omega_0) + \phi_z^*(\omega_0), W_\infty + \phi_z(0), w_m(\omega_0) + \phi_z(\omega_0)) \end{aligned}$$

where the superscript $*$ denotes the complex conjugate. Then,

$$\begin{aligned} \phi_x(\omega) * \phi_x(\omega) &= \begin{pmatrix} \phi_x^*(\omega_0)^2 \\ 2\phi_x^*(\omega_0)\phi_x(0) \\ 2\phi_x^*(\omega_0)\phi_x(\omega_0) + \phi_x(0)^2 \\ 2\phi_x(0)\phi_x(\omega_0) \\ \phi_x(\omega_0)^2 \end{pmatrix} \\ (i\omega\phi(\omega)) * (i\omega\phi(\omega)) &= \begin{pmatrix} (-i\omega_0\phi^*(\omega_0))^2 \\ 0 \\ 2(-i\omega_0\phi^*(\omega_0))(i\omega_0\phi(\omega_0)) \\ 0 \\ (i\omega_0\phi(\omega_0))^2 \end{pmatrix} \\ \phi_x(\omega) * (i\omega\phi(\omega)) &= \begin{pmatrix} -\phi_x^*(\omega_0)i\omega_0\phi^*(\omega_0) \\ -\phi_x(0)i\omega_0\phi^*(\omega_0) \\ \phi_x^*(\omega_0)i\omega_0\phi(\omega_0) - \phi_x(\omega_0)i\omega_0\phi^*(\omega_0) \\ \phi_x(0)i\omega_0\phi(\omega_0) \\ \phi_x(\omega_0)i\omega_0\phi(\omega_0) \end{pmatrix} \\ u(\omega) * u(\omega) &= \begin{pmatrix} u^*(\omega_0)^2 \\ 2u^*(\omega_0)u(0) \\ 2u^*(\omega_0)u(\omega_0) + u(0)^2 \\ 2u(\omega_0)u(0) \\ u(\omega_0)^2 \end{pmatrix} \end{aligned}$$

and similar expressions for $u(\omega) * u(\omega)$, $v(\omega) * v(\omega)$. In all these convolutions, the first element of the resulting vector corresponds to frequency component $\omega = -2\omega_0$, the second to $\omega = -\omega_0$, the third to $\omega = 0$, the fourth to $\omega = \omega_0$ and the fifth the $\omega = 2\omega_0$. Consequently, the pressure coefficient at $\omega = 0$ is calculated by substituting the third element of each of the convolution vector into equation 38, i.e.

$$\begin{aligned}
c_p(0) = & 1 - \frac{2u^*(\omega_0)u(\omega_0) + u(0)^2}{Q_\infty^2} - \frac{2v^*(\omega_0)v(\omega_0) + v(0)^2}{Q_\infty^2} - \frac{2w^*(\omega_0)w(\omega_0) + w(0)^2}{Q_\infty^2} \\
& + \frac{M_\infty^2}{Q_\infty^2} (2\phi_x^*(\omega_0)\phi_x(\omega_0) + \phi_x(0)^2) + \frac{2M_\infty^2}{Q_\infty^4} \omega_0^2 \phi^*(\omega_0)\phi(\omega_0) \\
& + \frac{2M_\infty^2}{Q_\infty^3} i\omega_0 (\phi_x^*(\omega_0)\phi(\omega_0) - \phi_x(\omega_0)\phi^*(\omega_0))
\end{aligned} \tag{39}$$

The pressure coefficient at the oscillation frequency, $\omega = \omega_0$, is obtained when using the fourth element of each of the convolution vectors, such that

$$\begin{aligned}
c_p(\omega_0) = & -2 \frac{u(\omega_0)u(0) + v(\omega_0)v(0) + w(\omega_0)w(0)}{Q_\infty^2} + \frac{2M_\infty^2}{Q_\infty^2} \phi_x(0)\phi_x(\omega_0) \\
& - \frac{2}{Q_\infty^2} i\omega_0 \phi(\omega_0) + \frac{2M_\infty^2}{Q_\infty^3} i\omega_0 \phi_x(0)\phi(\omega_0)
\end{aligned} \tag{40}$$

Finally, the pressure coefficient at twice the oscillation frequency, $\omega = 2\omega_0$, is obtained when using the fifth element of each convolution vector,

$$\begin{aligned}
c_p(2\omega_0) = & - \frac{u(\omega_0)^2 + v(\omega_0)^2 + w(\omega_0)^2}{Q_\infty^2} + \frac{M_\infty^2}{Q_\infty^2} \phi_x(\omega_0)^2 \\
& - \frac{M_\infty^2}{Q_\infty^4} \omega_0^2 \phi(\omega_0)^2 + \frac{2M_\infty^2}{Q_\infty^3} i\omega_0 \phi_x(\omega_0)\phi(\omega_0)
\end{aligned} \tag{41}$$

Equations 39 and 41 are nonlinear in the oscillatory potential and velocities and will not be used in the present work. In particular, equation 39 gives the zero frequency component of an oscillatory pressure, in other words the mean pressure. The steady pressure in the absence of motion is obtained by setting $\omega = 0$ directly in equation 38, such that

$$c_{p_0} = 1 - \frac{u(0)^2 + v(0)^2 + w(0)^2}{Q_\infty^2} + \frac{M_\infty^2}{Q_\infty^2} \phi_x(0)^2 \tag{42}$$

Equation 40 for $c_p(\omega_0)$ is linear in the oscillatory potential and velocities and can therefore be used for linear flutter analysis. Substituting for ω_0 from

$$\omega_0 = \frac{2Q_\infty k}{c_0}$$

leads to

$$\begin{aligned}
c_p(k) = & -2 \frac{u(k)u(0) + v(k)v(0) + w(k)w(0)}{Q_\infty^2} + \frac{2M_\infty^2}{Q_\infty^2} \phi_x(0)\phi_x(k) \\
& - \frac{4ik}{c_0 Q_\infty} \phi(k) + \frac{4ikM_\infty^2}{c_0 Q_\infty^2} \phi_x(0)\phi(k)
\end{aligned}$$

Writing out this latest expression for all the control points of all the panels on the surface leads to the vector expression

$$\begin{aligned} \mathbf{c}_p(k) = & -2 \frac{\mathbf{u}(k) \circ \mathbf{u}(0) + \mathbf{v}(k) \circ \mathbf{v}(0) + \mathbf{w}(k) \circ \mathbf{w}(0)}{Q_\infty^2} + \frac{2M_\infty^2}{Q_\infty^2} \phi_x(0) \circ \phi_x(k) \\ & - \frac{4ik}{c_0 Q_\infty} \phi(k) + \frac{4ikM_\infty^2}{c_0 Q_\infty^2} \phi_x(0) \circ \phi(k) \end{aligned} \quad (43)$$

We can also define the normalized potential and velocities $\bar{\phi}(k) = \phi(k)/Q_\infty$, $\bar{\mathbf{u}}(k) = \mathbf{u}(k)/Q_\infty$, $\bar{\mathbf{v}}(k) = \mathbf{v}(k)/Q_\infty$, $\bar{\mathbf{w}}(k) = \mathbf{w}(k)/Q_\infty$, $\bar{\mathbf{u}}_m(k) = \mathbf{u}_m(k)/Q_\infty$, $\bar{\mathbf{v}}_m(k) = \mathbf{v}_m(k)/Q_\infty$, $\bar{\mathbf{w}}_m(k) = \mathbf{w}_m(k)/Q_\infty$, $\bar{\phi}_x(k) = \phi_x(k)/Q_\infty$, $\bar{\phi}_y(k) = \phi_y(k)/Q_\infty$, $\bar{\phi}_z(k) = \phi_z(k)/Q_\infty$, $\bar{U}_\infty = U_\infty/Q_\infty$, $\bar{V}_\infty = V_\infty/Q_\infty$, $\bar{W}_\infty = W_\infty/Q_\infty$, such that

$$\begin{aligned} \mathbf{c}_p(k) = & -2(\bar{\mathbf{u}}(k) \circ \bar{\mathbf{u}}(0) + \bar{\mathbf{v}}(k) \circ \bar{\mathbf{v}}(0) + \bar{\mathbf{w}}(k) \circ \bar{\mathbf{w}}(0)) + 2M_\infty^2 \bar{\phi}_x(0) \circ \bar{\phi}_x(k) \\ & - \frac{4ik}{c_0} \bar{\phi}(k) + \frac{4ikM_\infty^2}{c_0} \bar{\phi}_x(0) \circ \bar{\phi}(k) \end{aligned} \quad (44)$$

In order to proceed further, we note that the normalized versions of equations 9, 10 and 11 become

$$\bar{\boldsymbol{\mu}}_n(k) = - \left(\frac{1}{\beta} \bar{\mathbf{u}}_m(k) \circ \mathbf{n}_\xi + \bar{\mathbf{v}}_m(k) \circ \mathbf{n}_\eta + \bar{\mathbf{w}}_m(k) \circ \mathbf{n}_\zeta \right) \quad (45)$$

$$\bar{\phi}(k) = -\mathbf{K}(k) \bar{\boldsymbol{\mu}}_n(k) \quad (46)$$

$$\bar{\phi}_x(k) = \mathbf{K}_x(k) \bar{\boldsymbol{\mu}}_n(k), \quad \bar{\phi}_y(k) = \mathbf{K}_y(k) \bar{\boldsymbol{\mu}}_n(k), \quad \bar{\phi}_z(k) = \mathbf{K}_z(k) \bar{\boldsymbol{\mu}}_n(k) \quad (47)$$

$$\bar{\mathbf{u}}(k) = \bar{\mathbf{u}}_m(k) + \bar{\phi}_x(k), \quad \bar{\mathbf{v}}(k) = \bar{\mathbf{v}}_m(k) + \bar{\phi}_y(k), \quad \bar{\mathbf{w}}(k) = \bar{\mathbf{w}}_m(k) + \bar{\phi}_z(k) \quad (48)$$

Let us treat the terms in equation 44 one by one. Substituting from expressions 45 to 48, the term $\bar{\mathbf{u}}(k) \circ \bar{\mathbf{u}}(0)$ becomes

$$\begin{aligned} \bar{\mathbf{u}}(k) \circ \bar{\mathbf{u}}(0) &= (\bar{\mathbf{u}}_m(k) + \bar{\phi}_x(k)) \circ \bar{\mathbf{u}}(0) = (\bar{\mathbf{u}}_m(k) + \mathbf{K}_x(k) \bar{\boldsymbol{\mu}}_n(k)) \circ \bar{\mathbf{u}}(0) \\ &= \bar{\mathbf{u}}_m(k) \circ \bar{\mathbf{u}}(0) - \left(\mathbf{K}_x(k) \left(\frac{1}{\beta} \bar{\mathbf{u}}_m(k) \circ \mathbf{n}_\xi + \bar{\mathbf{v}}_m(k) \circ \mathbf{n}_\eta + \bar{\mathbf{w}}_m(k) \circ \mathbf{n}_\zeta \right) \right) \circ \bar{\mathbf{u}}(0) \\ &= \bar{\mathbf{u}}_m(k) \circ \bar{\mathbf{u}}(0) - \frac{1}{\beta} \mathbf{K}_x(k) \circ \bar{\mathbf{u}}(0) (\bar{\mathbf{u}}_m(k) \circ \mathbf{n}_\xi) - \mathbf{K}_x(k) \circ \bar{\mathbf{u}}(0) (\bar{\mathbf{v}}_m(k) \circ \mathbf{n}_\eta) \\ &\quad - \mathbf{K}_x(k) \circ \bar{\mathbf{u}}(0) (\bar{\mathbf{w}}_m(k) \circ \mathbf{n}_\zeta) \end{aligned} \quad (49)$$

Similarly,

$$\begin{aligned} \bar{\mathbf{v}}(k) \circ \bar{\mathbf{v}}(0) &= \bar{\mathbf{v}}_m(k) \circ \bar{\mathbf{v}}(0) - \frac{1}{\beta} \mathbf{K}_y(k) \circ \bar{\mathbf{v}}(0) (\bar{\mathbf{u}}_m(k) \circ \mathbf{n}_\xi) - \mathbf{K}_y(k) \circ \bar{\mathbf{v}}(0) (\bar{\mathbf{v}}_m(k) \circ \mathbf{n}_\eta) \\ &\quad - \mathbf{K}_y(k) \circ \bar{\mathbf{v}}(0) (\bar{\mathbf{w}}_m(k) \circ \mathbf{n}_\zeta) \end{aligned} \quad (50)$$

$$\begin{aligned} \bar{\mathbf{w}}(k) \circ \bar{\mathbf{w}}(0) &= \bar{\mathbf{w}}_m(k) \circ \bar{\mathbf{w}}(0) - \frac{1}{\beta} \mathbf{K}_z(k) \circ \bar{\mathbf{w}}(0) (\bar{\mathbf{u}}_m(k) \circ \mathbf{n}_\xi) - \mathbf{K}_z(k) \circ \bar{\mathbf{w}}(0) (\bar{\mathbf{v}}_m(k) \circ \mathbf{n}_\eta) \\ &\quad - \mathbf{K}_z(k) \circ \bar{\mathbf{w}}(0) (\bar{\mathbf{w}}_m(k) \circ \mathbf{n}_\zeta) \end{aligned} \quad (51)$$

Furthermore,

$$\begin{aligned}
\bar{\phi}_x(0) \circ \bar{\phi}_x(k) &= \bar{\phi}_x(0) \circ (\mathbf{K}_x(k) \bar{\boldsymbol{\mu}}_n(k)) \\
&= -\mathbf{K}_x(k) \circ \bar{\phi}_x(0) \left(\frac{1}{\beta} \bar{\mathbf{u}}_m(k) \circ \mathbf{n}_\xi + \bar{\mathbf{v}}_m(k) \circ \mathbf{n}_\eta + \bar{\mathbf{w}}_m(k) \circ \mathbf{n}_\zeta \right) \\
&= -\frac{1}{\beta} \mathbf{K}_x(k) \circ \bar{\phi}_x(0) (\bar{\mathbf{u}}_m(k) \circ \mathbf{n}_\xi) - \mathbf{K}_x(k) \circ \bar{\phi}_x(0) (\bar{\mathbf{v}}_m(k) \circ \mathbf{n}_\eta) \\
&\quad - \mathbf{K}_x(k) \circ \bar{\phi}_x(0) (\bar{\mathbf{w}}_m(k) \circ \mathbf{n}_\zeta)
\end{aligned} \tag{52}$$

while

$$\begin{aligned}
\bar{\phi}(k) &= -\mathbf{K}(k) \bar{\boldsymbol{\mu}}_n(k) \\
&= \mathbf{K}(k) \left(\frac{1}{\beta} \bar{\mathbf{u}}_m(k) \circ \mathbf{n}_\xi + \bar{\mathbf{v}}_m(k) \circ \mathbf{n}_\eta + \bar{\mathbf{w}}_m(k) \circ \mathbf{n}_\zeta \right) \\
&= \frac{1}{\beta} \mathbf{K}(k) (\bar{\mathbf{u}}_m(k) \circ \mathbf{n}_\xi) + \mathbf{K}(k) (\bar{\mathbf{v}}_m(k) \circ \mathbf{n}_\eta) \\
&\quad + \mathbf{K}(k) (\bar{\mathbf{w}}_m(k) \circ \mathbf{n}_\zeta)
\end{aligned} \tag{53}$$

and, finally,

$$\begin{aligned}
\bar{\phi}_x(0) \circ \bar{\phi}(k) &= \bar{\phi}_x(0) \circ (\mathbf{K}(k) \bar{\boldsymbol{\mu}}_n(k)) \\
&= \mathbf{K}(k) \circ \bar{\phi}_x(0) \left(\frac{1}{\beta} \bar{\mathbf{u}}_m(k) \circ \mathbf{n}_\xi + \bar{\mathbf{v}}_m(k) \circ \mathbf{n}_\eta + \bar{\mathbf{w}}_m(k) \circ \mathbf{n}_\zeta \right) \\
&= \frac{1}{\beta} \mathbf{K}(k) \circ \bar{\phi}_x(0) (\bar{\mathbf{u}}_m(k) \circ \mathbf{n}_\xi) + \mathbf{K}(k) \circ \bar{\phi}_x(0) (\bar{\mathbf{v}}_m(k) \circ \mathbf{n}_\eta) \\
&\quad + \mathbf{K}(k) \circ \bar{\phi}_x(0) (\bar{\mathbf{w}}_m(k) \circ \mathbf{n}_\zeta)
\end{aligned} \tag{54}$$

Substituting equations 49 to 54 into equation 44 leads to

$$\begin{aligned}
\mathbf{c}_p(k) &= -2\bar{\mathbf{u}}_m(k) \circ \bar{\mathbf{u}}(0) + \frac{2}{\beta} \mathbf{K}_x(k) \circ \bar{\mathbf{u}}(0) (\bar{\mathbf{u}}_m(k) \circ \mathbf{n}_\xi) + 2\mathbf{K}_x(k) \circ \bar{\mathbf{u}}(0) (\bar{\mathbf{v}}_m(k) \circ \mathbf{n}_\eta) \\
&\quad + 2\mathbf{K}_x(k) \circ \bar{\mathbf{u}}(0) (\bar{\mathbf{w}}_m(k) \circ \mathbf{n}_\zeta) - 2\bar{\mathbf{v}}_m(k) \circ \bar{\mathbf{v}}(0) + \frac{2}{\beta} \mathbf{K}_y(k) \circ \bar{\mathbf{v}}(0) (\bar{\mathbf{u}}_m(k) \circ \mathbf{n}_\xi) \\
&\quad + 2\mathbf{K}_y(k) \circ \bar{\mathbf{v}}(0) (\bar{\mathbf{v}}_m(k) \circ \mathbf{n}_\eta) + 2\mathbf{K}_y(k) \circ \bar{\mathbf{v}}(0) (\bar{\mathbf{w}}_m(k) \circ \mathbf{n}_\zeta) - 2\bar{\mathbf{w}}_m(k) \circ \bar{\mathbf{w}}(0) \\
&\quad + \frac{2}{\beta} \mathbf{K}_z(k) \circ \bar{\mathbf{w}}(0) (\bar{\mathbf{u}}_m(k) \circ \mathbf{n}_\xi) + 2\mathbf{K}_z(k) \circ \bar{\mathbf{w}}(0) (\bar{\mathbf{v}}_m(k) \circ \mathbf{n}_\eta) \\
&\quad + 2\mathbf{K}_z(k) \circ \bar{\mathbf{w}}(0) (\bar{\mathbf{w}}_m(k) \circ \mathbf{n}_\zeta) - \frac{2M_\infty^2}{\beta} \mathbf{K}_x(k) \circ \bar{\phi}_x(0) (\bar{\mathbf{u}}_m(k) \circ \mathbf{n}_\xi) \\
&\quad - 2M_\infty^2 \mathbf{K}_x(k) \circ \bar{\phi}_x(0) (\bar{\mathbf{v}}_m(k) \circ \mathbf{n}_\eta) - 2M_\infty^2 \mathbf{K}_x(k) \circ \bar{\phi}_x(0) (\bar{\mathbf{w}}_m(k) \circ \mathbf{n}_\zeta) \\
&\quad - \frac{4ik}{c_0\beta} \mathbf{K}(k) (\bar{\mathbf{u}}_m(k) \circ \mathbf{n}_\xi) - \frac{4ik}{c_0} \mathbf{K}(k) (\bar{\mathbf{v}}_m(k) \circ \mathbf{n}_\eta) - \frac{4ik}{c_0} \mathbf{K}(k) (\bar{\mathbf{w}}_m(k) \circ \mathbf{n}_\zeta) \\
&\quad + \frac{4ikM_\infty^2}{c_0\beta} \mathbf{K}(k) \circ \bar{\phi}_x(0) (\bar{\mathbf{u}}_m(k) \circ \mathbf{n}_\xi) + \frac{4ikM_\infty^2}{c_0} \mathbf{K}(k) \circ \bar{\phi}_x(0) (\bar{\mathbf{v}}_m(k) \circ \mathbf{n}_\eta) \\
&\quad + \frac{4ikM_\infty^2}{c_0} \mathbf{K}(k) \circ \bar{\phi}_x(0) (\bar{\mathbf{w}}_m(k) \circ \mathbf{n}_\zeta)
\end{aligned}$$

This latest expression can be tidied up by grouping the terms in $(\bar{\mathbf{u}}_m(k) \circ \mathbf{n}_\xi)$, $(\bar{\mathbf{v}}_m(k) \circ \mathbf{n}_\eta)$ and $(\bar{\mathbf{w}}_m(k) \circ \mathbf{n}_\zeta)$ with the help of the coefficients

$$\begin{aligned}\bar{\mathbf{C}}_0(k) &= -2\mathbf{K}_x(k) \circ \bar{\mathbf{u}}(0) - 2\mathbf{K}_y(k) \circ \bar{\mathbf{v}}(0) - 2\mathbf{K}_z(k) \circ \bar{\mathbf{w}}(0) + 2M_\infty^2 \mathbf{K}_x(k) \circ \bar{\phi}_x(0) \\ \bar{\mathbf{C}}_1(k) &= 2\mathbf{K}(k) - 2M_\infty^2 \mathbf{K}(k) \circ \bar{\phi}_x(0)\end{aligned}\quad (55)$$

Consequently, the final expression for the oscillatory pressure coefficient on the surface becomes

$$\begin{aligned}\mathbf{c}_p(k) &= -\frac{1}{\beta} \bar{\mathbf{C}}_0(k)(\mathbf{n}_\xi \circ \bar{\mathbf{u}}_m(k)) - 2\bar{\mathbf{u}}(0) \circ \bar{\mathbf{u}}_m(k) - \bar{\mathbf{C}}_0(k)(\mathbf{n}_\eta \circ \bar{\mathbf{v}}_m(k)) - 2\bar{\mathbf{v}}(0) \circ \bar{\mathbf{v}}_m(k) \\ &\quad - \bar{\mathbf{C}}_0(k)(\mathbf{n}_\zeta \circ \bar{\mathbf{w}}_m(k)) - 2\bar{\mathbf{w}}(0) \circ \bar{\mathbf{w}}_m(k) - \frac{2ik}{c_0\beta} \bar{\mathbf{C}}_1(k)(\mathbf{n}_\xi \circ \bar{\mathbf{u}}_m(k)) \\ &\quad - \frac{2ik}{c_0} \bar{\mathbf{C}}_1(k)(\mathbf{n}_\eta \circ \bar{\mathbf{v}}_m(k)) - \frac{2ik}{c_0} \bar{\mathbf{C}}_1(k)(\mathbf{n}_\zeta \circ \bar{\mathbf{w}}_m(k))\end{aligned}\quad (56)$$

A.1 Linearized pressure on the surface

The first order oscillatory pressure equation is obtained by neglecting all nonlinear terms in equation 2, such that

$$c_p(\omega) = -\frac{2\phi_x(\omega)}{Q_\infty} - \frac{2}{Q_\infty^2} i\omega\phi(\omega)$$

Substituting for $\omega = 2kQ_\infty/c_0$ yields the linearized pressure coefficient on the panels

$$\mathbf{c}_p(k) = -2\bar{\phi}_x(k) - \frac{4ik}{c_0} \bar{\phi}(k)\quad (57)$$

Substituting from equations 45 to 47 in expression 57 leads to

$$\begin{aligned}\mathbf{c}_p(k) &= -2\mathbf{K}_x(k)\bar{\boldsymbol{\mu}}_n(k) + \frac{4ik}{c_0} \mathbf{K}(k)\bar{\boldsymbol{\mu}}_n(k) \\ &= 2\mathbf{K}_x(k) \left(\frac{1}{\beta} \bar{\mathbf{u}}_m(k) \circ \mathbf{n}_\xi + \bar{\mathbf{v}}_m(k) \circ \mathbf{n}_\eta + \bar{\mathbf{w}}_m(k) \circ \mathbf{n}_\zeta \right) \\ &\quad - \frac{4ik}{c_0} \mathbf{K}(k) \left(\frac{1}{\beta} \bar{\mathbf{u}}_m(k) \circ \mathbf{n}_\xi + \bar{\mathbf{v}}_m(k) \circ \mathbf{n}_\eta + \bar{\mathbf{w}}_m(k) \circ \mathbf{n}_\zeta \right)\end{aligned}\quad (58)$$

which is the linearized equivalent of equation 56.

B Nonlinear pressure derivatives for rigid body motion

The pressure coefficient at the oscillation frequency, k , also referred to as the oscillatory pressure, is given by equation 18

$$\mathbf{c}_p(k) = -\frac{1}{\beta} \bar{\mathbf{C}}_0(k)(\mathbf{n}_\xi \circ \bar{\mathbf{u}}_m(k)) - 2\bar{\mathbf{u}}(0) \circ \bar{\mathbf{u}}_m(k) - \bar{\mathbf{C}}_0(k)(\mathbf{n}_\eta \circ \bar{\mathbf{v}}_m(k)) - 2\bar{\mathbf{v}}(0) \circ \bar{\mathbf{v}}_m(k)$$

$$\begin{aligned}
& -\bar{\mathbf{C}}_0(k)(\mathbf{n}_\zeta \circ \bar{\mathbf{w}}_m(k)) - 2\bar{\mathbf{w}}(0) \circ \bar{\mathbf{w}}_m(k) - \frac{2ik}{c_0\beta}\bar{\mathbf{C}}_1(k)(\mathbf{n}_\xi \circ \bar{\mathbf{u}}_m(k)) \\
& - \frac{2ik}{c_0}\bar{\mathbf{C}}_1(k)(\mathbf{n}_\eta \circ \bar{\mathbf{v}}_m(k)) - \frac{2ik}{c_0}\bar{\mathbf{C}}_1(k)(\mathbf{n}_\zeta \circ \bar{\mathbf{w}}_m(k))
\end{aligned} \tag{59}$$

Rigid-body motion is defined here as the translation and rotation of the centre of gravity of a body in a body-fixed coordinate system, whereby the x axis is aligned with the chord or fuselage centreline, the y axis is aligned with the span and the z axis is perpendicular to the other two axes. To avoid confusion with the symbols used for the fluid velocities, the translation velocities are denoted by $\dot{x}(t)$, $\dot{y}(t)$ and $\dot{z}(t)$. The rotations are denoted by $\phi(t)$, $\theta(t)$, $\psi(t)$ for the roll, pitch and yaw angles. Assuming that the free stream vector is given by $\mathbf{Q}_\infty = (U_\infty, V_\infty, W_\infty)$ and assuming that all rotation angles are small, the relative velocities between the flow and the body are given by

$$\begin{aligned}
\mathbf{u}_m(t) &= V_\infty\psi(t) - W_\infty\theta(t) - \dot{\theta}(t)\mathbf{z}_c + \dot{\psi}(t)\mathbf{y}_c - \dot{x}(t) \\
\mathbf{v}_m(t) &= -U_\infty\psi(t) + W_\infty\phi(t) + \dot{\phi}(t)\mathbf{z}_c - \dot{\psi}(t)\mathbf{x}_c - \dot{y}(t) \\
\mathbf{w}_m(t) &= U_\infty\theta(t) - V_\infty\phi(t) + \dot{\theta}(t)\mathbf{x}_c - \dot{\phi}(t)\mathbf{y}_c - \dot{z}(t)
\end{aligned} \tag{60}$$

where the first two terms in each velocity component are due to the rotation of the freestream relative to the body-fixed axes, the next two terms are due to the rotational velocities of the centre of gravity and the last terms due to the translation velocities of the centre of gravity. The $N \times 1$ vectors \mathbf{x}_c , \mathbf{y}_c , \mathbf{z}_c , are the coordinates of the N panel control points, assuming that the centre of the coordinate system is the centre of gravity; consequently the relative velocity vectors $\mathbf{u}_m(t)$, $\mathbf{v}_m(t)$, $\mathbf{w}_m(t)$ are also $N \times 1$. Applying the Fourier transform to equations 60 leads to

$$\begin{aligned}
\mathbf{u}_m(\omega) &= V_\infty\psi(\omega) - W_\infty\theta(\omega) - i\omega\theta(\omega)\mathbf{z}_c + i\omega\psi(\omega)\mathbf{y}_c - i\omega x(\omega) \\
\mathbf{v}_m(\omega) &= -U_\infty\psi(\omega) + W_\infty\phi(\omega) + i\omega\phi(\omega)\mathbf{z}_c - i\omega\psi(\omega)\mathbf{x}_c - i\omega y(\omega) \\
\mathbf{w}_m(\omega) &= U_\infty\theta(\omega) - V_\infty\phi(\omega) + i\omega\theta(\omega)\mathbf{x}_c - i\omega\phi(\omega)\mathbf{y}_c - i\omega z(\omega)
\end{aligned} \tag{61}$$

Recall the definition of the reduced frequency $k = \omega c_0 / 2Q_\infty$, such that $\omega = 2kQ_\infty / c_0$. Dividing equations 61 throughout by Q_∞ leads to

$$\begin{aligned}
\bar{\mathbf{u}}_m(k) &= \bar{V}_\infty\psi(k) - \bar{W}_\infty\theta(k) - \frac{2ik}{c_0}\theta(k)\mathbf{z}_c + \frac{2ik}{c_0}\psi(k)\mathbf{y}_c - \frac{2ik}{c_0}x(k) \\
\bar{\mathbf{v}}_m(k) &= -\bar{U}_\infty\psi(k) + \bar{W}_\infty\phi(k) + \frac{2ik}{c_0}\phi(k)\mathbf{z}_c - \frac{2ik}{c_0}\psi(k)\mathbf{x}_c - \frac{2ik}{c_0}y(k) \\
\bar{\mathbf{w}}_m(k) &= \bar{U}_\infty\theta(k) - \bar{V}_\infty\phi(k) + \frac{2ik}{c_0}\theta(k)\mathbf{x}_c - \frac{2ik}{c_0}\phi(k)\mathbf{y}_c - \frac{2ik}{c_0}z(k)
\end{aligned} \tag{62}$$

Aircraft aerodynamic stability derivatives are usually expressed as derivatives of non-dimensional aerodynamic load coefficients with respect to non-dimensional quantities

$$\begin{aligned}
\bar{u}(t) &= \frac{1}{Q_\infty}\dot{x}(t), \quad \bar{v}(t) = \frac{1}{Q_\infty}\dot{y}(t), \quad \bar{w}(t) = \frac{1}{Q_\infty}\dot{z}(t) \\
\bar{\ddot{u}}(t) &= \frac{c_0}{2Q_\infty^2}\ddot{x}(t), \quad \bar{\ddot{v}}(t) = \frac{b}{2Q_\infty^2}\ddot{y}(t), \quad \bar{\ddot{w}}(t) = \frac{c_0}{2Q_\infty^2}\ddot{z}(t)
\end{aligned}$$

$$\begin{aligned}\bar{p}(t) &= \frac{b}{2Q_\infty} \dot{\phi}(t), \quad \bar{q}(t) = \frac{c_0}{2Q_\infty} \dot{\theta}(t), \quad \bar{r}(t) = \frac{b}{2Q_\infty} \dot{\psi}(t) \\ \bar{\dot{p}}(t) &= \left(\frac{b}{2Q_\infty}\right)^2 \ddot{\phi}(t), \quad \bar{\dot{q}}(t) = \left(\frac{c_0}{2Q_\infty}\right)^2 \ddot{\theta}(t), \quad \bar{\dot{r}}(t) = \left(\frac{b}{2Q_\infty}\right)^2 \ddot{\psi}(t)\end{aligned}$$

where b is the span. In the frequency domain, these definitions become

$$\begin{aligned}\bar{u}(k) &= \left(\frac{2ik}{c_0}\right) x(k), \quad \bar{v}(k) = \left(\frac{2ik}{c_0}\right) y(k), \quad \bar{w}(k) = \left(\frac{2ik}{c_0}\right) z(k) \\ \bar{\dot{u}}(k) &= \frac{c_0}{2} \left(\frac{2ik}{c_0}\right)^2 x(k), \quad \bar{\dot{v}}(k) = \frac{b}{2} \left(\frac{2ik}{c_0}\right)^2 y(k), \quad \bar{\dot{w}}(k) = \frac{c_0}{2} \left(\frac{2ik}{c_0}\right)^2 z(k) \\ \bar{p}(k) &= \frac{b}{2} \left(\frac{2ik}{c_0}\right) \phi(k), \quad \bar{q}(k) = \frac{c_0}{2} \left(\frac{2ik}{c_0}\right) \theta(k), \quad \bar{r}(k) = \frac{b}{2} \left(\frac{2ik}{c_0}\right) \psi(k) \\ \bar{\dot{p}}(k) &= \left(\frac{b}{2}\right)^2 \left(\frac{2ik}{c_0}\right)^2 \phi(k), \quad \bar{\dot{q}}(k) = \left(\frac{c_0}{2}\right)^2 \left(\frac{2ik}{c_0}\right)^2 \theta(k), \quad \bar{\dot{r}}(k) = \left(\frac{b}{2}\right)^2 \left(\frac{2ik}{c_0}\right)^2 \psi(k)\end{aligned} \tag{63}$$

In order to obtain the derivatives of $\mathbf{c}_p(k)$ with respect to $\bar{u}(k)$ and $\bar{\dot{u}}(k)$, equations 62 are substituted into equation 59, after setting $\bar{y}(k) = \bar{z}(k) = \phi(k) = \theta(k) = \psi(k) = 0$. Then, equation 59 becomes

$$\begin{aligned}\mathbf{c}_p(k) &= -\frac{1}{\beta} \bar{\mathbf{C}}_0(k) \left(\mathbf{n}_\xi \left(-\frac{2ik}{c_0} x(k) \right) \right) - 2\bar{\mathbf{u}}(0) \left(-\frac{2ik}{c_0} x(k) \right) \\ &\quad - \frac{2ik}{c_0\beta} \bar{\mathbf{C}}_1(k) \left(\mathbf{n}_\xi \left(-\frac{2ik}{c_0} x(k) \right) \right)\end{aligned}$$

where the Hadamard product is no longer required since $x(k)$ is a scalar. Substituting for $\bar{u}(k)$ and $\bar{\dot{u}}(k)$ from equations 63 leads to

$$\mathbf{c}_p(k) = \frac{1}{\beta} \bar{\mathbf{C}}_0(k) \mathbf{n}_\xi \bar{u}(k) + 2\bar{\mathbf{u}}(0) \bar{u}(k) + \frac{2}{c_0\beta} \bar{\mathbf{C}}_1(k) \mathbf{n}_\xi \bar{\dot{u}}(k)$$

Consequently, the pressure derivatives with respect to $\bar{u}(k)$ and $\bar{\dot{u}}(k)$ are given by

$$\mathbf{c}_{p_u}(k) = \frac{1}{\beta} \bar{\mathbf{C}}_0(k) \mathbf{n}_\xi + 2\bar{\mathbf{u}}(0) \tag{64}$$

$$\mathbf{c}_{p_{\dot{u}}}(k) = \frac{2}{c_0\beta} \bar{\mathbf{C}}_1(k) \mathbf{n}_\xi \tag{65}$$

Similarly, for the derivatives of $\mathbf{c}_p(k)$ with respect to $\bar{v}(k)$ and $\bar{\dot{v}}(k)$, we set $x(k) = z(k) = \phi(k) = \theta(k) = \psi(k) = 0$ in equations 62 and substitute them in equation 59 to obtain

$$\begin{aligned}\mathbf{c}_p(k) &= -\bar{\mathbf{C}}_0(k) \mathbf{n}_\eta \left(-\frac{2ik}{c_0} y(k) \right) - 2\bar{\mathbf{v}}(0) \left(-\frac{2ik}{c_0} y(k) \right) \\ &\quad - \frac{2ik}{c_0} \bar{\mathbf{C}}_1(k) \mathbf{n}_\eta \left(-\frac{2ik}{c_0} y(k) \right)\end{aligned}$$

Substituting for $\bar{v}(k)$ and $\bar{\dot{v}}(k)$ from equations 63 leads to the pressure derivatives

$$\mathbf{c}_{p_v}(k) = \bar{\mathbf{C}}_0(k)\mathbf{n}_\eta + 2\bar{\mathbf{v}}(0) \quad (66)$$

$$\mathbf{c}_{p_{\dot{v}}}(k) = \frac{2}{b}\bar{\mathbf{C}}_1(k)\mathbf{n}_\eta \quad (67)$$

Repeating the procedure for the derivatives of $\mathbf{c}_p(k)$ with respect to \bar{w} and $\bar{\dot{w}}$, we obtain

$$\mathbf{c}_{p_w}(k) = \bar{\mathbf{C}}_0(k)\mathbf{n}_\zeta + 2\bar{\mathbf{w}}(0) \quad (68)$$

$$\mathbf{c}_{p_{\dot{w}}}(k) = \frac{2}{c_0}\bar{\mathbf{C}}_1(k)\mathbf{n}_\zeta \quad (69)$$

The derivatives with respect to $\phi(k)$, $\bar{p}(k)$ and $\bar{\dot{p}}(k)$ are obtained by setting $x(k) = y(k) = z(k) = \theta(k) = \psi(k) = 0$ in equations 62 and substituting them into equation 59, so that

$$\begin{aligned} \mathbf{c}_p(k) = & -\bar{\mathbf{C}}_0(k) \left(\mathbf{n}_\eta \circ \left(\bar{W}_\infty \phi(k) + \frac{2ik}{c_0} \phi(k) \mathbf{z}_c \right) \right) - 2\bar{\mathbf{v}}(0) \circ \left(\bar{W}_\infty \phi(k) + \frac{2ik}{c_0} \phi(k) \mathbf{z}_c \right) \\ & -\bar{\mathbf{C}}_0(k) \left(\mathbf{n}_\zeta \circ \left(-\bar{V}_\infty \phi(k) - \frac{2ik}{c_0} \phi(k) \mathbf{y}_c \right) \right) - 2\bar{\mathbf{w}}(0) \circ \left(-\bar{V}_\infty \phi(k) - \frac{2ik}{c_0} \phi(k) \mathbf{y}_c \right) \\ & -\frac{2ik}{c_0} \bar{\mathbf{C}}_1(k) \left(\mathbf{n}_\eta \circ \left(\bar{W}_\infty \phi(k) + \frac{2ik}{c_0} \phi(k) \mathbf{z}_c \right) \right) \\ & -\frac{2ik}{c_0} \bar{\mathbf{C}}_1(k) \left(\mathbf{n}_\zeta \circ \left(-\bar{V}_\infty \phi(k) - \frac{2ik}{c_0} \phi(k) \mathbf{y}_c \right) \right) \end{aligned}$$

Substituting from equations 63 for $\bar{p}(k)$ and $\bar{\dot{p}}(k)$ results in the derivatives

$$\mathbf{c}_{p_\phi}(k) = -\bar{\mathbf{C}}_0(k)\mathbf{n}_\eta\bar{W}_\infty - 2\bar{\mathbf{v}}(0)\bar{W}_\infty + \bar{\mathbf{C}}_0(k)\mathbf{n}_\zeta\bar{V}_\infty + 2\bar{\mathbf{w}}(0)\bar{V}_\infty \quad (70)$$

$$\begin{aligned} \mathbf{c}_{p_p}(k) = & \frac{2}{b} \left(-\bar{\mathbf{C}}_0(k)(\mathbf{n}_\eta \circ \mathbf{z}_c) - 2\bar{\mathbf{v}}(0) \circ \mathbf{z}_c + \bar{\mathbf{C}}_0(k)(\mathbf{n}_\zeta \circ \mathbf{y}_c) + 2\bar{\mathbf{w}}(0)\mathbf{y}_c \right. \\ & \left. -\bar{\mathbf{C}}_1(k)\mathbf{n}_\eta\bar{W}_\infty + \bar{\mathbf{C}}_1(k)\mathbf{n}_\zeta\bar{V}_\infty \right) \end{aligned} \quad (71)$$

$$\mathbf{c}_{p_{\dot{p}}}(k) = \left(\frac{2}{b} \right)^2 \left(-\bar{\mathbf{C}}_1(k)(\mathbf{n}_\eta \circ \mathbf{z}_c) + \bar{\mathbf{C}}_1(k)(\mathbf{n}_\zeta \circ \mathbf{y}_c) \right) \quad (72)$$

Setting $x(k) = y(k) = z(k) = \phi(k) = \psi(k) = 0$ in equations 62 and substituting them into equation 59 leads to

$$\begin{aligned} \mathbf{c}_p(k) = & -\frac{1}{\beta}\bar{\mathbf{C}}_0(k) \left(\mathbf{n}_\xi \circ \left(-\bar{W}_\infty \theta(k) - \frac{2ik}{c_0} \theta(k) \mathbf{z}_c \right) \right) - 2\bar{\mathbf{u}}(0) \circ \left(-\bar{W}_\infty \theta(k) - \frac{2ik}{c_0} \theta(k) \mathbf{z}_c \right) \\ & -\bar{\mathbf{C}}_0(k) \left(\mathbf{n}_\zeta \circ \left(\bar{U}_\infty \theta(k) + \frac{2ik}{c_0} \theta(k) \mathbf{x}_c \right) \right) - 2\bar{\mathbf{w}}(0) \circ \left(\bar{U}_\infty \theta(k) + \frac{2ik}{c_0} \theta(k) \mathbf{x}_c \right) \\ & -\frac{2ik}{c_0\beta} \bar{\mathbf{C}}_1(k) \left(\mathbf{n}_\xi \circ \left(-\bar{W}_\infty \theta(k) - \frac{2ik}{c_0} \theta(k) \mathbf{z}_c \right) \right) \\ & -\frac{2ik}{c_0} \bar{\mathbf{C}}_1(k) \left(\mathbf{n}_\zeta \circ \left(\bar{U}_\infty \theta(k) + \frac{2ik}{c_0} \theta(k) \mathbf{x}_c \right) \right) \end{aligned}$$

Substituting from equations 63 for $\bar{q}(k)$ and $\bar{\dot{q}}(k)$ leads to

$$\mathbf{c}_{p_\theta}(k) = \frac{1}{\beta} \bar{\mathbf{C}}_0(k) \mathbf{n}_\xi \bar{W}_\infty + 2\bar{\mathbf{u}}(0) \bar{W}_\infty - \bar{\mathbf{C}}_0(k) \mathbf{n}_\zeta \bar{U}_\infty - 2\bar{\mathbf{w}}(0) \bar{U}_\infty \quad (73)$$

$$\begin{aligned} \mathbf{c}_{p_q}(k) &= \frac{2}{c_0} \left(\frac{1}{\beta} \bar{\mathbf{C}}_0(k) (\mathbf{n}_\xi \circ \mathbf{z}_c) + 2\bar{\mathbf{u}}(0) \circ \mathbf{z}_c - \bar{\mathbf{C}}_0(k) (\mathbf{n}_\zeta \circ \mathbf{x}_c) - 2\bar{\mathbf{w}}(0) \circ \mathbf{x}_c \right. \\ &\quad \left. + \frac{1}{\beta} \bar{\mathbf{C}}_1(k) \mathbf{n}_\xi \bar{W}_\infty - \bar{\mathbf{C}}_1(k) \mathbf{n}_\zeta \bar{U}_\infty \right) \end{aligned} \quad (74)$$

$$\mathbf{c}_{p_{\dot{q}}}(k) = \left(\frac{2}{c_0} \right)^2 \left(\frac{1}{\beta} \bar{\mathbf{C}}_1(k) (\mathbf{n}_\xi \circ \mathbf{z}_c) - \bar{\mathbf{C}}_1(k) (\mathbf{n}_\zeta \circ \mathbf{x}_c) \right) \quad (75)$$

Finally, setting $x(k) = y(k) = z(k) = \phi(k) = \theta(k) = 0$ in equations 62 and substituting them into equation 59 leads to

$$\begin{aligned} \mathbf{c}_p(k) &= -\frac{1}{\beta} \bar{\mathbf{C}}_0(k) \left(\mathbf{n}_\xi \circ \left(\bar{V}_\infty \psi(k) + \frac{2ik}{c_0} \psi(k) \mathbf{y}_c \right) \right) - 2\bar{\mathbf{u}}(0) \circ \left(\bar{V}_\infty \psi(k) + \frac{2ik}{c_0} \psi(k) \mathbf{y}_c \right) \\ &\quad - \bar{\mathbf{C}}_0(k) \left(\mathbf{n}_\eta \circ \left(-\bar{U}_\infty \psi(k) - \frac{2ik}{c_0} \psi(k) \mathbf{x}_c \right) \right) - 2\bar{\mathbf{v}}(0) \circ \left(-\bar{U}_\infty \psi(k) - \frac{2ik}{c_0} \psi(k) \mathbf{x}_c \right) \\ &\quad - \frac{2ik}{c_0 \beta} \bar{\mathbf{C}}_1(k) \left(\mathbf{n}_\xi \circ \left(\bar{V}_\infty \psi(k) + \frac{2ik}{c_0} \psi(k) \mathbf{y}_c \right) \right) \\ &\quad - \frac{2ik}{c_0} \bar{\mathbf{C}}_1(k) \left(\mathbf{n}_\eta \circ \left(-\bar{U}_\infty \psi(k) - \frac{2ik}{c_0} \psi(k) \mathbf{x}_c \right) \right) \end{aligned}$$

and the pressure derivatives in the yaw direction become

$$\mathbf{c}_{p_\psi}(k) = -\frac{1}{\beta} \bar{\mathbf{C}}_0(k) \mathbf{n}_\xi \bar{V}_\infty - 2\bar{\mathbf{u}}(0) \bar{V}_\infty + \bar{\mathbf{C}}_0(k) \mathbf{n}_\eta \bar{U}_\infty + 2\bar{\mathbf{v}}(0) \bar{U}_\infty \quad (76)$$

$$\begin{aligned} \mathbf{c}_{p_r}(k) &= \frac{2}{b} \left(-\frac{1}{\beta} \bar{\mathbf{C}}_0(k) (\mathbf{n}_\xi \circ \mathbf{y}_c) - 2\bar{\mathbf{u}}(0) \circ \mathbf{y}_c + \bar{\mathbf{C}}_0(k) (\mathbf{n}_\eta \circ \mathbf{x}_c) + 2\bar{\mathbf{v}}(0) \circ \mathbf{x}_c \right. \\ &\quad \left. - \frac{1}{\beta} \bar{\mathbf{C}}_1(k) \mathbf{n}_\xi \bar{V}_\infty + \bar{\mathbf{C}}_1(k) \mathbf{n}_\eta \bar{U}_\infty \right) \end{aligned} \quad (77)$$

$$\mathbf{c}_{p_{\dot{r}}}(k) = \left(\frac{2}{b} \right)^2 \left(-\frac{1}{\beta} \bar{\mathbf{C}}_1(k) (\mathbf{n}_\xi \circ \mathbf{y}_c) + \bar{\mathbf{C}}_1(k) (\mathbf{n}_\eta \circ \mathbf{x}_c) \right) \quad (78)$$

It should be noted that $c_0/2$ in expressions 64 to 78 can be replaced by any other reference chordwise length. Similarly, $b/2$ can be replaced by any other reference spanwise length.

C Pressure derivatives for pitching and plunging motion

Pitching and plunging motion is a special guess of rigid body motion whereby only two degrees of freedom, pitch $\alpha(t)$ and plunge $h(t)$ displacements; the latter is defined positive

downwards. The coordinate system is usually not centred on the pitch axis, so that the motion-induced velocities are given by a modified version of equations 22

$$\begin{aligned}\mathbf{u}_m(\omega) &= -W_\infty\alpha(\omega) - i\omega\alpha(\omega)(\mathbf{z}_c - z_f) \\ \mathbf{v}_m(\omega) &= \mathbf{0} \\ \mathbf{w}_m(\omega) &= U_\infty\alpha(\omega) + i\omega\alpha(\omega)(\mathbf{x}_c - x_f) + i\omega h(k)\end{aligned}$$

where θ has been replaced by α for compatibility with Theodorsen theory, q has been replaced by $i\omega\alpha$ and w has been replaced by $i\omega h$. All other degrees of freedom have been set to zero. Note that Theodorsen theory ignores the $\mathbf{u}_m(\omega)$ velocity and only makes use of the upwash $\mathbf{w}_m(\omega)$. Substituting for $\omega = 2kQ_\infty/c_0$ and dividing throughout by Q_∞ leads to

$$\begin{aligned}\bar{\mathbf{u}}_m(k) &= -\bar{W}_\infty\alpha(k) - \frac{2ik}{c_0}\alpha(k)(\mathbf{z}_c - z_f) \\ \bar{\mathbf{v}}_m(k) &= \mathbf{0} \\ \bar{\mathbf{w}}_m(k) &= \bar{U}_\infty\alpha(k) + \frac{2ik}{c_0}\alpha(k)(\mathbf{x}_c - x_f) + \frac{2ik}{c_0}h(k)\end{aligned}\tag{79}$$

The pressure coefficient at the oscillation frequency, k , is still given by equation 18

$$\begin{aligned}\mathbf{c}_p(k) &= -\frac{1}{\beta}\bar{\mathbf{C}}_0(k)(\mathbf{n}_\xi \circ \bar{\mathbf{u}}_m(k)) - 2\bar{\mathbf{u}}(0) \circ \bar{\mathbf{u}}_m(k) - \bar{\mathbf{C}}_0(k)(\mathbf{n}_\eta \circ \bar{\mathbf{v}}_m(k)) - 2\bar{\mathbf{v}}(0) \circ \bar{\mathbf{v}}_m(k) \\ &\quad - \bar{\mathbf{C}}_0(k)(\mathbf{n}_\zeta \circ \bar{\mathbf{w}}_m(k)) - 2\bar{\mathbf{w}}(0) \circ \bar{\mathbf{w}}_m(k) - \frac{2ik}{c_0\beta}\bar{\mathbf{C}}_1(k)(\mathbf{n}_\xi \circ \bar{\mathbf{u}}_m(k)) \\ &\quad - \frac{2ik}{c_0}\bar{\mathbf{C}}_1(k)(\mathbf{n}_\eta \circ \bar{\mathbf{v}}_m(k)) - \frac{2ik}{c_0}\bar{\mathbf{C}}_1(k)(\mathbf{n}_\zeta \circ \bar{\mathbf{w}}_m(k))\end{aligned}\tag{80}$$

Setting $\alpha(k) = 0$ in equations 79 and substituting into equation 80 leads to

$$\mathbf{c}_p(k) = -\bar{\mathbf{C}}_0(k) \left(\mathbf{n}_\zeta \frac{2ik}{c_0} h(k) \right) - 2\bar{\mathbf{w}} \frac{2ik}{c_0} h(k) - \frac{2ik}{c_0} \bar{\mathbf{C}}_1(k) \left(\mathbf{n}_\zeta \frac{2ik}{c_0} h(k) \right)$$

Writing the pressure coefficient as

$$\mathbf{c}_p(k) = ik\mathbf{c}_{p_h}(k)h(k) + (ik)^2\mathbf{c}_{p_h^2}(k)h(k)$$

leads to the plunge pressure derivatives

$$\mathbf{c}_{p_h}(k) = -\frac{2}{c_0}\bar{\mathbf{C}}_0(k)\mathbf{n}_\zeta - \frac{4}{c_0}\bar{\mathbf{w}}(0)\tag{81}$$

$$\mathbf{c}_{p_h^2}(k) = -\left(\frac{2}{c_0}\right)^2\bar{\mathbf{C}}_1(k)\mathbf{n}_\zeta\tag{82}$$

Setting $h(k) = 0$ in equations 79 and substituting into equation 80 leads to

$$\mathbf{c}_p(k) = -\frac{1}{\beta}\bar{\mathbf{C}}_0(k) \left(\mathbf{n}_\xi \circ \left(-\bar{W}_\infty\alpha(k) - \frac{2ik}{c_0}\alpha(k)(\mathbf{z}_c - z_f) \right) \right)$$

$$\begin{aligned}
& -2\bar{\mathbf{u}}(0) \circ \left(-\bar{W}_\infty \alpha(k) - \frac{2ik}{c_0} \alpha(k) (\mathbf{z}_c - z_f) \right) \\
& -\bar{C}_0(k) \left(\mathbf{n}_\zeta \circ \left(\bar{U}_\infty \alpha(k) + \frac{2ik}{c_0} \alpha(k) (\mathbf{x}_c - x_f) \right) \right) \\
& -2\bar{\mathbf{w}}(0) \circ \left(\bar{U}_\infty \alpha(k) + \frac{2ik}{c_0} \alpha(k) (\mathbf{x}_c - x_f) \right) \\
& -\frac{2ik}{c_0 \beta} \bar{C}_1(k) \left(\mathbf{n}_\xi \circ \left(-\bar{W}_\infty \alpha(k) - \frac{2ik}{c_0} \alpha(k) (\mathbf{z}_c - z_f) \right) \right) \\
& -\frac{2ik}{c_0} \bar{C}_1(k) \left(\mathbf{n}_\zeta \circ \left(\bar{U}_\infty \alpha(k) + \frac{2ik}{c_0} \alpha(k) (\mathbf{x}_c - x_f) \right) \right)
\end{aligned}$$

Finally, writing the pressure coefficient as

$$\mathbf{c}_p(k) = \mathbf{c}_{p_\alpha}(k) \alpha(k) + ik \mathbf{c}_{p_{\dot{\alpha}}}(k) \alpha(k) + (ik)^2 \mathbf{c}_{p_{\ddot{\alpha}}}(k) \alpha(k)$$

leads to the plunge pressure derivatives

$$\mathbf{c}_{p_\alpha}(k) = \frac{\bar{W}_\infty}{\beta} \bar{C}_0(k) \mathbf{n}_\xi + 2\bar{W}_\infty \bar{\mathbf{u}}(0) - \bar{U}_\infty \bar{C}_0(k) \mathbf{n}_\zeta - 2\bar{U}_\infty \bar{\mathbf{w}}(0) \quad (83)$$

$$\begin{aligned}
\mathbf{c}_{p_{\dot{\alpha}}}(k) &= \frac{2}{c_0 \beta} \bar{C}_0(k) (\mathbf{n}_\xi \circ (\mathbf{z}_c - z_f)) + \frac{4}{c_0} \bar{\mathbf{u}}(0) \circ (\mathbf{z}_c - z_f) \\
& - \frac{2}{c_0} \bar{C}_0(k) (\mathbf{n}_\zeta \circ (\mathbf{x}_c - x_f)) - \frac{4}{c_0} \bar{\mathbf{w}}(0) \circ (\mathbf{x}_c - x_f) \\
& + \frac{2\bar{W}_\infty}{c_0 \beta} \bar{C}_1(k) \mathbf{n}_\xi - \frac{2\bar{U}_\infty}{c_0} \bar{C}_1(k) \mathbf{n}_\zeta \quad (84)
\end{aligned}$$

$$\mathbf{c}_{p_{\ddot{\alpha}}}(k) = \left(\frac{2}{c_0} \right)^2 \frac{1}{\beta} \bar{C}_1(k) (\mathbf{n}_\xi \circ (\mathbf{z}_c - z_f)) - \left(\frac{2}{c_0} \right)^2 \bar{C}_1(k) (\mathbf{n}_\zeta \circ (\mathbf{x}_c - x_f)) \quad (85)$$

C.1 Linearised pressure derivatives for pitching and plunging motion

Equations 81 to 85 give the pressure derivatives obtained from the second order oscillatory pressure equation 80. Their linearized equivalents are obtained from the linearized pressure equation 58

$$\begin{aligned}
\mathbf{c}_p(k) &= 2\mathbf{K}_x(k) \left(\frac{1}{\beta} \bar{\mathbf{u}}_m(k) \circ \mathbf{n}_\xi + \bar{\mathbf{v}}_m(k) \circ \mathbf{n}_\eta + \bar{\mathbf{w}}_m(k) \circ \mathbf{n}_\zeta \right) \\
& - \frac{4ik}{c_0} \mathbf{K}(k) \left(\frac{1}{\beta} \bar{\mathbf{u}}_m(k) \circ \mathbf{n}_\xi + \bar{\mathbf{v}}_m(k) \circ \mathbf{n}_\eta + \bar{\mathbf{w}}_m(k) \circ \mathbf{n}_\zeta \right) \quad (86)
\end{aligned}$$

Setting $\alpha(k) = 0$ in equations 79 and substituting into equation 86 leads to

$$\mathbf{c}_p(k) = 2\mathbf{K}_x(k) \mathbf{n}_\zeta \frac{2ik}{c_0} h(k) - \frac{4ik}{c_0} \mathbf{K}(k) \mathbf{n}_\zeta \frac{2ik}{c_0} h(k)$$

such that the linearized pressure derivatives in the plunge direction become

$$\mathbf{c}_{p_h}(k) = \frac{4}{c_0} \mathbf{K}_x(k) \mathbf{n}_\zeta \quad (87)$$

$$\mathbf{c}_{p_{\dot{h}}}(k) = -\frac{8}{c_0^2} \mathbf{K}(k) \mathbf{n}_\zeta \quad (88)$$

Setting $h(k) = 0$ in equations 79 and substituting into equation 86 results in

$$\begin{aligned} \mathbf{c}_p(k) = & \frac{2}{\beta} \mathbf{K}_x(k) \left(\left(-\bar{W}_\infty \alpha(k) - \frac{2ik}{c_0} \alpha(k) (\mathbf{z}_c - \mathbf{z}_f) \right) \circ \mathbf{n}_\xi \right) \\ & + 2 \mathbf{K}_x(k) \left(\left(\bar{U}_\infty \alpha(k) + \frac{2ik}{c_0} \alpha(k) (\mathbf{x}_c - \mathbf{x}_f) \right) \circ \mathbf{n}_\zeta \right) \\ & - \frac{4ik}{c_0 \beta} \mathbf{K}(k) \left(\left(-\bar{W}_\infty \alpha(k) - \frac{2ik}{c_0} \alpha(k) (\mathbf{z}_c - \mathbf{z}_f) \right) \circ \mathbf{n}_\xi \right) \\ & - \frac{4ik}{c_0} \mathbf{K}(k) \left(\left(\bar{U}_\infty \alpha(k) + \frac{2ik}{c_0} \alpha(k) (\mathbf{x}_c - \mathbf{x}_f) \right) \circ \mathbf{n}_\zeta \right) \end{aligned}$$

Consequently, the linearized pressure derivatives in the plunge direction are

$$\mathbf{c}_{p_\alpha}(k) = -\frac{2\bar{W}_\infty}{\beta} \mathbf{K}_x(k) \mathbf{n}_\xi + 2\bar{U}_\infty \mathbf{K}_x(k) \mathbf{n}_\zeta \quad (89)$$

$$\begin{aligned} \mathbf{c}_{p_\alpha}(k) = & -\frac{4}{c_0 \beta} \mathbf{K}_x(k) (\mathbf{n}_\xi \circ (\mathbf{z}_c - \mathbf{z}_f)) + \frac{4}{c_0} \mathbf{K}_x(k) (\mathbf{n}_\zeta \circ (\mathbf{x}_c - \mathbf{x}_f)) \\ & + \frac{4\bar{W}_\infty}{c_0 \beta} \mathbf{K}(k) \mathbf{n}_\xi - \frac{4\bar{U}_\infty}{c_0} \mathbf{K}(k) \mathbf{n}_\zeta \end{aligned} \quad (90)$$

$$\mathbf{c}_{p_{\dot{\alpha}}}(k) = \frac{8}{c_0^2 \beta} \mathbf{K}(k) (\mathbf{n}_\xi \circ (\mathbf{z}_c - \mathbf{z}_f)) - \frac{8}{c_0^2} \mathbf{K}(k) (\mathbf{n}_\zeta \circ (\mathbf{x}_c - \mathbf{x}_f)) \quad (91)$$

D Nonlinear pressure derivatives for flexible motion

The pressure coefficient at the oscillation frequency, k , is still given by equation 18

$$\begin{aligned} \mathbf{c}_p(k) = & -\frac{1}{\beta} \bar{\mathbf{C}}_0(k) (\mathbf{n}_\xi \circ \bar{\mathbf{u}}_m(k)) - 2\bar{\mathbf{u}}(0) \circ \bar{\mathbf{u}}_m(k) - \bar{\mathbf{C}}_0(k) (\mathbf{n}_\eta \circ \bar{\mathbf{v}}_m(k)) - 2\bar{\mathbf{v}}(0) \circ \bar{\mathbf{v}}_m(k) \\ & - \bar{\mathbf{C}}_0(k) (\mathbf{n}_\zeta \circ \bar{\mathbf{w}}_m(k)) - 2\bar{\mathbf{w}}(0) \circ \bar{\mathbf{w}}_m(k) - \frac{2ik}{c_0 \beta} \bar{\mathbf{C}}_1(k) (\mathbf{n}_\xi \circ \bar{\mathbf{u}}_m(k)) \\ & - \frac{2ik}{c_0} \bar{\mathbf{C}}_1(k) (\mathbf{n}_\eta \circ \bar{\mathbf{v}}_m(k)) - \frac{2ik}{c_0} \bar{\mathbf{C}}_1(k) (\mathbf{n}_\zeta \circ \bar{\mathbf{w}}_m(k)) \end{aligned} \quad (92)$$

For flexible motion, the motion-induced relative velocities on the surface are given by equations 23

$$\begin{aligned} \bar{\mathbf{u}}_m(k) &= \bar{V}_\infty \tilde{\Phi}_\psi \mathbf{q}(k) - \bar{W}_\infty \tilde{\Phi}_\theta \mathbf{q}(k) - \frac{2ik}{c_0} \tilde{\Phi}_x \mathbf{q}(k) \\ \bar{\mathbf{v}}_m(k) &= -\bar{U}_\infty \tilde{\Phi}_\psi \mathbf{q}(k) + \bar{W}_\infty \tilde{\Phi}_\phi \mathbf{q}(k) - \frac{2ik}{c_0} \tilde{\Phi}_y \mathbf{q}(k) \\ \bar{\mathbf{w}}_m(k) &= \bar{U}_\infty \tilde{\Phi}_\theta \mathbf{q}(k) - \bar{V}_\infty \tilde{\Phi}_\phi \mathbf{q}(k) - \frac{2ik}{c_0} \tilde{\Phi}_z \mathbf{q}(k) \end{aligned} \quad (93)$$

Setting $\tilde{\Phi}_\phi = \tilde{\Phi}_\theta = \tilde{\Phi}_\psi = \tilde{\Phi}_y = \tilde{\Phi}_z = \mathbf{0}$ and substituting equations 93 into 92 leads to

$$\begin{aligned} \mathbf{c}_p(k) &= -\frac{1}{\beta} \bar{\mathbf{C}}_0(k) \left(\mathbf{n}_\xi \circ \left(-\frac{2ik}{c_0} \tilde{\Phi}_x \mathbf{q}(k) \right) \right) - 2\bar{\mathbf{u}}(0) \circ \left(-\frac{2ik}{c_0} \tilde{\Phi}_x \mathbf{q}(k) \right) \\ &\quad - \frac{2ik}{c_0\beta} \bar{\mathbf{C}}_1(k) \left(\mathbf{n}_\xi \circ \left(-\frac{2ik}{c_0} \tilde{\Phi}_x \mathbf{q}(k) \right) \right) \end{aligned}$$

We then write $\mathbf{c}_p(k)$ in the form

$$\mathbf{c}_p(k) = ik\mathbf{c}_{p\ddot{x}}(k)\mathbf{q}(k) + (ik)^2\mathbf{c}_{p\dot{x}}(k)\mathbf{q}(k)$$

where the pressure derivatives due to motion parallel to the $\tilde{\Phi}_x$ components of the mode shapes are given by

$$\mathbf{c}_{p\ddot{x}}(k) = \frac{2}{c_0\beta} \bar{\mathbf{C}}_0(k) \left(\mathbf{n}_\xi \circ \tilde{\Phi}_x \right) + \frac{4}{c_0} \bar{\mathbf{u}}(0) \circ \tilde{\Phi}_x \quad (94)$$

$$\mathbf{c}_{p\dot{x}}(k) = \frac{4}{c_0^2\beta} \bar{\mathbf{C}}_1(k) \left(\mathbf{n}_\xi \circ \tilde{\Phi}_x \right) \quad (95)$$

Similarly, the pressure derivatives do to motion parallel to the $\tilde{\Phi}_y$ components of the mode shapes become

$$\mathbf{c}_{p\ddot{y}}(k) = \frac{2}{c_0} \bar{\mathbf{C}}_0(k) \left(\mathbf{n}_\eta \circ \tilde{\Phi}_y \right) + \frac{4}{c_0} \bar{\mathbf{v}}(0) \circ \tilde{\Phi}_y \quad (96)$$

$$\mathbf{c}_{p\dot{y}}(k) = \frac{4}{c_0^2} \bar{\mathbf{C}}_1(k) \left(\mathbf{n}_\eta \circ \tilde{\Phi}_y \right) \quad (97)$$

while the pressure derivatives in the $\tilde{\Phi}_z$ direction are

$$\mathbf{c}_{p\ddot{z}}(k) = \frac{2}{c_0} \bar{\mathbf{C}}_0(k) \left(\mathbf{n}_\zeta \circ \tilde{\Phi}_z \right) + \frac{4}{c_0} \bar{\mathbf{w}}(0) \circ \tilde{\Phi}_z \quad (98)$$

$$\mathbf{c}_{p\dot{z}}(k) = \frac{4}{c_0^2} \bar{\mathbf{C}}_1(k) \left(\mathbf{n}_\zeta \circ \tilde{\Phi}_z \right) \quad (99)$$

Next, we set $\tilde{\Phi}_\theta = \tilde{\Phi}_\psi = \tilde{\Phi}_x = \tilde{\Phi}_y = \tilde{\Phi}_z = \mathbf{0}$ and substitute equations 93 into 92 to obtain

$$\begin{aligned} \mathbf{c}_p(k) &= -\bar{\mathbf{C}}_0(k) \left(\mathbf{n}_\eta \circ \left(\bar{W}_\infty \tilde{\Phi}_\phi \mathbf{q}(k) \right) \right) - 2\bar{\mathbf{v}}(0) \circ \left(\bar{W}_\infty \tilde{\Phi}_\phi \mathbf{q}(k) \right) \\ &\quad - \bar{\mathbf{C}}_0(k) \left(\mathbf{n}_\zeta \circ \left(-\bar{V}_\infty \tilde{\Phi}_\phi \mathbf{q}(k) \right) \right) - 2\bar{\mathbf{w}}(0) \circ \left(-\bar{V}_\infty \tilde{\Phi}_\phi \mathbf{q}(k) \right) \\ &\quad - \frac{2ik}{c_0} \bar{\mathbf{C}}_1(k) \left(\mathbf{n}_\eta \circ \left(\bar{W}_\infty \tilde{\Phi}_\phi \mathbf{q}(k) \right) \right) - \frac{2ik}{c_0} \bar{\mathbf{C}}_1(k) \left(\mathbf{n}_\zeta \circ \left(-\bar{V}_\infty \tilde{\Phi}_\phi \mathbf{q}(k) \right) \right) \end{aligned}$$

The pressure coefficient equation is written as

$$\mathbf{c}_p(k) = \mathbf{c}_{p_\phi}(k)\mathbf{q}(k) + ik\mathbf{c}_{p_{\dot{\phi}}}(k)\mathbf{q}(k)$$

where

$$\begin{aligned} \mathbf{c}_{p_\phi}(k) &= -\bar{W}_\infty \bar{\mathbf{C}}_0(k) \left(\mathbf{n}_\eta \circ \tilde{\mathbf{\Phi}}_\phi \right) - 2\bar{W}_\infty \bar{\mathbf{v}}(0) \circ \tilde{\mathbf{\Phi}}_\phi \\ &\quad + \bar{V}_\infty \bar{\mathbf{C}}_0(k) \left(\mathbf{n}_\zeta \circ \tilde{\mathbf{\Phi}}_\phi \right) + 2\bar{V}_\infty \bar{\mathbf{w}}(0) \circ \tilde{\mathbf{\Phi}}_\phi \end{aligned} \quad (100)$$

$$\mathbf{c}_{p_\phi}(k) = -\frac{2\bar{W}_\infty}{c_0} \bar{\mathbf{C}}_1(k) \left(\mathbf{n}_\eta \circ \tilde{\mathbf{\Phi}}_\phi \right) + \frac{2\bar{V}_\infty}{c_0} \bar{\mathbf{C}}_1(k) \left(\mathbf{n}_\zeta \circ \tilde{\mathbf{\Phi}}_\phi \right) \quad (101)$$

Again, we set $\tilde{\mathbf{\Phi}}_\phi = \tilde{\mathbf{\Phi}}_\psi = \tilde{\mathbf{\Phi}}_x = \tilde{\mathbf{\Phi}}_y = \tilde{\mathbf{\Phi}}_z = \mathbf{0}$ and substitute equations 93 into 92 to obtain

$$\begin{aligned} \mathbf{c}_p(k) &= -\frac{1}{\beta} \bar{\mathbf{C}}_0(k) \left(\mathbf{n}_\xi \circ \left(-\bar{W}_\infty \tilde{\mathbf{\Phi}}_\theta \mathbf{q}(k) \right) \right) - 2\bar{\mathbf{u}}(0) \circ \left(-\bar{W}_\infty \tilde{\mathbf{\Phi}}_\theta \mathbf{q}(k) \right) \\ &\quad - \bar{\mathbf{C}}_0(k) \left(\mathbf{n}_\zeta \circ \left(\bar{U}_\infty \tilde{\mathbf{\Phi}}_\theta \mathbf{q}(k) \right) \right) - 2\bar{\mathbf{w}}(0) \circ \left(\bar{U}_\infty \tilde{\mathbf{\Phi}}_\theta \mathbf{q}(k) \right) \\ &\quad - \frac{2ik}{c_0\beta} \bar{\mathbf{C}}_1(k) \left(\mathbf{n}_\xi \circ \left(-\bar{W}_\infty \tilde{\mathbf{\Phi}}_\theta \mathbf{q}(k) \right) \right) - \frac{2ik}{c_0} \bar{\mathbf{C}}_1(k) \left(\mathbf{n}_\zeta \circ \left(\bar{U}_\infty \tilde{\mathbf{\Phi}}_\theta \mathbf{q}(k) \right) \right) \end{aligned}$$

so that the pressure derivatives in the $\tilde{\mathbf{\Phi}}_\theta$ direction become

$$\begin{aligned} \mathbf{c}_{p_\theta}(k) &= \frac{\bar{W}_\infty}{\beta} \bar{\mathbf{C}}_0(k) \left(\mathbf{n}_\xi \circ \tilde{\mathbf{\Phi}}_\theta \right) + 2\bar{W}_\infty \bar{\mathbf{u}}(0) \circ \tilde{\mathbf{\Phi}}_\theta \\ &\quad - \bar{U}_\infty \bar{\mathbf{C}}_0(k) \left(\mathbf{n}_\zeta \circ \tilde{\mathbf{\Phi}}_\theta \right) - 2\bar{U}_\infty \bar{\mathbf{w}}(0) \circ \tilde{\mathbf{\Phi}}_\theta \end{aligned} \quad (102)$$

$$\mathbf{c}_{p_\theta}(k) = \frac{2\bar{W}_\infty}{c_0\beta} \bar{\mathbf{C}}_1(k) \left(\mathbf{n}_\xi \circ \tilde{\mathbf{\Phi}}_\theta \right) - \frac{2\bar{U}_\infty}{c_0} \bar{\mathbf{C}}_1(k) \left(\mathbf{n}_\zeta \circ \tilde{\mathbf{\Phi}}_\theta \right) \quad (103)$$

Finally, setting $\tilde{\mathbf{\Phi}}_\phi = \tilde{\mathbf{\Phi}}_\theta = \tilde{\mathbf{\Phi}}_x = \tilde{\mathbf{\Phi}}_y = \tilde{\mathbf{\Phi}}_z = \mathbf{0}$ and repeating the procedure yields

$$\begin{aligned} \mathbf{c}_p(k) &= -\frac{1}{\beta} \bar{\mathbf{C}}_0(k) \left(\mathbf{n}_\xi \circ \left(\bar{V}_\infty \tilde{\mathbf{\Phi}}_\psi \mathbf{q}(k) \right) \right) - 2\bar{\mathbf{u}}(0) \circ \left(\bar{V}_\infty \tilde{\mathbf{\Phi}}_\psi \mathbf{q}(k) \right) \\ &\quad - \bar{\mathbf{C}}_0(k) \left(\mathbf{n}_\eta \circ \left(-\bar{U}_\infty \tilde{\mathbf{\Phi}}_\psi \mathbf{q}(k) \right) \right) - 2\bar{\mathbf{v}}(0) \circ \left(-\bar{U}_\infty \tilde{\mathbf{\Phi}}_\psi \mathbf{q}(k) \right) \\ &\quad - \frac{2ik}{c_0\beta} \bar{\mathbf{C}}_1(k) \left(\mathbf{n}_\xi \circ \left(\bar{V}_\infty \tilde{\mathbf{\Phi}}_\psi \mathbf{q}(k) \right) \right) - \frac{2ik}{c_0} \bar{\mathbf{C}}_1(k) \left(\mathbf{n}_\eta \circ \left(-\bar{U}_\infty \tilde{\mathbf{\Phi}}_\psi \mathbf{q}(k) \right) \right) \end{aligned}$$

so that the pressure derivatives in the $\tilde{\mathbf{\Phi}}_\psi$ direction become

$$\begin{aligned} \mathbf{c}_{p_\psi}(k) &= -\frac{\bar{V}_\infty}{\beta} \bar{\mathbf{C}}_0(k) \left(\mathbf{n}_\xi \circ \tilde{\mathbf{\Phi}}_\psi \mathbf{q}(k) \right) - 2\bar{V}_\infty \bar{\mathbf{u}}(0) \circ \tilde{\mathbf{\Phi}}_\psi \\ &\quad + \bar{U}_\infty \bar{\mathbf{C}}_0(k) \left(\mathbf{n}_\eta \circ \tilde{\mathbf{\Phi}}_\psi \right) + 2\bar{U}_\infty \bar{\mathbf{v}}(0) \circ \tilde{\mathbf{\Phi}}_\psi \end{aligned} \quad (104)$$

$$\mathbf{c}_{p_\psi}(k) = -\frac{2\bar{V}_\infty}{c_0\beta} \bar{\mathbf{C}}_1(k) \left(\mathbf{n}_\xi \circ \tilde{\mathbf{\Phi}}_\psi \right) + \frac{2\bar{U}_\infty}{c_0} \bar{\mathbf{C}}_1(k) \left(\mathbf{n}_\eta \circ \tilde{\mathbf{\Phi}}_\psi \right) \quad (105)$$